Aus dem Institut für Toxikologie und Pharmakologie für Naturwissenschaftler
Universitätsklinikum Schleswig-Holstein Campus Kiel

Characterization of the LysR-type Transcriptional Regulator HsdR Gene and Its Adjacent Short-chain Dehydrogenase/Reductase SDRx Gene in *Comamonas testosteroni* ATCC 11996

Dissertation
zur Erlangung des Doktorgrades
der Agrar- und Ernährungswissenschaftlichen Fakultät
der Christian-Albrechts-Universität zu Kiel

vorgelegt von
M. Sc. Wenjie Gong
aus Wugang, Hunan, P. R. China

Kiel, 2011

Dekanin: Prof. Dr. Karin Schwarz
1. Berichterstatter: Prof. Dr. Edmund Maser
2. Berichterstatter: Prof. Dr. Frank Döring
Tag der mündlichen Prüfung: 08.11.2011

Gedruckt mit der Genehmigung der Agrar- und Ernährungswissenschaftlichen Fakultät
der Christian-Albrechts-Universität zu Kiel

Contents

Summary

3α-hydroxysteroid dehydrogenase/carbonyl reductase (3α-HSD/CR) from *Comamonas testosteroni* (*C. testosteroni*) is a key enzyme in the degradation of steroid compounds in soil and water. Interestingly, 3α-HSD/CR gene (*hsdA*) expression can be induced by steroids like testosterone and progesterone. Thus, the regulatory mechanism of 3α-HSD/CR induction has attracted considerable attention of our group. Previously, it has been shown that induction of *hsdA* expression by steroids is a derepression where steroid inducers bind to two repressors, RepA and RepB, thereby preventing blocking of *hsdA* transcription and translation, respectively.

In the present study, a new LysR-type transcriptional factor HsdR for 3α-HSD/CR expression in *C. testosteroni* was identified. The *hsdR* gene locates 2.58 kb downstream of the *hsdA* gene on the *C. testosteroni* ATCC 11996 chromosome with an orientation opposite to *hsdA*. The *hsdR* gene was cloned and the recombinant HsdR protein was overproduced, and an anti-HsdR polyclonal antibody was subsequently prepared. While heterologous transformation systems revealed that HsdR activates the expression of the *hsdA* gene, electrophoretic mobility shift assays (EMSA) showed that HsdR specifically binds to the *hsdA* promoter region. Furthermore, the activity of HsdR is dependent on the decreased repression by RepA. *in vitro* binding assays clearly indicated that HsdR can contact with RNA polymerase. Interestingly, an *hsdR* disrupted mutant expressed low levels of 3α-HSD/CR compared to wild type *C. testosteroni* after testosterone induction. In addition, HsdR itself cannot be induced by testosterone. As a member of LysR-type regulators, HsdR may also repress it own expression. Here, electrophoretic mobility shift assays indicated that HsdR specifically binds to its own promoter. As expected, mutated HsdR expression in an *hsdR-gfp* fusion mutant and an *hsdR* gene disrupted mutant of *C. testosteroni* increased compared to that in the wild type strain, largely because autorepression of HsdR in these mutants is prevented. This result revealed that HsdR negatively regulates its own expression. Phylogenetic analyses indicated that HsdR is related to the contact-regulated gene A (CrgA) from *Neisseria meningitidis*, which exists as an octamer. To detect the active form of HsdR, three truncated proteins,

HsdRΔN (residues 1-86 deleted), HsdRΔC (residues 221-303 deleted), and HsdRΔNC (residues 1-86 and 221-303 deleted), were constructed and purified. These deleted domains are important for the positive control of HsdR on 3α-HSD/CR expression. Western blotting indicated that HsdR may also exist as an octamer, where the central domain is crucial for the multimerization of HsdR. Unexpectedly, gel filtration chromatography showed that there are two dominant oligomers (octamer and hexamer) present for HsdR and its truncated proteins. Taken together, HsdR is a positive transcription factor for 3α-HSD/CR expression in *C. testosteroni*, and it may also negatively regulate its own expression.

In addition, a novel gene *SDRx*, which is divergently transcribed from the *hsdR* gene, was found to be a member of the short-chain dehydrogenase/reductase (SDR) superfamily. The open reading frame of this *SDRx* consists of 768 bp and translates into a protein of 255 amino acids. Two consensus sequences of the SDR superfamily were found, an N-terminal Gly-*X*-*X*-*X*-Gly-*X*-Gly cofactor-binding motif and a Tyr-*X*-*X*-*X*-Lys segment (residues 160-164 in the SDRx sequence) essential for catalytic activity of SDR proteins. Phylogenetic analyses indicated that the novel SDRx gene from *C. testosteroni*, which is active in steroid metabolism, is related to 7α-hydroxysteroid dehydrogenase (7α-HSD). Degradation of the steroids testosterone and estradiol decreased in the *SDRx* knock-out mutant strain. Furthermore, growth on the steroids cholic acid, estradiol and testosterone was impaired in the *SDRx* knock-out strain. Combined, the novel SDRx in *C. testosteroni* was identified as 7α-HSD that is involved in steroid degradation.

Zusammenfassung

Die 3α-Hydroxysteroid-Dehydrogenase/Carbonyl-Reduktase (3α-HSD/CR) von *C. testosteroni* ist ein Schlüsselenzym im Abbau von Steroid-Verbindungen in Boden und Wasser. Bemerkenswerterweise kann die Expression des 3α-HSD/CR Gens (*hsdA*) durch Steroide wie Testosteron und Progesteron induziert werden. Die Aufklärung dieses Regulationsmechanismus der 3α-HSD/CR Induktion ist Gegenstand intensiver Forschung. Bisher hat sich gezeigt, dass die Induktion der *hsdA* Expression durch Steroide eigentlich eine Derepression darstellt, bei der Steroid-Induktoren an zwei Repressoren (RepA und RepB) binden, diese inaktivieren und so die Expression einleiten.

In der vorliegenden Studie wurde ein neuer LysR-artiger Transkriptionsfaktor (*hsdR*) der 3α-HSD/CR Expression in *C. testosteroni* identifiziert. Das *hsdR*-Gen ist 2,58 kb stromabwärts des *hsdA*-Gens im Genom von *C. testosteroni* ATCC 11996 in entgegengesetzter Leserichtung lokalisiert. Das *hsdR*-Gen wurde in *E. coli*-Zellen kloniert, überexprimiert und gereinigt. Mit dem rekombinanten Protein wurde ein polyklonaler Antikörper gewonnen. Während mit heterologen Transformations-Systemen gezeigt wurde, dass *hsdR* die Expression des *hsdA*-Gens induziert, konnte durch „band-shift"-Versuche nachgewiesen werden, dass *hsdR* spezifisch an die *hsdA* Promotor-Region bindet. Dabei ist die HsdR-Aktivität eng mit der *hsdA*-Repression durch RepA verbunden, insofern als HsdR erst nach der Freigabe des Promotors durch RepA aktiv wird. Weiterhin zeigten *in-vitro* Bindungsstudien, dass *hsdR* an RNA-Polymerase bindet. Wie erwartet, ließen sich in *hsdR* knock-out Mutanten nach Testosteron-Induktion nur erniedrigte 3α-HSD/CR Level im Vergleich zum Wildtyp finden.

Die hsdR-Expression wiederum ist nicht durch Testosteron induzierbar. Von LysR-Typ Regulatoren ist bekannt, dass sie im Sinne einer feed-back Regulation ihre eigene Expression unterdrücken können. Es konnte durch weitere „band-shift"-Versuche gezeigt werden, dass HsdR an seinen eigenen Promotor bindet. Wie erwartet war die Expression eines hsdR-gfp Fusionsproteins und einer hsdR-Disruptionsmutante erhöht im Vergleich zum

Wildtyp, da in diesen Mutanten die Autorepression nicht stattfinden konnte.
Folglich wird *hsdR* ebenfalls durch einen feed-back Mechanismus reguliert.

hsdR ähnelt dem Kontakt-regulierten Gen A (CrgA) von *Neisseria meningitidis*, einem Octamer, wie sich durch phylogenetische Untersuchungen nachweisen ließ. Für weitere Analysen wurden drei Deletionsmutanten von hsdR hergestellt, denen folgende Aminosäuren fehlten: HsdRΔN (1-86); HsdRΔC (221-303); HsdRΔNC (1-86 und 221-303). Diese deletierten Domänen sind wichtig für die positive HsdR-regulierte 3α-HSD/CR Expression. Western-Blot-Ergebnisse mit diesen Mutanten zeigten, dass HsdR ebenfalls als Octamer vorliegen könnte und die zentrale Domäne entscheidend für die Multimerisierung ist. Ergebnisse aus Gelfiltrations Versuchen mit dem Wildtyp-Protein sowie den Deletionsmutanten deuten das Vorliegen von zwei Oligomeren (Octamer und Hexamer) an. Zusammenfassend ist *hsdR* als positiver Transkriptionsfaktor der 3α-HSD/CR Expression in *C. testosteroni* identifiziert worden, der die eigene Expression negativ reguliert.

Darüber hinaus wurde ein neues SDR-Gen (*SDRx*) gefunden, das abweichend von *hsdR* transkribiert wird. Der open-reading-frame von *SDRx* umfasst 768 bp, die für ein Protein aus 255 Aminosäuren kodieren. Zwei Konsensus-Sequenzen der SDR-Superfamilie wurden gefunden, das *N*-terminale Gly-XXX-Gly-X-Gly-Cofaktor-Bindungsmotiv und ein Tyr-XXX-Lys-Segment (Aminosäuren 160-164 in der SDRx Sequenz), das essentiell für die katalytische Aktivität der SDR-Proteine ist. Phylogenetische Analysen lassen vermuten, dass das neu gefundene *SDRx*-Gen in *C. testosteroni* homolog zu einer 7α-Hydroxysteroid-Dehydrogenase (7α-HSD) ist, die am Steroidstoffwechsel beteiligt ist. Dies steht im Einklang mit der Beobachtung, dass der Abbau der Steroide Testosteron und Östradiol in *SDRx* knock-out Mutanten verringert ist. Außerdem war das Wachstum des *SDRx* knock-out-Stamms mit den Steroiden Cholsäure, Estradiol oder Testosteron als Kohlenstoffquelle geringer als das des Wildtyps.

Abbreviations

α	alpha
3α-HSD/CR	3 alpha-Hydroxysteroid Dehydrogenase/ Carbonyl Reductase
7α-HSD	7 alpha-Hydroxysteroid Dehydrogenase
AA	amino acid
ABS	activation binding site
ABTS	2'-azino-di-(3-ethylbenzthiazoline-6-sulfonate)
ADH	alcohol dehydrogenase/reductase superfamily
Ap	ampicillin
AP	alkaline phosphatase
APS	ammonium persulfate
ATCC	American Type Culture Collection
BLAST	Basic Local Alignment Search Tool
BSA	bovine serum albumin
C. testosteroni	*Comamonas testosteroni*
cm	centimeter
d	day
DBD	DNA binding domain
DIG	digoxigenin
DNA	deoxyribonucleic acid
DSMZ	Deutsche Sammlung von Mikroorganismen und Zellkulturen
DTT	dithiothreitol
E. coli	*Escherichia coli*
EDTA	ethylene diamine tetraacetic acid
ELISA	enzyme-linked immunosorbent assay
EMSA	electrophoretic mobility shift assays
GFP	green fluorescent protein
h	hour
HPLC	high performance liquid chromatography
HTH	helix-turn-helix
HsdR	3 alpha-Hydroxysteroid Dehydrogenase/ Carbonyl Reductase gene Regulator
IPTG	isopropyl-β-D-thiogalactoside
LTTRs	LysR-type transcriptional regulators
LH	linker helix
kb	kilo basepair
Km	kanamycin
MDR	Medium-chain Dehydrogenase/Reductase
M	molar
mA	milliampere
mM	millimolar

min	minute
ml/mg	milliliter/milligram
mM	millimolar
MOPS	3-(*N*-morpholino)propanesulfonic acid
µg	microgram
µl	microliter
NADH	nicotinamide adenine dinucleotide reduced
NADPH	nicotinamide adenine dinucleotide phosphate reduced
NBT/BCIP	nitroblue tetrazolium/5-bromo-4-chloro-3-indolyl phosphate
Ni-NTA	nickel-nitrilotriacetic acid
nm	nanometer
OD	optical density
OP	operator
PBS	phosphate buffered saline
PCR	polymerase chain reaction
pM	picomolar
PVDF	polyvinylidene fluoride membrane
RBS	repressor binding site
RD	regulatory domain
RNA	ribonucleic acid
RNAP	RNA polymerase
rpm	revolution per minute
RT	room temperature
SAP	shrimp alkaline phosphatase
SDS-PAGE	sodium dodecyl sulphate-polyacrylamide gel electrophoresis
sec	second
SIN	Standard I Nutrient broth medium
SLS	sodium lauroyl sarcosinate
TAE	tris-acetate-EDTA
TBE	tris-boric acid-EDTA
TEMED	N, N, N', N'-tetramethylethylene diamine
UV	ultraviolet
V	voltage
wHTH	winged helix-turn-helix

1. Introduction

1.1 Steroid Degradation in bacteria

Steroids are a class of terpenoid lipids characterized by a carbon skeleton of four fused rings: three cyclohexane rings (designated as rings A, B, and C) and one cyclopentane ring (the D ring) (Fig. 1-1). The steroids vary by the functional groups attached to this four ring core and by the oxidation state of the rings. Examples of steroids include the dietary fat cholesterol, the sex hormones estradiol and testosterone, and the anti-inflammatory drug dexamethasone. Hundreds of distinct steroids have been found in plants, animals, and fungi. All steroids are made in cells either from the sterol lanosterol (animals and fungi) or from cycloartenol (plants). Both lanosterol and cycloartenol are derived from the cyclization of the triterpene squalene.

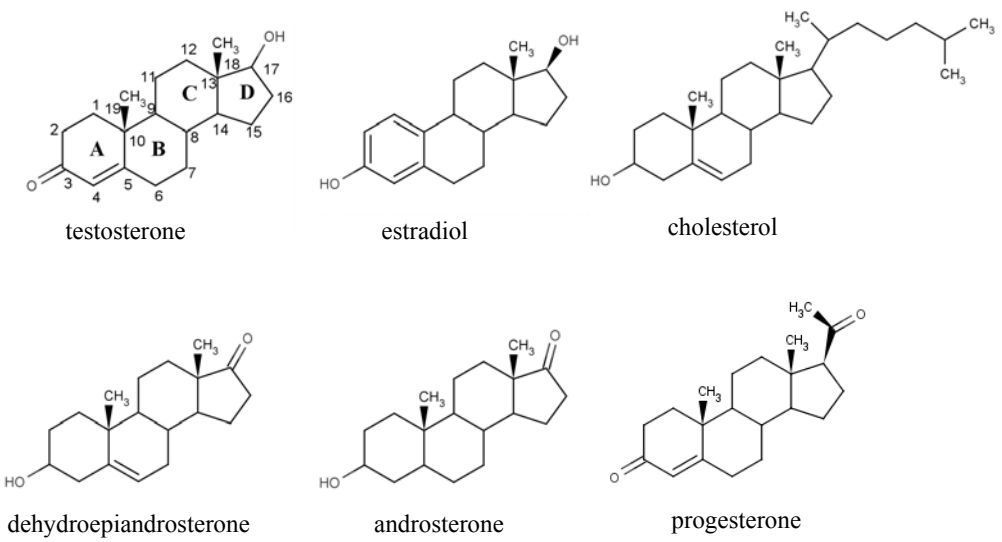

Fig. 1-1. Molecular formula of steroids. Steroids are formed by four fused rings (A to D), varying in the functional groups attached to the four fused rings.

The most important role of steroids in most organisms is as hormones. Steroids such as estradiol, excreted by humans and livestock, are frequently detected in the environment and are likely to cause endocrine-disrupting effects in aquatic wildlife (Sumpter and Johnson, 2005), therefore, concerns about negative ecological effects of steroid hormones have resulted in an increased interest with regard to the elimination of these compounds in soil,

sediments, and during wastewater treatment. As a potential means of producing bioactive steroids from natural and low-cost sterols, such as β-sitosterol and cholesterol, the bacterial catabolism of steroids also has attracted considerable attention (Kieslich, 1985).

Several species of bacteria, including *Nocardia restrictus*, *Comamonas testosteroni* (*C. testosteroni*) and *Rhodococcus erythropolis* SQ1 (*R. erythropolis* SQ1) are known for their ability to utilize testosterone, cholesterol and various other steroids as sole carbon and energy sources (van der Geize *et al*., 2000; van der Geize *et al*., 2001; van der Geize *et al*., 2002a; van der Geize *et al*., 2002b; Horinouchi *et al*., 2010). *C. testosteroni* is a Gram-negative bacterium that belongs to the beta group of Proteobacteria (Tamaoka *et al*., 1987). *Comamonas* strains have been isolated from soil, water and mud, but also from the gastrointestinal tract in humans (Barbaro *et al*., 1987; Garcia Valdes *et al*., 1988). These strictly aerobic, nonfermentative, chemoorganotrophic bacteria rarely attack sugars, but grow well on organic acids and amino acids (Balows *et al*., 1992). Moreover, *C. testosteroni* strains are able to use steroids as the sole carbon source and may be an attractive means for the removal of these stable compounds from the environment. *Rhodococcus* is a genus of mycolic-acid-containing actinomycetes that display a wide range of metabolic capabilities, degrading a variety of environmental pollutants and transforming or synthesizing compounds with possible useful applications (Warhurst *et al*., 1994; Bell *et al*., 1998; van der Geize *et al*., 2004). A well-known feature of *Rhodococci* is their ability to degrade a range of naturally occurring steroids, including cholesterol and phytosterols, e.g., β-sitosterol (van der Geize *et al*., 2004).

Over the past decades, new technological breakthroughs in genomics and transcriptomics facilitate the elucidation of steroid metabolism by these bacteria. With transcriptomics and gene deletion studies, van der Geize reported that the catabolism of cholesterol by *Rhodococcus sp*. strain RHA1 (van der Geize *et al*., 2007) is similar to that of testosterone and 4-androstene-3,17-dione (4-AD) by *C. testosteroni* TA441 (Horinouchi *et al*., 2001; Horinouchi *et al*., 2003a; Horinouchi *et al*., 2003b; Horinouchi *et al*., 2004a; Horinouchi *et al*., 2004b; Horinouchi *et al*., 2005; Horinouchi *et al*., 2010) and *R. erythropolis* SQ1 (van der

Geize *et al*., 2000; van der Geize *et al*., 2001; van der Geize *et al*., 2002a; van der Geize *et al*., 2002b; van der Geize *et al*., 2008). Studies in these species indicate that the steroid is transformed to 4-AD. The steps of this transformation are steroid-dependent (Fig. 1-2). For example, the branched alkyl sidechain of cholesterol is degraded via β-oxidation (van der Geize *et al*., 2007). Testosterone is converted to 4-AD via dehydrogenation of the 17β-hydroxy group catalyzed by 17β-hydroxysteroid dehydrogenase (17β-HSD) (Fig. 1-2). Two steps are needed for the conversion of androsterone to 4-AD, androsterone is first catalyzed by 3α-hydroxysteroid dehydrogenase/carbonyl reductase (3α-HSD/CR) to yield androstanedione (Talalay *et al*., 1952; Möbus *et al*., 1998; Maser *et al*., 2000), then 3-ketosteroid-Δ^4(5α)-dehydrogenase (TesI) is responsible for the conversion of androstanedione to 4-AD (Horinouchi *et al*., 2003a) (Fig. 1-2).

In bacteria, a ketone group at C-3 position and double bonds at Δ1 and Δ4 are responsible for steroid degradation via aromatization of the A-ring (Fig. 1-2). In *Rhodococcus sp.* RHA1, 3-ketosteroid-Δ1-dehydrogenase (KstD) (TesH in *C. testosteroni* TA441) is involved in the conversion of 4-AD to 1,4-androstene-3,17-dione (ADD). Following 9α-hydroxylation results in automatic cleavage of ring B and aromatization of ring A, yielding 3-hydroxy-9,10-secoandrosta-1,3,5(10)-triene-9,17-dione (3-HSA). 3-ketosteroid-9α-hydroxylase (KshAB) in *Rhodococcus sp.* RHA1 (ORF17 in *C. testosteroni* TA441) is involved in the above reaction. C-4 of 3-HSA is hydroxylated by hydroxylase HsaAB in *Rhodococcus sp.* RHA1 (TesA1A2 in *C. testosteroni* TA441), to yield 3,4-dihydroxy-9,10-secoandrosta-1,3,5(10)-triene-9,17-dione (3,4-DHSA), which is followed by cleavage between C-4 and C-5 by *meta*-cleavage enzyme (HsaC in *Rhodococcus sp.* RHA1 or TesB in *C. testosteroni* TA441), yielding 4,5-9,10-diseco-3-hydroxy-5,9,17-trioxoandrosta-1(10),2-diene-4-oic acid (4,9-DHSA). Following hydrolysis by a hydratase HsaD in *Rhodococcus sp.* RHA1 (TesD in *C. testosteroni* TA441), 4,9-DHSA is converted to 2-hydroxy-hexa-2,4-dienoate (2-HHD) and 9,17-dioxo-1,2,3,4,10,19-hexanorandrostan-5-oate (DOHNAA). 2-HHD is transformed to central metabolites by the successive actions of a hydratase (HsaE in *Rhodococcus sp.* RHA1 or TesE in *C. testosteroni* TA441), an aldolase (HsaF in *Rhodococcus sp.* RHA1 or TesG in *C. testosteroni* TA441), and a propionaldehyde dehydrogenase (HsaG in *Rhodococcus sp.* RHA1

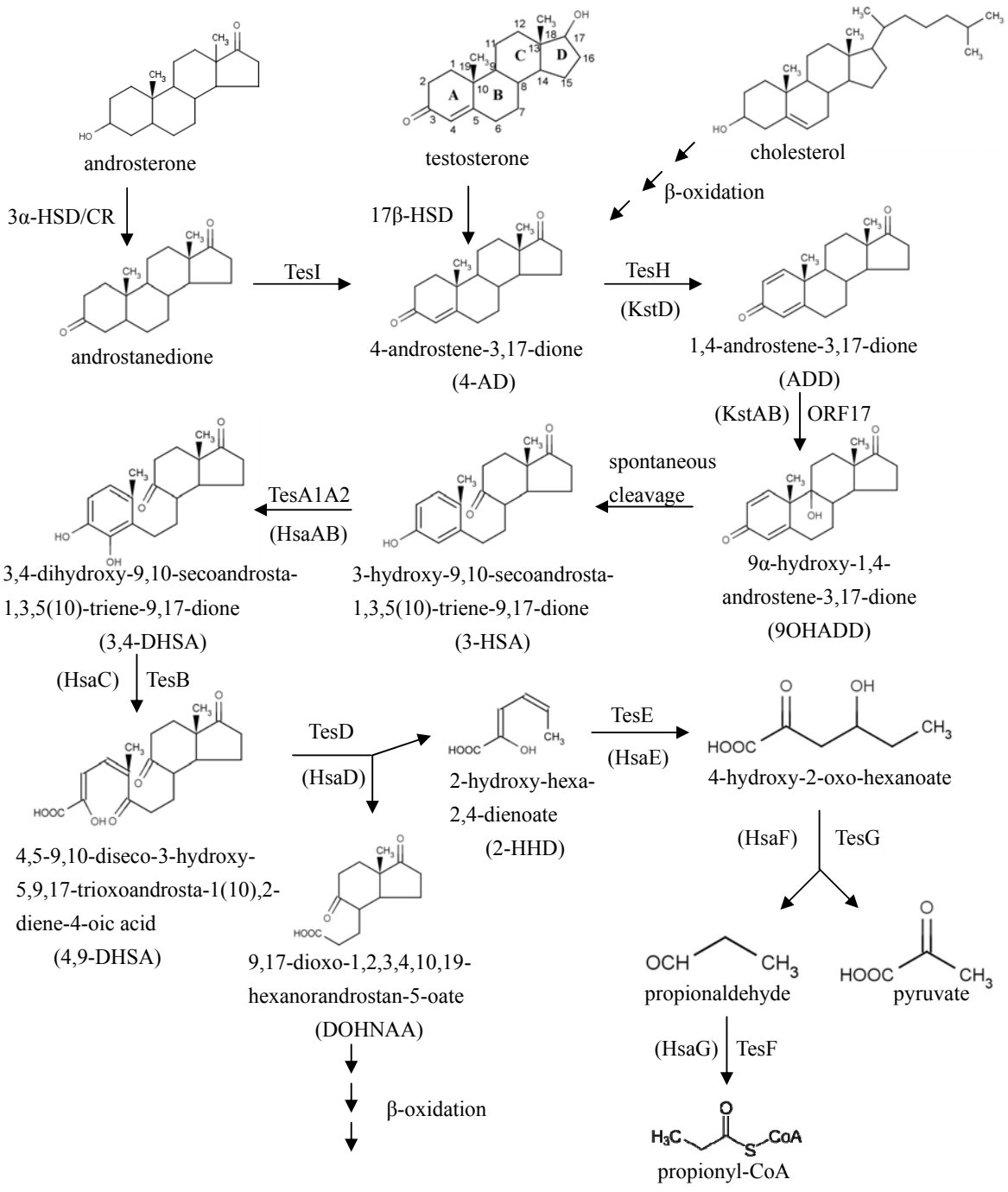

Fig. 1-2. Proposed steroid degradation pathway in *C. testosteroni* (Horinouchi *et al*., 2010; Möbus and Maser, 1998) and *Rhodococcus* sp. RHA1 (van der Geize *et al*., 2007). The catabolism of steroids in *C. testosteroni* is similar to that in *Rhodococcus* sp. RHA1. Catabolic enzymes indicated in brackets are originated from *Rhodococcus sp.* RHA1 (for details see text). The full names of enzymes are indicated in the text.

or TesF in *C. testosteroni* TA441). In *Rhodococcus equi*, the propionate moiety of DOHNAA is removed via β-oxidation (Miclo and Germain, 1992). Although many genes involved in steroid catabolism have been identified, many of the pathway enzymes are still poorly characterized, particularly those involved in degrading the bicycloalkanone originating from rings C and D. Detailed knowledge of steroid catabolism is essential for engineering strains for the biotransformation of sterols.

As presented above, most of the catabolic enzymes of cholesterol by *Rhodococcus sp.* RHA1 shared the same functions with that involved in testosterone degradation by *C. testosteroni* TA441 (van der Geize *et al*., 2007). Unexpectedly they also have sufficient sequence similarity to each other. For example, sequences of KstD, KshAB are 40-47% identical to those of orthologs in *C. testosteroni* TA441 that act sequentially to transform 4-AD to 3-HSA (van der Geize *et al*., 2007). Further degradation of 3-HSA by *Rhodococcus sp.* RHA1 was predicted to be specified by seven genes, annotated as *hsa*. The encoded proteins share significant amino acid sequence similarity (31-42%) with the *tes*-encoded enzymes of *C. testosteroni* TA441 that transform 3-HSA during growth on testosterone (Horinouchi *et al*., 2003a; Horinouchi *et al*., 2004b; van der Geize *et al*., 2007).

High throughout techniques, such as genomics and proteomics, facilitate the elucidation of the aerobic degradation of steroids via aromatization. Further characterization of these pathways will provide important insights for engineering strains for the biotransformation of sterols and may help characterize the global regulatory networks of steroid catabolism. Moreover, elucidation of the steroid catabolic pathways plays an important role in synthesizing steroid compounds in bacterial system.

1.2 3α-HSD/CR and Regulation of its Expression

The short-chain dehydrogenase/reductase (SDR) superfamily comprises a wide range of prokaryotic and eukaryotic enzymes involved in functions as diverse as the metabolism of steroids, sugars, aromatic hydrocarbons and prostaglandins, the fixation of nitrogen and the

synthesis of antibiotics (Persson *et al*., 1991; Jörnvall *et al*., 1995). The superfamily is made up of enzymes averaging 250-350 amino acids in length which function independently of metal cofactors, and its members are readily distinguishable from those of the medium-chain dehydrogenase/reductase (MDR) and long-chain alcohol dehydrogenase superfamilies (ADH) (Persson *et al*., 1991; Jörnvall *et al*., 1995). All SDR proteins share a residue identity of typically 15-30% in pairwise comparison (Kallberg *et al*., 2002), but with highly conserved specific sequence motifs as well as highly conserved folding patterns. Their general primary structure is composed of a cofactor-binding region at the N-terminal part, a catalytic active site and a substrate-binding region in the central part, and a C-terminal extension important for oligomerization. Analyses of the three-dimensional structure of the SDRs characterized so far shows that both NAD(H) and NADP(H) bind to the classical βαβ motif of the Rossmann fold which is a frequently occurring motif in nucleotide binding proteins, such as dehydrogenases. It depends on their predominant function as a dehydrogenase or reductase whether they use either NAD(H) or NADP(H) as cosubstrate (Duax *et al*., 2000).

As described above, *C. testosteroni* is able to use steroids as the sole carbon and energy source. Interestingly, the catabolic enzymes for steroid degradation are usually not constitutively expressed, but are induced by their respective steroid substrates (Marcus *et al*., 1956; Oppermann *et al*., 1996; Möbus *et al*., 1997). Hence, steroids play a particularly important role in certain prokaryotes, as they may simultaneously serve both as signal molecules and carbon source. 3α-hydroxysteroid dehydrogenase/carbonyl reductase, 3α-HSD/CR, which belongs to the SDR family, was characterized in *C. testosteroni* ATCC 11996 and has been identified as a steroid-inducible enzyme (Oppermann and Maser, 1996; Möbus and Maser, 1999). The 3α-HSD/CR primary structure shows two sequence motifs which are common to the members of the SDR family. These are the N-terminal Gly^{8}-*X*-*X*-*X*-Gly^{12}-*X*-Gly^{14} cofactor binding motif and the Tyr^{155}-*X*-*X*-*X*-Lys^{159} motif which is structurally located in the active site and forms together with the conserved Ser^{114} a catalytic triad (numbering according to the 3α-HSD/CR primary structure) (Möbus and Maser, 1998). Most SDR enzymes are either homodimers or homotetramers (Jörnvall *et al*., 1995), and the crystal structure of 3α-HSD/CR reveals one homodimer per asymmetric unit representing the

physiologically active unity (Grimm *et al*., 2000; Hoffmann *et al*., 2007).

Since the pioneering work of Talalay and co-workers (Marcus and Talalay, 1956; Talalay *et al*., 1952), it is well known that 3α-HSD/CR is one of the first enzymes of the steroid-catabolic pathway (Fig. 1-2) and therefore plays an important role in steroid metabolism. In previous investigations, 3α-HSD/CR has been identified to catalyze the oxidoreduction at position 3 of the steroid nucleus of a variety of C_{19-27} steroids, including androstanedione, 5α-dihydrotestosterone, androsterone, cholic acid, and the steroid antibiotic fusidic acid (Maser *et al*., 2000). This reaction is of significance in the initiation of the complete degradation of these relatively inert substrates. Surprisingly, this enzyme is also capable of catalyzing the carbonyl reduction of a variety of nonsteroidal xenobiotic aldehydes and ketones such as metyrapone, *p*-nitrobenzaldehyde and the insecticide NKI 42255 (Maser *et al*., 2000). It has been demonstrated that this substrate pluripotency not only enhances the metabolic capacity of insecticide degradation but also increases the resistance of *C. testosteroni* towards the steroid antibiotic fusidic acid (Oppermann *et al*., 1996).

3α-HSD/CR from *C. testosteroni* is one of the enzymes, whose expression is induced by steroids such as testosterone and progesterone (Talalay *et al*., 1952; Marcus and Talalay, 1956; Oppermann *et al*., 1993; Oppermann *et al*., 1996), and which causes interest in the mode of the molecular regulation of its gene (*hsdA*). In previous investigations, our group identified two genes involved in *hsdA* regulation and reported a “two repressor model” to control *hsdA* gene expression (Fig. 1-3). Repressor A (RepA) was found to be a transcriptional repressor for 3α-HSD/CR expression (Xiong and Maser, 2001; Xiong *et al*., 2003a). In the absence of inducing steroids, the RepA protein binds to operator sequences (Op1 and Op2) upstream of *hsdA* and a DNA loop structure is formed, therefore, it blocks *hsdA* transcription (Xiong *et al*., 2003b). In the presence of appropriate steroids, however, these bind to RepA, which is then released from the operator region. Upon dissociation of the repressor from the operator, RNA polymerase binds to the promoter, and transcription of *hsdA* is initiated. In addition, it has been demonstrated that the expression of 3α-HSD/CR is closely related to the distance between Op1 and Op2. Repressor B (RepB) turned out to be a translational repressor, which

can bind to the ribosomal binding site (RBS) of 3α-HSD/CR mRNA, thereby interfering with *hsdA* translation (Xiong *et al*., 2003a). In the presence of appropriate steroids, RepB is dissociated from the mRNA of 3α-HSD/CR and translation of 3α-HSD/CR initiates (Fig. 1-3). Hence, induction of *hsdA* expression by steroids in fact is a derepression of *hsdA* transcription and translation.

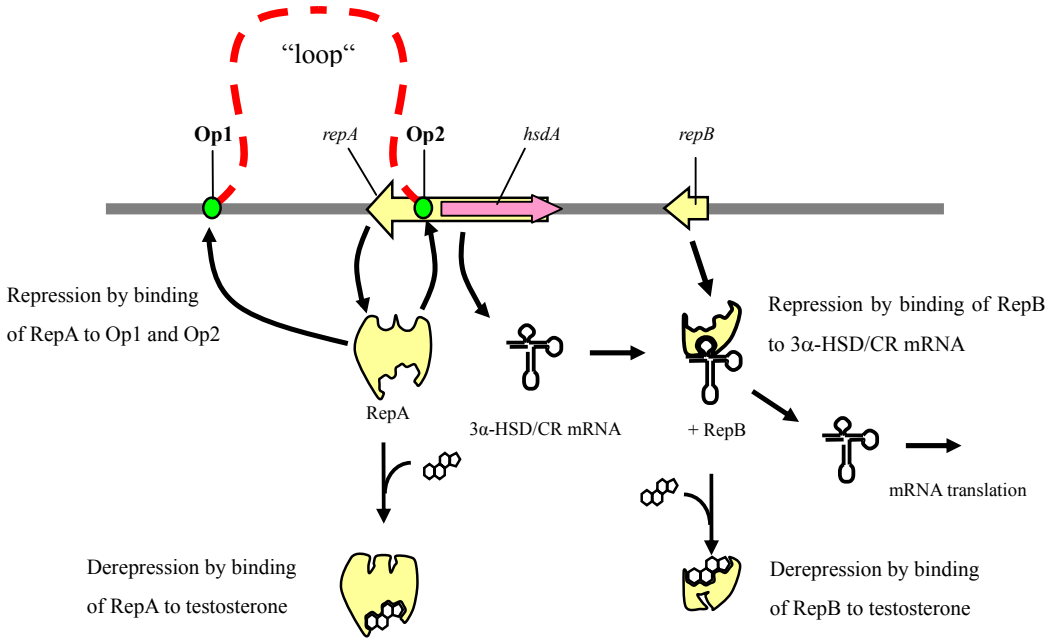

Fig. 1-3. A model on the transcriptional and translational regulation of *hsdA* in *C. testosteroni* (Xiong and Maser, 2001; Xiong *et al*., 2003a). In the absence of inducing steroids, RepA blocks transcription of *hsdA* and RepB blocks translation of the 3α-HSD/CR mRNA. In the presence of appropriate steroids, however, these bind to both negative regulators, leading to a dissociation of RepA from the operater region and to a release of RepB from the 3α-HSD/CR mRNA. Hence, induction of *hsdA* expression by steroids in fact is a derepression of *hsdA* transcription and translation.

Recently, the activator gene *teiR* (testosterone inducible regulator) for induced *hsdA* gene expression has been found 55.135 kb upstream of the *hsdA* gene and shown to have the same transcriptional direction as the *hsdA* gene. TeiR was cloned and characterized to be an important sensor protein for steroid chemotaxis and steroid degradation in *C. testosteroni* (Göhler *et al*., 2008). Moreover, as a signaling mechanism in the steroid transduction chain in *C. testosteroni* cells, a histidine kinase mechanism has been proposed (Göhler *et al*., 2008).

1.3 LysR-type Transcriptional Regulator Family

The LysR-type transcriptional regulator (LTTR) family, formally documented by Henikoff *et al*. (Henikoff *et al*., 1988), is a well-characterized group of transcriptional regulators. They are highly conserved and ubiquitous amongst bacteria, with functional orthologues identified in archaea and eukaryotic organisms (Pérez-Rueda and Collado-Vides, 2001; Sun and Klein, 2004; Stec *et al*., 2006). Currently it comprises the largest known family of prokaryotic DNA-binding proteins, more than 3,800 proteins have been found to be members of this family and the number is rising steadily (Henikoff *et al*., 1988; Pareja *et al*., 2006). The genes controlled by LTTRs have a diversity of functions, including the synthesis of virulence factors, CO_2- and N_2-fixation, antibiotic resistance, cell division, quorum sensing, oxidative stress responses, degradation of aromatic compounds and the biosynthesis of amino acids, and so on (Schell, 1993; Deghmane *et al*., 2000; Deghmane *et al*., 2002; Cao *et al*., 2001; Gerischer, 2002; Kim *et al*., 2004; Russell *et al*., 2004; Tropel and van der Meer, 2004; Byrne *et al*., 2007; Lu *et al*., 2007; Sperandio *et al*., 2007; Maddocks and Oyston, 2008). Proteins belonging to LTTRs typically activate promoters transcribed divergently from their own genes in response to small inducer molecules, and extensive researches revealed that target gene or operon genes regulated by LTTRs can also be located elsewhere on the bacterial chromosome (Heroven and Dersch, 2006; Hernández-Lucas *et al*., 2008). In addition, most LTTRs repress their own synthesis (Henikoff *et al*., 1988; Schell, 1993).

1.3.1 Structure and Function of LTTRs

1.3.1.1 Highly Conserved N-terminal DNA Binding Domain

Studies of amino acid composition and secondary structure have helped to identify many LTTRs. LysR-type regulators are similar in size (300-350 residues) and contain a predicted helix-turn-helix (HTH) motif (Suzuki and Brenner, 1995) between 20-80 residues at the N terminus (Fig. 1-4). The typical HTH motif comprises a three-helical bundle with an open conformation. The second and third helices of the bundle interact with DNA, the third being inserted into the major groove of the DNA double helix (Brennan and Matthews, 1989; Huffman and Brennan, 2002; Aravind *et al*., 2005). The HTH motif in LysR-type family

members, however, has evolved to be the winged helix variety (wHTH), which possesses two β-strands between the third helix and the linker helix hinge (LH) (Sainsbury *et al*., 2009; Monferrer *et al*., 2010). This region containing wHTH shows the highest degree of amino acid sequence similarity among family members and is believed to participate in DNA-binding according to mutational studies performed on several LTTRs, such as NahR (Schell *et al*., 1990), OxyR (Kullik *et al*., 1995), GcvA (Jourdan and Stauffer, 1998), CysB (Lochowska *et al*., 2001) and CrgA (Deghmane and Taha, 2003). In addition, mutational analyses indicated that residues 27-29 of CysB, lying in the turn region between the α2 and α3 helices, comprise an 'activating region' (AR) that is crucial for positive control of the *cysP* promoter, but not for DNA binding and inducer response activities of CysB (Lochowska *et al*., 2004).

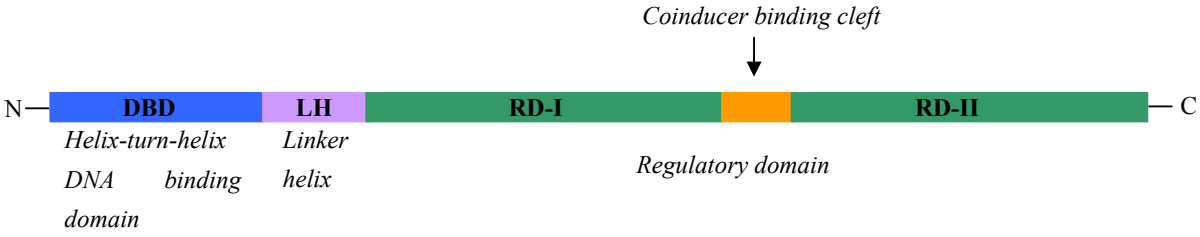

Fig. 1-4. Schematic representation of domain structures of LTTRs. LysR-type regulators have a highly conserved N-terminal helix-turn-helix DNA binding domain, joined by Linker helix to the C-terminal regulatory domain, which can respond to coinducer molecules (Schell, 1993; Muraoka *et al*., 2003).

1.3.1.2 Less Conserved C-terminal Coinducer Binding Domain

The winged HTH joined by LH, involved in oligomerization, to a C-terminal regulatory domain as depicted in Fig. 1-4 (Schell, 1993; Muraoka *et al*., 2003), which is relatively less conserved at the amino acid level. The regulatory domains of LTTRs share a similar fold with periplasmic substrate-binding proteins (Tyrrell *et al*., 1997) and constitute two distinct α/β subdomains (RDI and RDII) which are connected by two cross-over regions that form a hinge or cleft, which is likely to accommodate the coinducer (Stec *et al*., 2006). In addition to respond to effector molecules, the regulatory domains can also respond directly to redox-active compounds through the thiol groups of cysteine residues (Kullik *et al*., 1995; Choi *et al*., 2001). Mutational studies have identified two regions located between residues 95 to 173 and residues 196 to 206 that are involved in inducer recognition and response (Schell, 1993;

Lochowska *et al*., 2001).

Low-molecular-weight coinducers are required for LTTRs in the positive control of transcription, although most family members bind their target promoters irrespective of the presence of the coinducers. Mutational studies of regulators NodD, CysB, AmpR and OxyR established that the residues 95, 123, 154 (NodD); 149, 165 (CysB); 102, 135 (AmpR) and 234 (OxyR) were involved in coinducer recognition and response; mutations in these regions led to a coinducer-independent phenotype in each case (Burn *et al*., 1989; Mclver *et al*., 1989; Storz *et al*., 1990; Bartowsky and Normark, 1991; Renna *et al*., 1993; Colyer and Kredich, 1994; Colyer and Kredich, 1996). CatM and BenM which are paralogous LTTRs from *Acinetobacter baylyi* ADP1 respond to a metabolite formed during benzoate consumption, *cis,cis*-muconate. However, unlike CatM, BenM also responds to benzoate as an effector (Ezezika *et al*., 2006). The co-factor binding domain in both regulators has been well defined. Structural studies identified the binding site for coinducer lying between RDI and RDII of both regulators, which is the same case as that of CysB, Cbl and TsaR (Lochowska *et al*., 2001; Stec *et al*., 2006; Monferrer *et al*., 2010). RDI and RDII were shown to be connected by two hinge-like, antiparallel β-strands which provide flexibility to the protein, enabling the two domains to rotate relatively to each other. BenM has a unique feature compared to other LTTRs in that it can bind to two different coinducers. Benzoate binds a second region in BenM that is not present in CatM. The secondary site is located in a highly hydrophobic region of RDI and alters the conformation of BenM once the coinducer is bound. The altered conformation still enables *cis,cis*-muconate to bind at the primary binding site and produces a synergistic effect resulting in very high levels of transcriptional regulation. It is thought that occupation of the secondary site alters the salt bridges formed between glutamate residues and arginine residues within the primary binding site, producing an altered protein conformation but not affecting the capacity to bind *cis,cis*-muconate (Ezezika *et al*., 2007).

1.3.1.3 LTTRs Act as Homotetramer or Homooctamer

Extensive studies have demonstrated that LTTRs often act as a tetramer to perform their function. ClcR and CatR have been identified as dimers in solution, but two dimers are

needed to bind on target DNA (Parsek *et al*., 1992; Coco *et al*., 1994; McFall *et al*., 1997a). CatM, BenM, TsaR, and CbnR were found to form tetramers (Bundy *et al*., 2002; Clark *et al*. 2002; Muraoka *et al*., 2003; Monferrer *et al*., 2010). Until now, there are few LTTRs that their crystal structures have been resolved, structures of CatM, BenM, CysB, and Cbl were resolved only on the regulatory regions, largely because the HTH domain being particularly difficult to crystallize due to the high degree of flexibility found in the 'wing' region.

Despite the abundance of LTTRs, only three full-length structures have been reported, those of CbnR, CrgA and TsaR (Muraoka *et al*., 2003; Sainsbury *et al*., 2009; Monferrer *et al*., 2010). CbnR from *Ralstonia eutropha* NH9, which regulates an operon involved in the degradation of chlorocatechols, was the first crystallized LysR-type regulator (Muraoka *et al*., 2003). CbnR was found to form a homotetramer, which seems to be a biologically active form. The tetramer can be regarded as a dimer of dimers, whereby each dimer is composed of two subunits in different conformations. In the CbnR tetramer, the DNA-binding domains are located at the V-shaped bottom of the main body of the tetramer, and seem to be suitable to interact with a long stretch of the promoter DNA, which is approximately 60 bp. The four DNA-binding domains have no interactions with each other, whereas the main body of the tetramer is composed of four intertwined regulatory domains (residues 88 to 294 of each subunit) (Muraoka *et al*., 2003).

Recently, the crystal structure of the contact-regulated gene A (CrgA), an LTTR from *Neisseria meningitides* (*N. meningitides*) which has been implicated in host-pathogen interactions, has been resolved (Sainsbury *et al*., 2009). CrgA was initially identified as being induced upon contact of *N. meningitidis* with human epithelial cells (Deghmane *et al*., 2000) and appears to be part of a group of genes that are co-ordinately upregulated during initial adhesion (Morelle *et al*., 2003). CrgA is an autorepressor and activates the expression of the divergently orientated gene, modulator of drug activity gene (*mdaB*), a putative quinone NADPH oxidoreductase, suggesting that it may be involved in the response of *Neisseria* to oxidative stress (Ieva *et al*., 2005; Hong *et al*., 2008). The crystal structure indicated that CrgA exists as an octameric assembly state, and it's the first of a novel subclass of LTTRs

that form octameric rings (Sainsbury *et al*., 2009). CrgA assembles into square-like hollow octameric rings with dimensions of 125 × 125 × 67Å. The regulatory domains are sandwiched between the DBDs that are located in pairs (DBD pairs) at the four corners of the disc. Each subunit forms an N-term interface with one adjacent subunit, principally through their equivalent N-terminal domains (residues 1-89) and to a second subunit, through their regulatory domains (RD interface) (Sainsbury *et al*., 2009).

The crystal structure of TsaR, which is from *C. testosteroni* T-2 and regulates the expression of *tsaMBCD* involved in the degradation of *para*-toluenesulfonate (TSA), showed that the tetramer is formed by two dimers according to a twofold axis (Monferrer *et al*., 2010). The tetramer arises through association of the alternate C-terminal subdomains (RDI to RDII and vice versa) of an extended and a compact promoter belonging to opposed dimers. The tetramer has a squared, rather flat shape with approximate dimensions of 100 Å x 80 Å x 50 Å. It presents a central cavity with a funnel shape, wider on one side of the tetramer (45 Å x 20 Å), and much narrower on the opposite side (12 Å x 9 Å). Structure of full-length TsaR reveals an open conformation of the tetrameric LTTR fold, whereas CbnR presents additional contacts in opposing C-terminal domains that close the ring (Monferrer *et al*., 2010).

1.3.2 Mechanisms of Transcriptional Regulation of LTTRs

LTTRs are dual function regulators acting as both autorepressors and activators of target promoters, frequently of genes co-located with the LTTRs in the chromosome. However, subgroups of LTTRs are now also known to catalyze positive autoregulation, or act as transcriptional repressors of other target genes (Maddocks and Oyston, 2008). As described above, most LTTRs are known to be functionally active as tetramers, as such there are multiple binding sites on the DNA of the target promoter region. DNase I footprinting studies suggest a common regulatory mechanism for many LTTR members in which in the absence of inducer, a high affinity repressor binding site (RBS), located at -80 to -50 relative to the transcriptional start site of the target gene, is necessary and sufficient for both activation and autorepression. RBS was characterized by the presence of an imperfect dyad symmetry within the consensus sequence T-N_{11}-A, which is referred to as ‘LTTR box’ (Schell, 1993).

An activation binding site (ABS), located near the -35 regulatory region of the target gene, is essential for inducing target gene expression via interaction with RNA polymerase. Generally the T-N_{11}-A motif is not present in the ABS region. In addition, three binding sites including RBS and ABS have been described in a number of LTTRs such as BenM, CatM, CysB and TsaR (Lochowska *et al*., 2001; Ezezika *et al*., 2006; Monferrer *et al*., 2010).

The studies of several LTTRs have indicated that they can cause DNA to bend between 50º and 100º and that the degree of DNA bending is determined by the presence or absence of the coinducer. A conformational change upon ligand binding causes some LTTRs to move a variable number of base pairs from a more proximal ABS site to a more distal ABS site (ABS'), usually accompanied by a relaxation of the DNA bending angle. This is the basis of the so-called 'sliding dimer' hypothesis of LTTR activation (Fig. 1-5). LysR-type regulator ClcR, which is required for the induction of the *clcABD* operon involved in 3-chlorocatechol degradation in *Pseudomonas putida*, binds the *clcA* promoter irrespective of the presence of inducer. The DNase I protection pattern of ClcR with or without inducer has been determined (Coco *et al*., 1994; Parsek *et al*., 1994; McFall *et al*., 1997a; McFall *et al*., 1997b). In the absence of inducer 2-chloromuconate, two regions of the *clcA* promoter were protected by ClcR from -79 to -53 (RBS) and -37 to -28 (ABS) relative to the *clcA* transcriptional start site, with two areas of hypersensitivity at region -52/-51 and region -42. In the presence of inducer 2-chloromuconate, the hypersensitive band at -42 disappeared and occupation of the ABS shifted from -37 to -41 (McFall *et al*., 1997a). Circular permutation gel shift assays showed that ClcR bends the *clcA* promoter without inducer 2-chloromuconate to an estimated angle of 71º, the bending angle was relaxed to approximate 55º when 2-chloromuconate was added. The 'sliding dimer' hypothesis is also confirmed in other LysR-type regulators, such as CatM, BenM, AtzR, CysB, TsaR and so on (Lochowska *et al*., 2004; Ezezika *et al*., 2006; Porrúa *et al*., 2007; Monferrer *et al*., 2010).

Circular permutation analyses indicated that AtzR bends DNA upon binding to the *atzR-atzDEF* promoter region (Porrúa *et al*., 2007). The minimal relative mobility was estimated for a fragment centred at position -45 relative to the *atzDEF* transcriptional start site,

suggesting that this position is the bending centre of the AtzR binding site. The bending angle was estimated to be 71º. Both the location of the bending centre and the bending angle are similar to those obtained with other LTTRs (Wang *et al*., 1992; McFall *et al*., 1997b). In the presence of inducer cyanuric acid, the bending angle was decreased to 49º, and the bending centre was shifted 3-8 bp away from the *atzDEF* promoter. This result indicates that cyanuric acid sensing by AtzR provokes a relaxation of the AtzR-induced bend upstream from the *atzDEF* promoter. Taken together, DNA bending is the common mechanism of transcriptional activation for LysR-type regulators, which is dependent on the tetrameric nature of these transcriptional regulators.

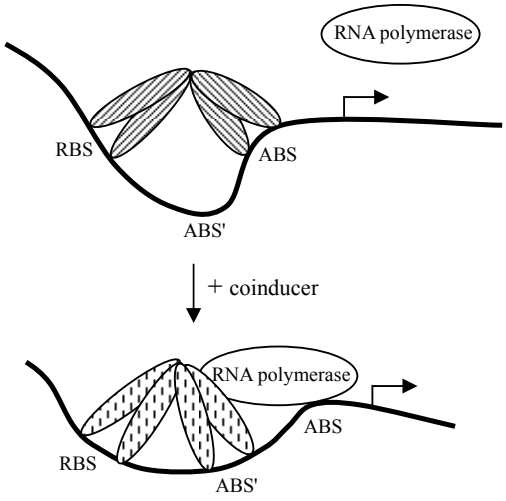

Fig. 1-5. Model of transcriptional regulation of LTTRs (McFall *et al*., 1997a; Ezezika *et al*., 2006; Porrúa *et al*., 2007; Monferrer *et al*., 2010). In the absence of coinducer, tetrameric LysR-type regulator binds to RBS and ABS sites and causes DNA bending; a conformational change of regulator upon coinducer binding causes regulator to move a variable number of base pairs from a more proximal ABS site to a more distal ABS site (ABS'), usually accompanied by a relaxation of the DNA bending angle, then regulator recruits RNA polymerase at the promoter region and promotes transcription of target gene or operon.

Although transcriptional activation of genes by LTTRs was extensively studied, less has been undertaken to elucidate the autoregulatory function. The RBS motif of genes divergently transcribed from their LTTR has been implicated as a possible autoregulatory site. Integrity of the RBS motif in the *atzR-atzDEF* intergenic region is not only required for high-affinity AtzR binding to activate the P*atzDEF* promoter, but also essential for the autorepression of

AtzR expression (Porrúa *et al*., 2007). Involvement of the ABS site in autorepression of AtzR was first reported by Porrúa *et al*. (Porrúa *et al*., 2007), that is, partial deletion of the ABS region prevents autorepression of *atzR*, despite the presence of an intact RBS overlapping the P*atzR* promoter. The affinity of purified AtzR binding to the ABS deleted probe moderately decreased relative to the wild type fragment, and the cyanuric acid-induced increase in complex mobility was less apparent in the ABS deleted probe than in the wild type probe. These led the author to propose that the lack of additional AtzR recognition sequences in this region may preclude high-affinity binding at the RBS, which may in turn prevent AtzR from competing with RNA polymerase for their overlapping binding sites (Porrúa *et al*., 2007).

Aim of the study

3α-HSD/CR from *C. testosteroni* is one of the first enzymes of the steroid-catabolic pathway. Interestingly, it can be induced by the steroids testosterone, progesterone, and cholic acid. The mechanism of 3α-HSD/CR induction by steroids has for long attracted the interest of our group. Previous investigations proposed a "two repressor model" for 3α-HSD/CR expression. Repressors RepA and RepB can inhibit the 3α-HSD/CR expression at the transcriptional and translational levels, respectively. In the presence of appropriate steroids, RepA and RepB can be released from the *hsdA* promoter or 3α-HSD/CR mRNA, respectively, therefore, 3α-HSD/CR expression increased.

On the chromosomal DNA of *C. testosteroni*, a novel transcriptional regulator gene, *hsdR*, was found to locate downstream of the *hsdA* gene. Sequence analyses revealed that HsdR is a member of the LysR-type transcription regulator family. In addition, a novel short-chain dehydrogenase/reductase gene, *SDRx*, was found to be divergently transcribed from the *hsdR* gene. In this study, we try to understand the following questions:

The first goal is to test if HsdR is involved in the regulation of 3α-HSD/CR expression and to elucidate the mechanism of its action.

The second is to find out if HsdR negatively regulates its own expression and to determine the active form of HsdR.

The third is to understand the function of SDRx in steroid degradation by *C. testoteroni* before determining the relationship between HsdR and SDRx, because LysR-type regulators generally regulate the expression of their divergently transcribed gene or operon.

2. Materials and Methods

2.1 Bacterial Strains, Media and Growth Conditions

For molecular cloning and gene expression, host strains *E. coli* HB101, *E. coli* BL21(DE3)pLysS and *C. testosteroni* ATCC 11996 were used, and the detailed information of these strains and related mutant strains is shown in Table 2-1.

Table 2-1 Bacterial strains used in this study

strain	relevant genotype	origin/reference
E. coli HB101	F^- mcrB mrr hsdS20($r_B^-m_B^-$) recA13 LeuB6 ara-14 proA2 lacY1 galK2 xyl5 mtl-1 rpsL20(Sm^R) glnV44 λ^-	Promega (Mannheim, Deutschland)
E. coli BL21(DE3)pLysS	F^- ompT gal dcm lon $hsdS_B(r_B^-m_B^-)$ λ(DE3) pLysS(cm^R)	Promega (Mannheim, Deutschland)
C. testosteroni ATCC 11996	strain ATCC 11996	ATCC/DSMZ*
CT-HsdR-Ko	*C. testosteroni* ATCC 11996 *hsdR*::pTOPOHsdR3-1	this study
C.T.HsdRGFP2	*C. testosteroni* ATCC 11996 *hsdR*::pTOPOHsdRGFP	this study
C.T.SDR-6	*C. testosteroni* ATCC 11996 *SDRx*::pTOPOSDR_{425}	this study

*ATCC: American Type Culture Collection; DSMZ: Deutsche Sammlung von Mikroorganismen und Zellkulturen.

Bacterial cells were grown in Standard I Nutrient broth medium (SIN) obtained from Merck (25 g/liter, containing 15.0 g of peptones, 3.0 g of yeast extract, 6.0 g of sodium chloride and 1.0 g of D (+) glucose), and incubated at 37 °C (*E. coli*) or 27 °C (*C. testosteroni*) in a shaker at 180 rpm. Growth media contained 100 μg/ml ampicillin and/or 30 μg/ml kanamycin if necessary.

2.2 Oligonucleotides

Table 2-2 Oligonucleotides used in this study

oligonucleotide	sequence (5'→3')	gene	modification
pHsdR-F	CATATGGATTTCAATGCGC	*hsdR*	*Nde*I
pHsdR-R	GGATCCAAGAGCGGTCATGC	*hsdR*	*Bam*HI
pHsdR-Ko-F	CTGCCGCCAGCGGGC	*hsdR*	
pHsdR-Ko-R	CAGTGCATGGGCTGC	*hsdR*	
pHsdRΔN-F	CATATGAGCGGGCTGCGAGGCA	*hsdR*	*Nde*I
pHsdRΔN-R	GGATCCAAGAGCGGTCCATGC	*hsdR*	*Bam*HI
pHsdRΔC-F	CATATGGATTTCAATGCGC	*hsdR*	*Nde*I
pHsdRΔC-R	GGATCCACACCAGGGCGCAGTGC	*hsdR*	*Bam*HI
pHsdR-L	GCTCTAGAATGGATTTCAATGCG	*hsdR*	
pHsdGFP-M	TCCTTTGCTAGCCATAGAGCG GTCCAT	*hsdR*	
pGFP-L	ATGGCTAGCAAAGGAG	*gfp*	
pGFP-R	TTATTTGTAGAGCTC	*gfp*	
pSDR-L	CATATGCAAGCATCTGCAC	*SDRx*	*Nde*I
pSDR-R	GGATCCAGAGCATCATGCCAC	*SDRx*	*Bam*HI
pSDR-Ko-F	CAGCAAGAGCTTTGTC	*SDRx*	
pSDR-Ko-R	TGAGCTGTGCGTTGTC	*SDRx*	
p7-1	AGGGGAATTACATCGTCCG TTTGCATGTAGCC	*hsdA* promoter	
pCla	CCGCATCGCGTATATCG	*hsdA* promoter	
pHsdR-SDR-L1	CGGGATCCGAGAGCTCGGCAACG	*hsdR-SDRx* intergenic region	*Bam*HI
pHsdR-SDR-R1	GGAATTCGGCTTGCGCCGGTGA	*hsdR-SDRx* intergenic region	*Eco*RI

2.3 Plasmids

Table 2-3 Plasmids used in this study

plasmid	phenotype	reference
pCR2.1-TOPO	TA cloning vector. Ap^r Km^r	Invitrogen
pUC18	multicopy-cloning vector. Ap^r	Invitrogen
pK18	multicopy-cloning vector. Km^r	Invitrogen
pET15b	expression vector for purification of proteins by nickel affinity chromatography. Ap^r	Novagen
p6	5.257-kb *Eco*RI fragment containing *hsdA* and its regulatory elements cloned into pUC18. Ap^r	Xiong and Maser, 2001
pAX1	*Avr*II-*Eco*RI fragment containing *hsdA* and its promoter cloned into pUC18. Ap^r	Xiong and Maser, 2001
pDel13n	deletion of the first 13 nucleotides in pAX1. Ap^r	Xiong *et al*., unpublished
P67	deletion of the *Mlu*I-*Avr*II fragment in p6, and 67 bp between Op1 and Op2. Ap^r	Xiong *et al*., 2003b
P67-3	deletion of the *Mlu*I-*Avr*II fragment in p6, and 64 bp between Op1 and Op2. Ap^r	Xiong *et al*., 2003b
P67-5	deletion of the *Mlu*I-*Avr*II fragment in p6, and 62 bp between Op1 and Op2. Ap^r	Xiong *et al*., 2003b
P67-7	deletion of the *Mlu*I-*Avr*II fragment in p6, and 60 bp between Op1 and Op2. Ap^r	Xiong *et al*., 2003b
pTOPOHsdR	*hsdR* cloned into pCR2.1-TOPO. Ap^r Km^r	this study
pKHsdR3	*hsdR* expressed from the *lac* promoter in pK18. Km^r	this study
pKtacHsdR1	*hsdR* expressed from the *tac* promoter in pKtac18. Km^r	this study
pET-HsdR2	pET15b plasmid overexpressing HsdR-His_6. Ap^r	this study
pTOPOHsdR3-1	fragment of *hsdR* between 251 bp and 650 bp cloned into pCR2.1-TOPO. Ap^r Km^r	this study
pTOPOHsdRGFP	*hsdR-gfp* transcriptional fusion in pCR2.1-TOPO. Ap^r Km^r	this study
pKHsdRΔN	fragment of *hsdR* between 259 bp and 912 bp cloned into pK18. Km^r	this study
pKHsdRΔC	fragment of *hsdR* between 1 bp and 660 bp cloned into pK18. Km^r	this study
pKHsdRΔNC	fragment of *hsdR* between 259 bp and 660 bp cloned into pK18. Km^r	this study
pET-HsdRΔN	pET15b plasmid overexpressing HsdRΔN-His_6. Ap^r	this study
pET-HsdRΔC	pET15b plasmid overexpressing HsdRΔC-His_6. Ap^r	this study
pET-HsdRΔNC	pET15b plasmid overexpressing HsdRΔNC-His_6. Ap^r	this study
pTOPOSDRx	*SDRx* cloned into pCR2.1-TOPO. Ap^r Km^r	this study
pET-SDRx	pET15b plasmid overexpressing SDRx-His_6. Ap^r	this study
$pTOPOSDR_{425}$	fragment of *SDRx* between 201 bp and 625 bp cloned into pCR2.1-TOPO. Ap^r Km^r	this study

* Km^r, kanamycin resistant; Ap^r, ampicillin resistant.

2.4 Instruments

PCR-cycler Mastercycler gradient and ThermoStat plus were purchased from Eppendorf. UV-transilluminator THERMAL IMAGING System FTI-500 and RNA/DNA calculator GeneQuant II were obtained from Pharmacia Biotech. Pharmacia ÄKTA protein purifier system was from Amersham Biosciences. SDS-PAGE electrophoresis apparatus was from Roth. Spectrophotometer UV Uvicon 810 was from Kontron. Incubator Hood TH 15 was from Edmund Bühler GmbH. Digital-pH-METER 646 was from Knick. Microplate Reader, POWER/PAC 300, and *E. coli* Pulser were from BIO-RAD. Vortex GENE 2 Digital was from Scientific Industries. EL_X50 Auto Strip Washer was from Bio-TEK Instruments. Centrifuge Biofuge *pico* was from Heraeus. Haake N3 Wasserbad B Fisons was from HAAKE. HPLC apparatus comprising Waters 2487 Dual λ absorbance Detector, Waters 717 plus Autosampler, and Waters 515 HPLC pump was obtained from Waters.

2.5 Chemicals

40% acrylamide: bisacrylamide solution (molar ratio of bisacrylamide:acrylamide is 1:37.5), EDTA, ethanol, phenol, chloroform, acetic acid, sodium dodecyl sulfate, di-sodium hydrogenphosphate, sodium dihydrogenphosphate, potassium chloride, Tween 20, urea, and hydrochloric acid were abtained from Roth. Glycerol, isopropanol, calcium chloride, boric acid, Standard I Nutrient Broth medium (SIN), and methanol were purchased from Merck (Darmstadt). Agrose, testosterone, estradiol, TEMED, dimethyl pimelimidate dihydrochloride and ethidium bromide were supplied by Sigma (Deisenhofen). Bovine serum albumin (BSA) was from Boehringer (Mammheim). Tris base, glycine, sodium hydroxide, sodium chloride were from Promega. Dithiothreitol (DTT) was from BIOMOL. 1 kb DNA ladder and dNTPs were from Fermentas. Ampicillin and agar were from AppliChem. Kanamycin was from CALBIOCHEM. Low melting point agarose was from Invitrogen. Sodium lauroyl sarcosinate and bromophenol blue were from Fluka (Neu-Ulm). Ammonium persulfate was from SERVA (Heidelberg).

2.6 Restriction Enzymes and Kits

Restriction enzymes and Vent DNA polymerase were from New England Biolabs. Shrimp alkaline phosphatase was from Usb. T4 DNA ligase and Taq DNA polymerase were from Fermentas. RNAse A was from Boehringer (Mammheim). TOPO TA cloning kit was from Invitrogen. QIAGEN Plasmid Midi Kit and Ni-NTA Spin Kit were from QIAGEN. DIG DNA labeling and Detection Kit was from Roth.

2.7 Amplification, Detection and Cloning of DNA

2.7.1 PCR

The amplification of specific DNA fragments is facilitated by polymerase chain reaction (PCR). Oligonucleotides that served as specific primers to amplify the DNA of interest are listed in Table 2-2. The reaction was done in a total volume of 20 µl containing 10 ng of template DNA, 1 µl of forward primer (100 pM), 1 µl of reverse primer (100 pM), 1 µl of dNTPs (100 mM), 10 µl of $MgCl_2$ (25 mM), 5 µl of 10x PCR buffer and H_2O (adding to 50 µl). The PCR program was shown as following: 2 min at 95 °C for pre-denaturation; 25 thermal cycles involving denaturation at 95 °C for 30 sec, annealing at 45 °C for 30 sec, extension at 72 °C for 30 sec; final extension at 72 °C for 10 min and storage at 4 °C. The PCR product was then analyzed by agarose gel electrophoresis.

2.7.2 Agarose Gel Electrophoresis

Agarose gel electrophoresis is commonly used to separate DNA fragments of more than 50 bp in size based on the size of the fragments, that is, longer fragments move more slowly in the gel than smaller fragments. For proper separation of fragments with different lengths, 0.8%-2% of agarose in 1x TAE buffer (40 mM Tris-acetate and 1 mM EDTA) was used. Before loading onto the gel, the DNA samples were mixed with 1 µl of 10x loading buffer (0.25% bromophenol blue, 1% SDS, and 50% glycerol). The gel electrophoresis was run at 100 mA and 1x TAE buffer was used as running buffer. After running for 30 min, the gel was transferred to the staining solution containing 10 µg/ml ethidium bromide, which can incorporate into the DNA and enables detection of the loaded DNA. Following staining for 5 min, washing the gel with water for another 5 min, subsequently the gel was documented

with UV light in a UV-transilluminator and the picture was printed out.

2.7.3 Estimation of DNA Concentration

To facilitate the molecular cloning and other experiments, DNA should be quantified by using a spectrophotometer which is based on the maximum absorption of DNA at the wavelength of λ = 260 nm. From the absorption (optical density=OD), the nucleic acid concentration can be calculated in µg/ml using a quartz cuvette with a thickness of 1 cm considering the following parameters:

$$\text{double stranded DNA (µg/ml)} = OD_{260} \times 50 \times \text{dilution factor}$$

For spectrophotometric estimation of DNA concentration, 15 µl of DNA diluted in 1:10 was added to the quartz cuvette with a thickness of 1 cm, and each sample was independently measured at least 3 times. For blank value determination, water or buffer was used dependent on the DNA-dilution reagent.

2.7.4 Digestion of DNA with Restriction Endonucleases

Restriction endonuclease digestion was performed with the enzymes and buffers from New England Biolabs according to the instruction given in the manuals. Reactions were generally performed in a total volume of 20 µl. Double digestions were done with suitable buffer which is compatible with both the chosen enzymes. All digestions were performed at 37 °C for 1 h.

To prevent the linearized vector from religation in the subsequent ligation reactions, the 5' end of the vector DNA was dephosphorylated. The DNA to be dephosphorylated was subjected to shrimp alkaline phosphatase (SAP) treatment after restriction reaction, where 1 unit of SAP was used in a 40 µl reaction volume containing 4 µl of 10x SAP reaction buffer and incubated at 37 °C for 15 min. Inactivation of the enzyme was performed by incubation at 65 °C for 5 min.

2.7.5 Phenol/Chloroform Extraction of DNA

After digestion with restriction enzymes, phenol/chloroform extraction was used to eliminate

proteins from DNA solutions. First, the DNA solution was filled up with H_2O to a final volume of 200 µl and subsequently an equal volume of phenol was added, then vigorously shaked and incubated at RT for 5 min. After centrifugation at 13,000 rpm for 1 min, the organic phase was discarded and 200 µl of chloroform was added. Mixing and centrifugation were repeated and the organic phase was discarded. After a second chloroform-step, 1/20 volume of 5 M NaCl and 2 volumes of absolute ethanol were added, and centrifugated at 13,000 rpm for 10 min. The supernatant was discarded and the sedimented nucleic acids were washed with 1 ml of 70% ethanol. Finally, the pellet was dissolved in 10 µl H_2O.

2.7.6 Ligation of DNA Fragments

Ligases catalyze the formation of phosphodiester bonds between the directly adjacent 3'-hydroxyl and 5'-phosphoryl termini of nucleic acid molecules, therefore, ligation of DNA fragments requires the presence of compatible ends and DNA ligase. 50 ng of restriction enzyme-digested vector DNA was incubated with a three- to fivefold molar excess of insert depending on the insert size. 1 unit of T4 DNA ligase was added in a final reaction volume of 10 µl. The ligation mixtures were incubated at 22 °C for 3 h, and inactivation of T4 DNA ligase was performed at 65 °C for 3 min and immediately placed on ice for 5 min.

2.7.7 Transformation

Before transforming of plasmid or ligation mixtures into competent *E. coli*, chemically competent *E. coli* was prepared with $CaCl_2$. 2 ml of SIN medium was inoculated with 20 µl of overnight culture. After it reached up to an OD_{600} of 0.5-0.6, 1 ml of cells was harvested at 13,000 rpm for 20 sec. The precipitated cells were gently resuspended in 1 ml of 0.1 M $CaCl_2$ and incubated on ice for 30 min. After centrifugation at 13,000 rpm for 20 sec, the precipitated bacteria were resuspended in 0.5 ml or 1 ml of $CaCl_2$ and incubated on ice for additional 30 min. For transformation, 100 µl of chemically competent cells was added to 1 µl plasmid DNA or ligation mixtures and incubated on ice for 30 min. During incubation plasmid DNA attaches to the outer membrane of the cells. The cells were heatshocked in 42 °C waterbath for 90 sec and immediately placed on ice for 5 min. During heatshock the

plasmid DNA is picked up into the bacteria. After addition of 400 µl of SIN medium, the competent cell mixtures were shaken at 110 rpm for 1 h at 37 °C to gain antibiotic resistance. The cell mixtures were plated on SIN agar plates (100 µg/ml ampicillin and/or 30 µg/ml kanamycin depending on the type of antibiotic resistance gene used). After 10 min, the plate was inverted and incubated at 37 °C overnight.

For transformation of plasmid DNA into *C. testosteroni* ATCC 11996, competent *C. testosteroni* ATCC 11996 was prepared with glycerol. The cells, the optical density of which was around 0.5-0.6, were placed on ice for 1 h. Then 1 ml of cells was harvested at 13,000 rpm for 20 sec. The pellet of *C. testosteroni* cells was resuspended in 1 ml of 10% glycerol and incubated on ice for 5 min. After centrifugation at 13,000 rpm for 20 sec, the precipitated bacteria were resuspended in 1 ml and incubated on ice for additional 5 min, they are ready to use for transformation. 100 µl of competent cells was added to 10 µg of desalted plasmid DNA, which was transformed into *C. testosteroni* by electroporation (1.8 kV, 1-cm cuvette, BIO-RAD). The competent cell mixtures were shaken at 110 rpm for 3 h at 27 °C to gain antibiotic resistance and then were plated on SIN agar plates (100 µg/ml ampicillin and/or 30 µg/ml kanamycin depending on the type of antibiotic resistance gene used). After 10 min, the plate was inverted and incubated at 27 °C overnight.

2.8 Preparation of Plasmid DNA

2.8.1 Mini Preparation of Plasmid DNA from *E. coli* (Alkaline Lysis Method)

Mini preparation of plasmid DNA was performed according to the alkaline lysis method. 1 ml of SIN medium containing relative antibiotics was inoculated with a single colony of bacterium, and incubated at 37 °C with continuous shaking for 5 h at 180 rpm. The cell culture was centrifuged at 13,000 rpm for 20 sec, and the supernatant was discarded. The pellet was resuspended by adding 100 µl of buffer P1 (50 mM Tris/HCl, pH 8.0, 10 mM EDTA, and 100 µg/ml RNAse A). After addition of 100 µl of buffer P2 (200 mM NaOH and 1% SDS) and gently shaking for several times, the mixtures were incubated at room temperature (RT) for 5 min. In this step the cellular membranes of the bacteria were lysed. To neutralize the mixtures and to precipitate chromosomal DNA and proteins, 100 µl of buffer

P3 (3 M potassium acetate, pH 5.5) was added and the mixtures were mixed gently giving curd-like appearance. After centrifugation at 13,000 rpm for 1 min, the supernatant containing plasmid DNA was transferred into another tube. 2 volumes of absolute ethanol were added to the supernatant, the mixtures were shaked and then centrifuged at 13,000 rpm for 7 min at RT. The pellet of plasmid DNA was washed with 70% ethanol to dissolve salts. The pellet was dissolved in 10 µl H_2O or TE buffer and stored at 4 °C.

2.8.2 Midi Preparation of Plasmid DNA

QIAGEN plasmid purification protocols are based on a modified alkaline lysis procedure, followed by binding of plasmid DNA to QIAGEN Anion-Exchange Resin under appropriate low-salt and pH conditions. RNA, proteins, and low-molecular-weight impurities are removed by a medium-salt wash. Plasmid DNA is eluted in a high-salt buffer and then concentrated and desalted by isopropanol precipitation. Thus, highly pure plasmid DNA in larger quantities can be obtained by using QIAGEN Midi Plasmid Kit.

To prepare a large amount of plasmid DNA, 50 ml of SIN medium was inoculated with 50 µl of overnight culture and incubated overnight on a shaker at 180 rpm. The incubated 50 ml bacterial culture was transferred into 50 ml Falcon tubes and centrifuged at 4,000 rpm for 10 min. The pellet was resuspended in 4 ml of buffer P1 (50 mM Tris-HCl, pH 8.0, 10 mM EDTA, and 100 µg/ml RNAse A) and the cells were finally lysed by addition of 4 ml of buffer P2 (200 mM NaOH and 1% SDS) with a gentle mix. The mixtures were incubated at RT for 5 min, then 4 ml of buffer P3 (3 M potassium acetate, pH 5.5) was added for neutralization and placed on ice for 15 min. The mixtures were centrifuged at 4,000 rpm for 10 min at 4 °C. Slowly the supernatant was transferred into the pre-equilibrated anion exchange column with 4 ml of buffer QBT (750 mM NaCl, 50 mM MOPS, pH 7.0, 15% isopropanol, and 0.15% Triton X-100). The solution was let to pass through the column by gravity flow, and the column-matrix binds the plasmid DNA. When all the solution was passed, the column was washed twice with buffer QC (1 M NaCl, 50 mM MOPS, pH 7.0, and 15% isopropanol), 10 ml buffer was used for each time. The solution was let to pass through the column completely. Finally, the plasmid DNA was eluted by adding 5 ml of QF buffer

(1.25 M NaCl, 50 mM Tris-HCl, pH 8.5, and 15% isopropanol). The eluted DNA was mixed with 0.7 volume of isopropanol. Centrifuged at 4 °C, 4,000 rpm for 10 min, the pellet was washed with 70% ethanol and centrifuged again as described above. The pellet of plasmid DNA was dissolved in 300 µl TE buffer.

2.9 Cloning of *hsdR* Gene from *C. testosteroni* and Subcloning of *hsdR* Gene Fragments

The *hsdR* gene was cloned from *C. testosteroni* ATCC 11996 chromosomal DNA in this lab by using forward primer pHsdR-F containing an *Nde*I site and reverse primer pHsdR-R containing a *Bam*HI site (Table 2-2). The full length *hsdR* gene was then subcloned into pCR2.1-TOPO to yield plasmid pTOPOHsdR, which after sequence confirmation (MWG) was used as template for further PCR reactions. To generate *hsdR* gene constructs that are controlled under the *lac* or the *tac* promoter, respectively, plasmid pTOPOHsdR was digested with *Kpn*I and *Xba*I and then the resulting fragment was ligated into either pK18 downstream from the *lac* promoter to yield pKHsdR3 or downstream from the *tac* promoter to yield pKtacHsdR1. To overexpress recombinant HsdR protein, the *Bam*HI-*Nde*I fragment of pTOPOHsdR was subcloned into pET15b downstream from the N-terminal His-tag coding sequence to yield pET-HsdR2, which was used for recombinant HsdR protein production.

To further analyze the oligomeric state of HsdR, three in frame *hsdR* deletions were constructed by using PCR. The first allele, HsdRΔN, in which the first N-terminal 86 codons were deleted, was amplified using primers HsdRΔN-F and HsdRΔN-R (Table 2-2). The second allele, HsdRΔN, in which codons between 221 and 303 were deleted, was obtained using primers HsdRΔC-F and HsdRΔC-R (Table 2-2). The third allele, HsdRΔNC, was the common part shared by HsdRΔN and HsdRΔC and amplified with primers HsdRΔN-F and HsdRΔC-R. To obtain these fragments, plasmid pKtacHsdR1 containing the full length *hsdR* gene was used as the template. The amplified fragments were first cloned into pCR2.1-TOPO, the recombinant plasmids were then digested with *Kpn*I and *Xba*I and ligated into plasmid pK18 to get pKHsdRΔN, pKHsdRΔC, and pKHsdRΔNC, respectively (Table 2-3). To

identify the effect of in frame *hsdR* deletions on *hsdA* expression, the recombinant pK18 plasmids were transformed into *E. coli* HB101 with plasmid pAX1 containing the *hsdA* gene, respectively, and the amount of 3α-HSD/CR was detected by using ELISA as described below.

To overproduce these truncated proteins, the recombinant pCR2.1-TOPO plasmids were digested with *Bam*HI and *Nde*I and ligated into pET15b (Novagen) that had been digested with *Bam*HI and *Nde*I. The recombinant plasmids were named pET-HsdRΔN, pET-HsdRΔC and pET-HsdRΔNC, respectively, and transformed into *E. coli* strain BL21(DE3)pLysS to overproduce HsdR truncated proteins. Ni-NTA His-tag column was used to purify these proteins.

2.10 Cloning of *SDRx* Gene from *C. testosteroni* and Subcloning of *SDRx* Gene Fragments

The *SDRx* gene from *C. testosteroni* ATCC11996 chromosomal DNA was amplified by PCR. The corresponding primers for PCR were designed as follows. The forward primer pSDR-L contained an *Nde*I site and the reverse primer pSDR-R contained a *Bam*HI site (Table 2-2). The full length SDRx gene was then cloned into pCR2.1-TOPO to yield plasmid pTOPOSDRx, which, after sequence confirmation (MWG), was used as template for further PCR reactions. Plasmid pTOPOSDRx was digested by restriction enzymes *Bam*HI and *Nde*I and then the resulting fragment was ligated into pET15b downstream from the N-terminal His-tag coding sequence to yield pET-SDRx.

2.11 Construction of Mutant Strains of *C. testosteroni*

2.11.1 Construction of an *hsdR* Disrupted Mutant Strain of *C. testosteroni*

An *hsdR* disrupted mutant of *C. testosteroni* was prepared by homologous integration. A DNA fragment ranging from 251 bp to 650 bp of the *hsdR* gene was generated by PCR using forward primer pHsdR-Ko-F and reverse primer pHsdR-Ko-R (Table 2-2) with plasmid pTOPOHsdR as template. The 400-bp fragment was cloned into pCR2.1-TOPO containing the kanamycin resistance gene to yield pTOPOHsdR3-1. Since plasmid pTOPOHsdR3-1

cannot replicate in *C. testosteroni*, and because of the sensitivity of wild type *C. testosteroni* to kanamycin, only mutants of *C. testosteroni* harbouring the kanamycin resistance gene of plasmid pTOPOHsdR3-1 integrated within the chromosomal DNA can grow in medium containing kanamycin. Accordingly, 10 μg of pTOPOHsdR3-1, which contains *hsdR* sequences homologous to *C. testosteroni* chromosomal DNA, was transformed into *C. testosteroni* by electroporation (1.8 kV, 1-cm cuvette, BIO-RAD). The cells were spread on 30 μg/ml kanamycin SIN agar plates and cultured in a 27 °C incubator overnight. The colonies were proven by PCR for homologous integration.

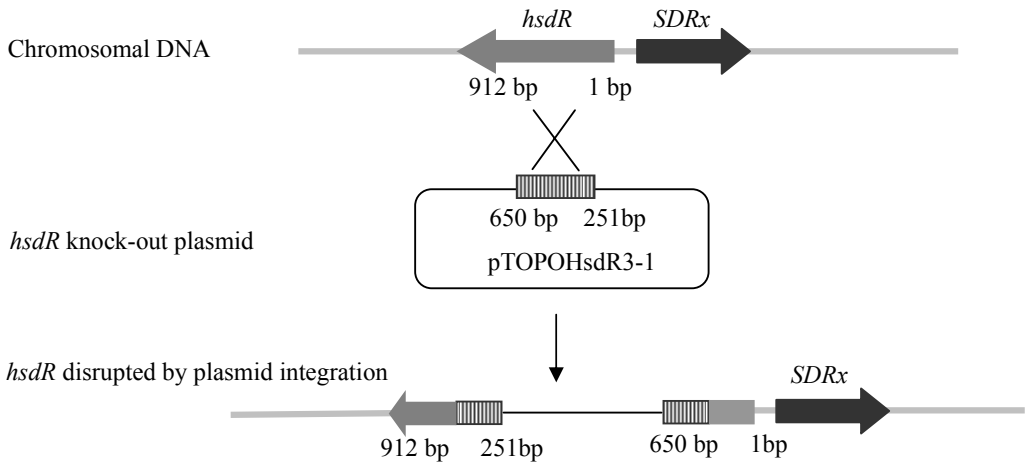

Fig. 2-1. Schematic representation of construction of an *hsdR* disrupted mutant strain of *C. testosteroni*. Plasmid pTOPOHsdR3-1 containing the central part of *hsdR* from 251 bp to 650 bp was electroporated into *C. testosteroni* and integrated into the chromosomal DNA of *C. testosteroni*, finally an *hsdR* disrupted mutant strain, CT-HsdR-Ko, was obtained.

2.11.2 Construction of an *hsdR-gfp* Fusion Mutant Strain of *C. testosteroni*

To further analyze the relationship between the structure of HsdR and its function, an *hsdR-gfp* fusion mutant of *C. testosteroni* was constructed. Double PCR was used to obtain an HsdR-GFP fragment. The *hsdR* gene was amplified by PCR using specific primers pHsdR-L and pHsdRGFP-M (Table 2-2) and plasmid pKHsdR3 as the template, *gfp* was amplified using primers pGFP-L and pGFP-R (Table 2-2) and plasmid pCR2.1-TOPO-GFP as the template. These two fragments were then used as the templates to construct an HsdR-GFP fragment by PCR using primers pHsdR-L and pGFP-R, the obtained fragment was cloned

into pCR2.1-TOPO to get pTOPOHsdRGFP, which was transformed into *C. testosteroni* by electroporation. This plasmid can be integrated into the chromosomal DNA of *C. testosteroni* via homologous recombination and the mutant strain can grow in medium containing kanamycin. To test if the *hsdA* expression is affected by the HsdR-GFP fusion protein, the *hsdR-gfp* fusion mutant and wild type *C. testosteroni* were induced by 0.5 mM testosterone and ELISA was used to detect the amount of HsdR and 3α-HSD/CR.

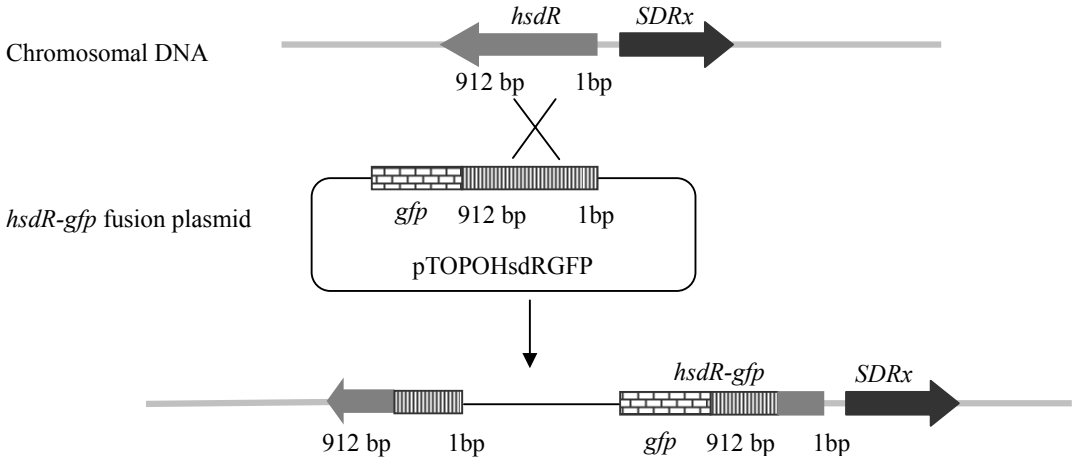

hsdR-gfp transcriptional fusion by plasmid integration

Fig. 2-2. Schematic representation of construction of an *hsdR-gfp* transcriptional fusion mutant strain of *C. testosteroni*. Plasmid pTOPOHsdRGFP containing the *hsdR-gfp* gene fragment was electroporated into *C. testosteroni* and integrated into the chromosomal DNA of *C. testosteroni*, finally an *hsdR-gfp* transcriptional fusion mutant strain, C.T.HsdRGFP2, was obtained.

2.11.3 Construction of an *SDRx* Disrupted Mutant Strain of *C. testosteroni*

An *SDRx* disrupted mutant of *C. testosteroni* was prepared by homologous integration. A central part of the *SDRx* gene from 201 bp to 625 bp was generated by PCR using forward primer pSDR-Ko-F and reverse primer pSDR-Ko-R (Table 2-2) with plasmid pTOPOSDRx as template. The PCR fragment was cloned into pCR2.1-TOPO to yield pTOPOSDR$_{425}$. Because of its sensitivity to kanamycin, only the mutant *C. testosteroni* in which pTOPOSDR$_{425}$ was integrated into the chromosomal DNA could grow in kanamycin-containing medium, while pTOPOSDR$_{425}$ could not replicate as a plasmid in *C. testosteroni*. Accordingly, 10 μg of pTOPOSDR$_{425}$ was transformed into *C. testosteroni* by electroporation

(1.8 kV, 1-cm cuvette, BIO-RAD), and the *SDRx* gene was disrupted upon integration of the plasmid into the chromosomal DNA. The cells were cultured and spread on SIN agar plates containing 30 μg/ml of kanamycin, and then cultured in a 27 °C incubator overnight. The colonies on the plates were cultured in 1 ml SIN medium containing 30 μg/ml of kanamycin and PCR was used to prove the integration.

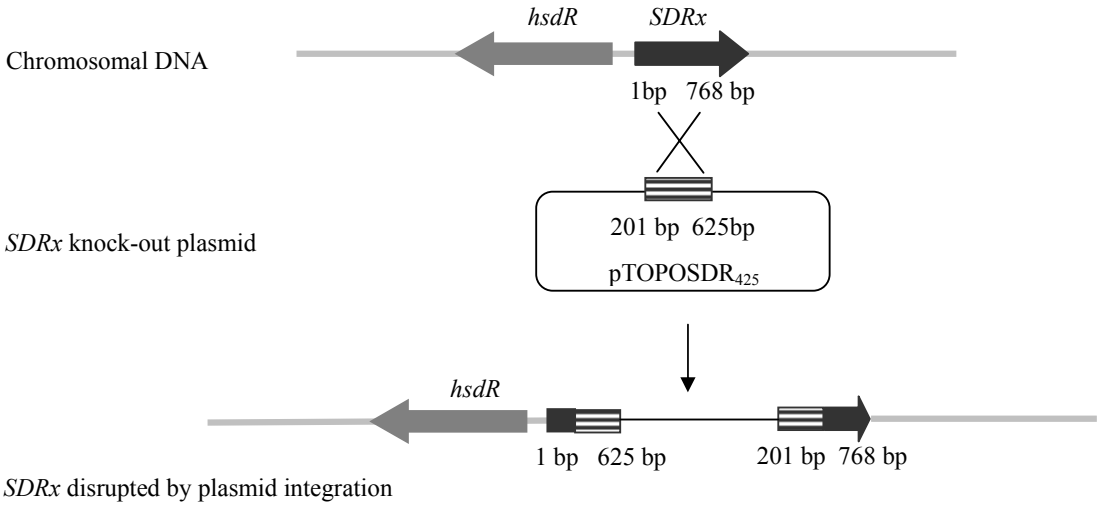

Fig. 2-3. Schematic representation of construction of an *SDRx* disrupted mutant strain of *C. testosteroni*. Plasmid pTOPOSDR$_{425}$ containing the central part of *SDRx* from 201 bp to 625 bp was electroporated into *C. testosteroni* and integrated into the chromosomal DNA of *C. testosteroni*, finally an *SDRx* disrupted mutant strain, C.T.SDR-6, was obtained.

2.12 Growth of Wild Type *C. testosteroni* and an *SDRx* Gene Knock-out Mutant Strain in the Presence of Steroids

To determine if disruption of the *SDRx* gene affects the utilization of steroids as the carbon source by *C. testosteroni*, wild type *C. testosteroni* and the *SDRx* gene knock-out mutant strain were incubated with 0.5 mM cholic acid, testosterone, and estradiol, respectively. After incubation at 27 °C overnight, the growth of each sample was detected through measurement of the optical density of the samples.

2.13 Overexpression and Purification of Proteins

Overexpression of HsdR and its truncated proteins was performed in *E. coli* strain BL21(DE3)pLysS with plasmid pET-HsdR2 or pET-HsdRΔN, pET-HsdRΔC and pET-HsdRΔNC (Table 2-3), respectively, and the recombinant proteins were extracted under native conditions and purified by their His-tag sequence. In brief, cells transformed with recombinant pET15b plasmids were grown at 37 °C in a shaker (180 rpm) in SIN medium supplemented with 100 μg/ml ampicillin. 100 μl of the overnight culture was used to inoculate 3 ml of fresh SIN medium. When the bacteria had grown to an optical density of 0.4-0.6 at 595 nm, target protein expression was induced by the addition of isopropyl-β-D-thiogalactoside (IPTG) to a final concentration of 1 mM. After induction for 4 h at 37 °C or overnight at RT, cells were harvested by centrifugation. The cell pellet was either stored at -80 °C for further usage or directly suspended in 200 μl of lysis buffer (50 mM sodium dihydrogenphosphate, 300 mM sodium chloride, and 10 mM imidazole, pH 8.0) containing different concentrations of sodium lauroyl sarcosinate (SLS). Cells were lyzed by freezing (-20 °C, 30 min) and thawing (RT, 30 min) 3 times, and the resulting mixtures were centrifuged at 13,000 rpm for 20 min. The supernatant was applied to a mini nickel-nitrilotriacetic acid (Ni-NTA) metal-affinity chromatography column (QIAGEN). After washing 2 times with 600 μl of washing buffer (50 mM sodium dihydrogenphosphate, 300 mM sodium chloride, 75 mM imidazole, and different concentrations of SLS, pH 8.0), HsdR was eluted from the column by applying 100 μl of elution buffer for 4 times (50 mM sodium dihydrogenphosphate, 300 mM sodium chloride, 250 mM imidazole and different concentrations of SLS, pH 8.0). Samples containing pure and soluble HsdR protein were assessed by SDS-polyacrylamide gel electrophoresis. Purification of RepA protein was performed as described previously (Xiong *et al*., 2003a).

Overexpression of SDRx was performed in *E. coli* strain BL21(DE3)pLysS harboring plasmid pET-SDRx, and the recombinant protein was extracted under denaturing conditions and purified by its His-tag sequence. Cells transformed with plasmid pET-SDRx were grown at 37 °C in a shaker (180 rpm), and maintenance of plasmids was ensured by adding 100 μg/ml ampicillin to the culture medium. An amount of 100 μl of the overnight culture was used to inoculate 3 ml of fresh SIN medium. At an OD_{595} of 0.6, expression was induced by

the addition of IPTG to a final concentration of 1 mM. After 4 h at 37 °C, cells were sedimented by centrifugation. The cell pellet was either stored at -80 °C for further usage or directly suspended in 200 µl of lysis buffer (8 M urea, pH 8.0). Cells were lyzed by freezing (-20 °C, 30 min) and thawing (RT, 30 min) 3 times, and the resulting mixtures were centrifuged (20 min, 13,000 rpm, 4 °C). The supernatant was applied to a mini Ni-NTA column (QIAGEN). After washing 2 times with 600 µl of washing buffer (8 M urea, pH 4.5) (QIAGEN), the SDRx protein was eluted from the column by applying 100 µl of elution buffer (8 M urea, pH 3.5) for 4 times.

2.14 Immunization and Preparation of Antisera against HsdR

On the first day, rabbits were injected subcutaneously with an emulsion of 0.5 ml ddH_2O and 0.5 ml incomplete Freund's adjuvant. For immunization, one microgram of purified HsdR protein was dissolved in an emulsion of 0.5 ml ddH_2O and 0.5 ml incomplete Freund's adjuvant, and rabbits were immunized on the following days: 7 d, 37 d, 67 d. The antiserum was collected at day 74 and antibody titer determination in the rabbit serum was performed by ELISA.

2.15 Protein Determination

Protein concentration was determined by the method of Bradford (Bradford 1976) with Roti-Quant solution (Roth) using bovine serum albumin (BSA) as standard. The principle of this method is based on the observation that the maximum absorption for an acidic solution of Coomassie Brillant Blue G-250 shifts from 465 nm to 595 nm when binding to protein occurs. Each time the assay was performed, a standard curve was prepared using BSA as protein standard (0-1 mg/ml); A595 was corrected for the blank. 20 µl of appropriately diluted samples or BSA was mixed with 980 µl of 1 volume of 5x staining solution, and the absorbance of the solution at 595 nm was measured at RT with a spectrophotometer (Kontron) after 10 min.

2.16 SDS-PAGE

In order to analyze the purity of recombinant proteins, polyacrylamide gels containing the

strong anionic detergent SDS were used. The polypeptides bind SDS and become negatively charged, and the amount of SDS bound is almost always proportional to the molecular weight of the polypeptide independent of its sequence (Laemmli, 1970). Thus, SDS-polypeptide complexes migrate through polyacrylamide gels in accordance with the size of the polypeptide.

In most cases, SDS-PAGE is carried out with a discontinuous buffer system in which the buffer in the reservoirs is of a pH and ionic strength different from that of the buffer used to cast the gel (Laemmli, 1970). The sample and the stacking gel contain Tris-HCl (pH 6.8), the upper and lower buffer reservoirs contain Tris-glycine (pH 8.3), and the resolving gel contains Tris-HCl (pH 8.8). All components of the system contain 0.1% SDS (Laemmli, 1970). 15% resolving gel (15 ml) is composed of the following components: 5.5 ml of 40% acrylamide: bisacrylamide solution, 3.8 ml of 1.5 M Tris-HCl (pH 8.8), 150 µl of 10% ammonium persulfate (APS), 150 µl of 10% SDS, 6 µl of TEMED and 5.5 ml of H_2O (Sambrook and Russel, 2001). The 5% stacking gel (10 ml) contained 1.25 ml of 40% acrylamide: bisacrylamide, 1.25 ml of 1 M Tris-HCl (pH 6.8), 100 µl of 10% APS, 100 µl of 10% SDS, 10 µl of TEMED, and 7.3 ml of H_2O (Sambrook and Russel, 2001). The electrophoresis was performed using the Roth electrophoresis apparatus Max Fill (Roth).

To load onto the polyacrylamide gel, samples were mixed with 5x loading buffer (250 mM Tris-HCl, pH 6.8, 500 mM dithiothreitol, 10% (w/v) SDS, 0.5% bromophenol blue and 50% (v/v) glycerol) and heat at 95 °C for 3 min. Subsequently, the samples were loaded onto the gel. The eletrophoresis chamber was completely filled with Tris/glycine-electrophoresis buffer (25 mM Tris base, 250 mM glycine, pH 8.3, and 0.1% SDS). The electrophoresis was run with a voltage of 100 V until the bromophenol blue reached the bottom of the resolving gel. Protein marker of known molecular weight was used upon SDS-PAGE. After electrophoresis, the proteins were visualized by staining the gel at RT for 30 min in staining solutions (dissolving 1.25 g of Coomassie Brilliant Blue R-250 in 1 L of methanol:acetic acid solution containing 500 ml of methanol, 400 ml of H_2O, and 100 ml of glacial acetic acid) (Sambrook and Russel, 2001). Destaining was carried out at RT for 30 min with destaining

buffer (250 ml of methanol, 75 ml of glacial acetic acid, and 675 ml of H_2O).

2.17 ELISA of 3α-HSD/CR and HsdR

Proteins for 3α-HSD/CR or HsdR ELISA detection were prepared from 3 ml of bacterial cell culture and subsequent centrifugation at 13,000 rpm for 10 sec. The pellet was washed 3 times with 1 ml of PBS (137 mM NaCl, 2.7 mM KCl, 10 mM Na_2HPO_4, and 2 mM KH_2PO_4, pH 7.4) and resuspended in 200 µl of PBS with 100 µg/ml of lysozyme. The suspension was frozen at -20 °C and thawed at RT for 3 times. Finally, the samples were centrifuged again at 13,000 rpm for 20 min. The supernatant was diluted into 1 mg/ml of total protein and used for 3α-HSD/CR or HsdR ELISA detections.

To quantify 3α-HSD/CR protein expression, an ELISA was established, and respective antibodies directed against 3α-HSD/CR from *C. testosteroni* were prepared in rabbits (Maser *et al*., 2000). For HsdR detection, antibodies against HsdR were prepared in rabbits as described above. ELISA plates were coated with protein samples containing 3α-HSD/CR or HsdR diluted in coating buffer (Na_2CO_3 1.59 g, $NaHCO_3$ 2.93 g, and NaN_3 0.2 g, pH 9.6 in 1 liter). As a standard 200, 100, 50, 25, 12.5, 6.25 ng of purified 3α-HSD/CR or HsdR was applied in coating buffer into the wells. After washing (washing buffer: NaCl 8 g, KH_2PO_4 0.2 g, Na_2HPO_4 1.5 g, KCl 0.2 g and Tween 20 0.5 ml, pH 7.4 in 1 liter), antibodies against 3α-HSD/CR or HsdR were added in a 1:1000 dilution. Following incubation for additional 30 min and washing 3 times, the secondary antibodies peroxidase-conjugated swine anti-rabbit immunoglobulin (DAKO, Denmark) were used in a 1:1000 dilution. The further procedure corresponded to that of the chloramphenicol acetyl transferase ELISA kit from Roth.

2.18 Electrophoretic Mobility Shift Assays (EMSA)

For gel mobility shift assays, a digoxigenin-11-dUTP-labeled 203-bp DNA fragment from -65 to +137 bp relative to the transcriptional start site of the *hsdA* gene was generated by PCR with forward primer p7-1 and reverse primer pCla, and plasmid p6 as template. For binding of HsdR to the *hsdR-SDRx* intergenic region, a 200-bp DNA fragment was amplified by PCR

with primers pHsdR-SDR-L1 and pHsdR-SDR-R1 and plasmid pKSphI1-2 as template, which was constructed in our lab and contains the *hsdR* gene, *hsdR-SDRx* intergenic region and the *SDRx* gene. Incubation mixtures (20 µl) contained 10 ng of labeled DNA fragment, 100 ng of herring sperm DNA, and different concentrations of purified HsdR and RepA protein in binding buffer consisting of 50 mM Tris-HCl (pH 8.0), 100 mM KCl, 12.5 mM $MgCl_2$, 1 mM EDTA, 5% glycerol, 100 µg/ml bovine serum albumin, and 1 mM DTT. After incubation at 27 °C for 30 min, samples were separated on 5% polyacrylamide nondenaturing gels in 0.05 M Tris borate/EDTA buffer (pH 8.3) for 2 h at 10 V/cm and blotted onto nitrocellulose membranes. Labeled DNA was visualized by chemiluminescence using the digoxigenin luminescence detection kit (Roth). The membrane was fixed at 80 °C for 1 h, and was washed with washing buffer (0.1 M maleic acid, 0.15 M NaCl, and 0.3% Tween 20). After blocking with 10 ml of blocking buffer (1% blocking reagent, 0.1 M maleic acid, and 0.15 M NaCl) for 30 min, the membrane was incubated with anti-DIG antibody conjugated with alkaline phosphatase for another 30 min. Following washing twice, the membrane was visualized overnight with addition of NBT/BCIP (nitroblue tetrazolium/5-bromo-4-chloro-3-indolyl phosphate). After desired spot or band intensities are achieved, the reaction was stopped by washing the membrane for 5 min with 50 ml of distilled waster.

2.19 HsdR-RNA Polymerase Interaction

300 ng RNA polymerase (a generous gift from Prof. Ruth Schmitz-Streit, Kiel University) was used to coat each well. The plate was incubated at 37 °C for 30 min. After washing, different amounts of purified HsdR diluted with washing buffer were added. Following incubation at 37 °C for 30 min, rabbit antibodies against HsdR diluted with washing buffer (1:1000) were added into the wells. After incubation for another 30 min at 37 °C and washing, washing buffer diluted (1:1000) peroxidase-conjugated swine anti-rabbit immunoglobulin (DAKO, Denmark) was added. Following a further incubation for 30 min at 37 °C and washing, 100 µl ABTS solution (2'-azino-di-(3-ethylbenzthiazoline-6-sulfonate) with H_2O_2 in glycin/citric acid buffer; Roth, Mannheim, Germany) was added into each well and incubated at 37 °C for 30 min. Finally, the samples were assayed in an ELISA reader at 415 nm with reference at 490 nm (BIO-RAD, Hercules, California).

2.20 NuPAGE and Western blotting

Protein analyses by SDS-PAGE were carried out according to Laemmli (Laemmli, 1970). To further analyze the full length HsdR and its truncated proteins, 1 µg of each protein was subjected to NuPAGE® Novex Bis-tris Mini Gels according to the manufacturer's instruction (Invitrogen). After electrophoresis, samples were transferred onto a polyvinylidene fluoride membrane (ProBlott PVDF-Membrane, Applied Biosystems, Weiterstadt, Germany). Following the electrotransfer of proteins, the membrane was blocked with 5% (w/v) milk powder in PBST (137 mM NaCl, 2.7 mM KCl, 10 mM Na_2HPO_4, 2 mM KH_2PO_4, and 0.1% Tween 20, pH 7.4) and gently shaken overnight at 4 °C. After washing twice with PBST, the membrane was then incubated with rabbit anti-HsdR polyclonal antibody which was diluted in 1:5,000 with 2.5% milk powder of PBST. After incubation at RT for 1 h, the membrane was washed twice with PBST, then incubated with 1:10,000 dilutions of peroxidase-conjugated anti-(rabbit IgG) antibody (Amersham Biosciences, Freiburg, Germany) for additional 1 h. Excess of conjugates was removed by washing the membrane 3 times with PBST. Immunodetection was performed with the protocol for the ECF detection kit provided by Amersham Biosciences using the Kodak X-OmAT films to detect the light emitted during the reaction of the substrate ECF with the peroxidase-linked secondary antibody.

2.21 HPLC

To further determine the function of SDRx in catabolic pathway of steroid compounds, wild type *C. testosteroni* and the *SDRx* gene knock-out mutant were incubated with 0.5 mM testosterone or estradiol, respectively. Samples were collected at different time points: 0 h, 6 h, 12 h and 24 h. The remaining testosterone or estradiol in the medium was extracted with ethyl acetate and then concentrated under vacuum conditions. The steroids were dissolved with 100 µl of HPLC running buffer (acetonitrile: H_2O in 50:50) and 50 µl thereof was subjected to a Waters HPLC chromatographic system consisting of a gradient pump, autosampler, and Dual λ absorbance detector. The mobile phase for HPLC analyses was acetonitrile: H_2O with a flow rate of 1 ml/min. In each case, 50 µl samples were injected into the HPLC system. Detection was performed at a wavelength of 254 nm for testosterone, and

two wavelengths (210 nm and 225 nm) for estradiol at RT. Under these chromatographic conditions testosterone and estradiol could be determined with retention times of testosterone and estradiol of 10 min and 8 min, respectively.

2.22 Gel Filtration Chromatography

Gel filtration chromatography was performed on a Pharmacia ÄKTA Protein Purifier system (Maser *et al*., 2000). Purified recombinant HsdR and its truncated proteins were applied to a Superdex 200 10/300 GL column (GE healthcare) in buffer (pH 8.0) containing 50 mM sodium dihydrogenphosphate, 300 mM sodium chloride and 0.3% SLS, and eluted with the same buffer at a flow rate of 0.5 ml/min. The molecular mass of HsdR and the truncated HsdR proteins was calculated by comparing its elution volume with that of appropriate standard proteins. The GL column was calibrated using the following molecular mass standards: β-amylase (206 kDa), albumin (67 kDa), carbonic anhydrase (29 kDa), and cytochrome C (13.6 kDa). Blue Dextran 2000 was used to calculate the void volume of the column. Molecular mass standards were run using a final volume of 250 µl (50 µl for each component).

2.23 Cross-linking of HsdR with Dimethyl Pimelimidate Dihydrochloride

The cross-linking reagent dimethyl pimelimidate dihydrochloride (DMP) is extensively used for identifying the multimerization of proteins that existed in an oligomeric state (DiBella *et al*., 2001; Horiguchi *et al*., 1997; Tellinghuisen *et al*., 2000). In the present study, oligomerization of HsdR was also tested using DMP (Sigma). 20 µl reaction mixtures contained 10 mM DMP, 5 µg purified HsdR protein and 10 µl of 50 mM triethanolamine-Cl, pH 8.2. After incubation at RT for 30 min, samples were subjected to SDS-PAGE.

2.24 Sequencing

Manufactured synthesis of oligonucleotides and DNA sequencing were performed by MWG (Ebersberg, Germany). Before further cloning, fragments prepared by PCR were cloned into pCR2.1-TOPO and then checked for correct sequence by MWG.

2.25 Phylogenetic Analyses and Sequence Alignment

The BLAST program (Altschul *et al*., 1990) was used to screen protein and DNA databases for proteins that share sequence similarity. Multiple sequence alignments were made according to the CLUSTAL W method (Higgins *et al*., 1994), and the similarity relationships were calculated applying bootstrap analyses (Efron *et al*., 1996).

3. Results

3.1 HsdR Positively Regulates *hsdA* Expression

3.1.1 Cloning, Sequence Alignments, and Phylogenetic Analyses of HsdR

A new transcriptional factor, HsdR, named from "3α-hydroxysteroid dehydrogenase/carbonyl reductase regulator" was identified in *C. testosteroni*. The *hsdR* gene locates 2.58 kb downstream of the *hsdA* gene on the *C. testosteroni* ATCC 11996 chromosome with an orientation opposite to *hsdA* (Fig. 3-1). The open reading frame of *hsdR* consists of 912 bp and translates into a protein of 303 amino acids, which is a member of the LysR-type transcriptional regulator family (LTTRs) as revealed by sequence analyses. The GenBank accession number of the nucleotide sequence of *hsdR* is JF747025.

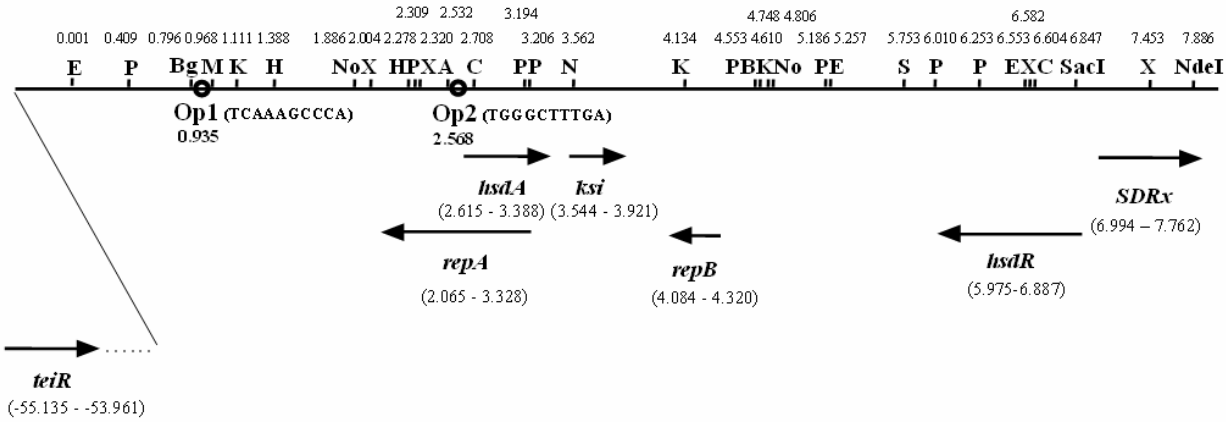

Fig. 3-1. Genetic organization of the *hsdA* gene and its regulatory elements. Two negative regulator genes, *repA* (Xiong and Maser, 2001) and *repB* (Xiong *et al*., 2003a), are located in the vicinity of the *hsdA* gene, and a positive regulator gene, *teiR* (Göhler *et al*., 2008), upstream of the *hsdA* gene. A novel transcriptional regulator gene, *hsdR*, encoding HsdR for *hsdA* expression, was identified 2.58 kb downstream of the *hsdA* gene. Adjacent to the *hsdR* gene, a novel short-chain dehydrogenase/reductase gene, *SDRx*, was found. Open reading frames are indicated as arrows and restriction sites are abbreviated as one-letter code (A, *Avr*II; B, *Bam*HI; Bg, *Bgl*II; Bs, *Bss*HI; C, *Cla*I; E, *Eco*RI; H, *Hind*III; K, *Kpn*I; M, *Mlu*I; N, *Nde*I; No, *Not*I; P, *Pst*I; X, *Xam*I). Op: operator; *ksi*: gene encoding ketosteroid isomerase.

A multiple alignment of HsdR with other retrieved LTTRs indicates that the identity of amino acids between HsdR and CrgA is 25.3%, which is higher than that between HsdR and other LTTRs (12.8~20.7%). The N-terminal DNA binding domain (DBD) is highly conserved among LTTRs as shown in Fig. 3-2, and the similarity of DBD (N-terminal 66 residues) between HsdR and CrgA is about 40%. The similarity between HsdR and other LTTRs was further confirmed

by phylogenetic analyses. As shown in the phylogenetic tree (Fig. 3-3), HsdR is related to CrgA, which is supported with the high bootstrap value and both of them form a cluster. It has been demonstrated that CrgA exists as an octamer and forms a novel subclass of LTTRs (Sainsbury *et al*., 2009).

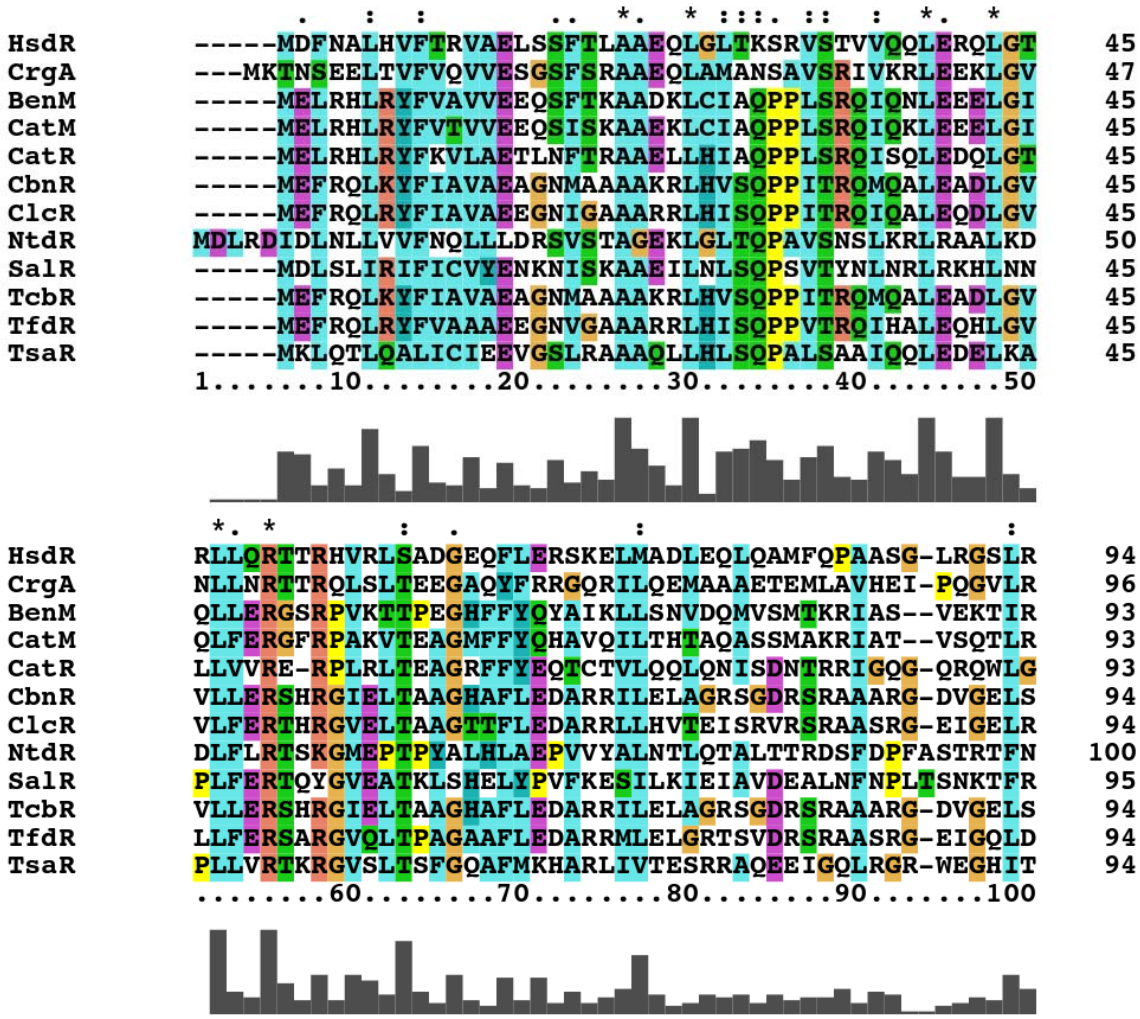

Fig. 3-2. Multiple sequence alignment of HsdR and other structurally characterized LysR-type transcriptional regulators (LTTRs). "*" indicates amino acids identical among all the proteins; ":" and "·" indicate amino acids of high and low similarity, respectively. Sequence alignment was performed using the CLUSTAL W. Swissprot or PDB accession numbers of these LTTRs are: BenM and CatM from *Acinetobacter baylyi*, O68014 and P07774; CatR from *Pseudomonas putida* (strain KT2440), Q88GK5; CbnR from *Ralstonia eutropha*, Q9WXC7; ClcR from *Pseudomonas putida*, Q706T8; CrgA from *Neisseria meningitidis*, Q9JPU9; NtdR from *Comamonas sp*. JS765, Q7WT52; SalR from *Acinetobacter sp*. (strain ADP1), Q9BBI3; TcbR from *Pseudomonas sp*. (strain P51), D27102; TfdR from *Ralstonia eutropha* JMP134, YP_025396; TsaR from *Comamonas testosteroni*, P94678.

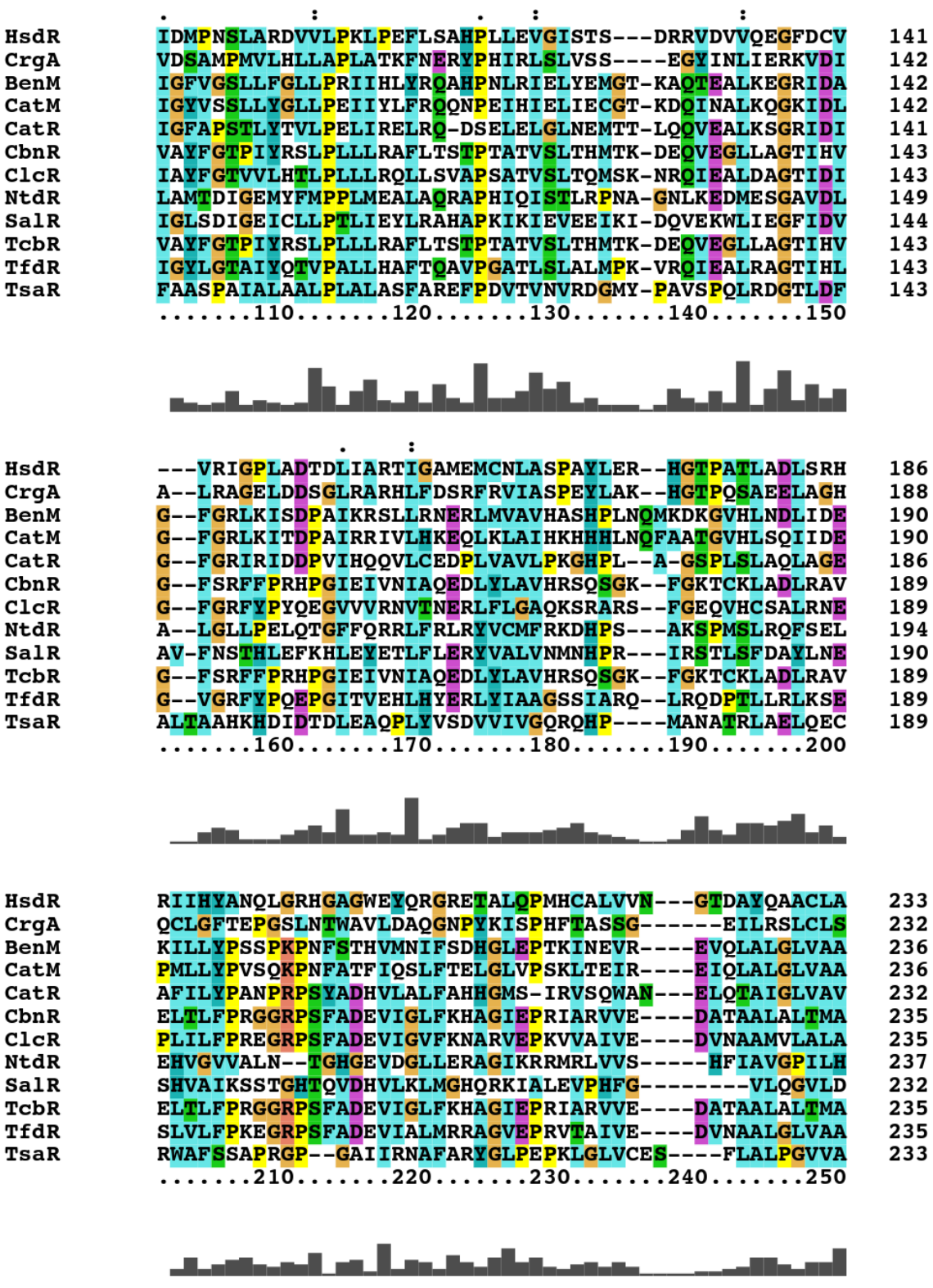

Fig. 3-2 (continued)

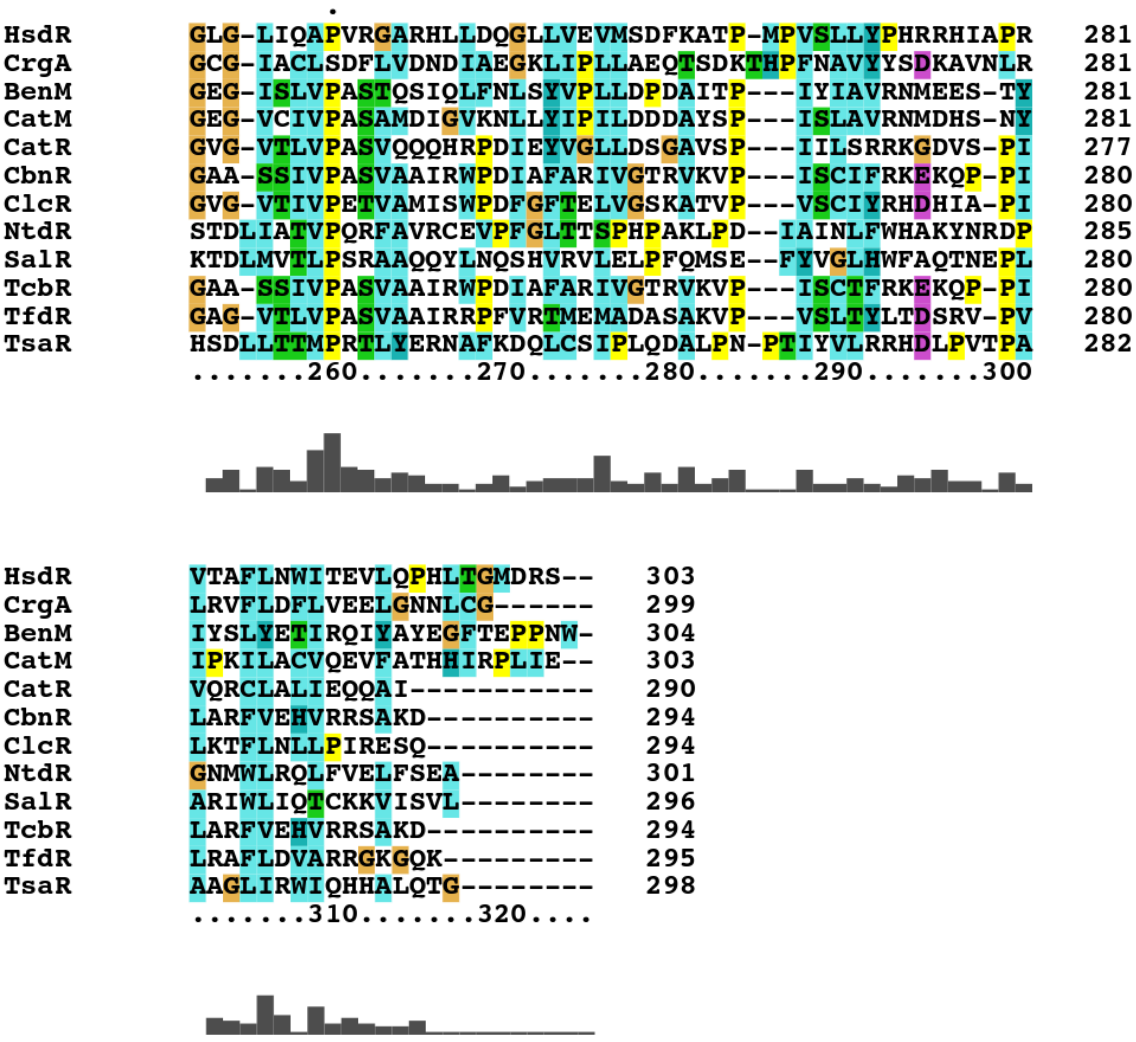

Fig. 3-2 (continued)

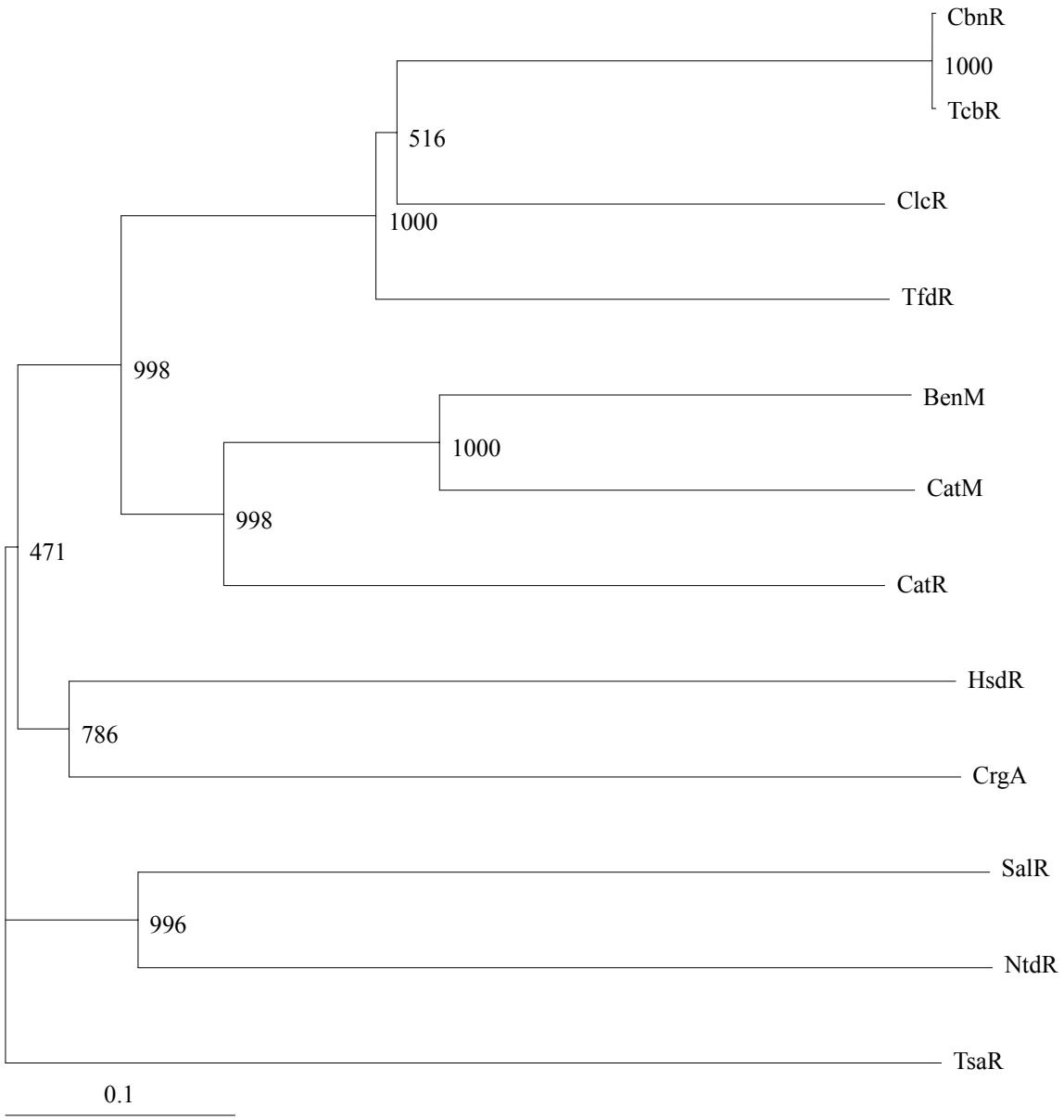

Fig. 3-3. Phylogenetic tree of HsdR and other LTTRs based on the amino acid sequences. The phylogenetic tree was constructed using CLUSTAL W. The horizontal line on the bottom left represents the evolutionary distance.

3.1.2 Overexpression and Purification of HsdR

To prepare purified HsdR protein, the *hsdR* gene was cloned from *C. testosteroni* ATCC 11996 into the expression vector pET15b, and subsequent overexpression in *E. coli* BL21(DE3)pLysS cells resulted in an HsdR protein with an N-terminal His-tag sequence. After induction with IPTG at RT overnight, overexpressed HsdR was first dissolved in 0.6% sodium lauroyl

sarcosinate (SLS) detergent and then purified in one step using nickel-chelate chromatography under native conditions. The molecular mass of the recombinant protein (33.4 kDa) plus the His-tag sequence (2.2 kDa) as seen on the SDS-polyacrylamide gel (35.6 kDa) was identical to that predicted from the amino acid sequence (Fig. 3-4). The purified protein was used for binding assays to DNA and RNA polymerase, as well as for the preparation of polyclonal antibodies.

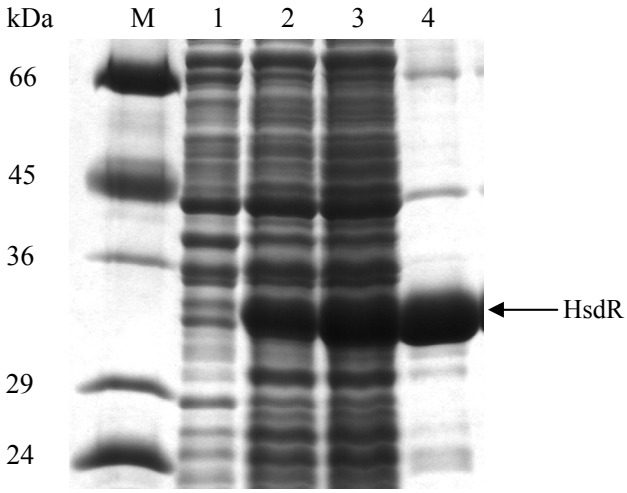

Fig. 3-4. Purification of HsdR protein. Recombinant HsdR protein induced at RT was lyzed with lysis buffer containing various concentrations of sodium lauroyl sarcosinate (SLS). After centrifugation, the supernatant of the samples was analyzed by SDS-PAGE (Lane 1 without SLS; Lane 2 with 0.3 % SLS; lane 3 with 0.6 % SLS). HsdR was purified on a Ni-NTA column by its N-terminal His-tag sequence. Lane 4, eluate from the coloumn.

3.1.3 Activation of *hsdA* Expression by HsdR

For the identification of HsdR as an activator of *hsdA* expression, plasmid pKHsdR3, containing the *hsdR* gene (Table 2-3), was co-transformed into *E. coli* HB101 with plasmids p6, pAX1 or pDel13n, respectively. After co-transformation with pKHsdR3, the expression levels of 3α-HSD/CR with pAX1 increased compared to the control vector pK18, but not with p6 (Fig. 3-5).

According to previous findings of our group, there are two operators (Op1 and Op2) present in plasmid p6 which form a DNA-loop structure upon binding of both with repressor RepA (Xiong and Maser, 2001). In addition, Op2 overlaps the -10 region of the *hsdA* promoter region (Xiong and Maser, 2001). Both loop structure and the occupation of the *hsdA* promoter by RepA lead to a strong repression of *hsdA* gene expression (Xiong and Maser, 2001). Since in pAX1 there is only operator Op2 present, the DNA-loop structure cannot be formed, such that *hsdA* expression

already increases with empty control vector pK18. However, after co-transformation with plasmid pKHsdR3, an increased expression of *hsdA* could be observed. Thus, HsdR drives *hsdA* gene expression as a transcriptional activator (Fig. 3-5).

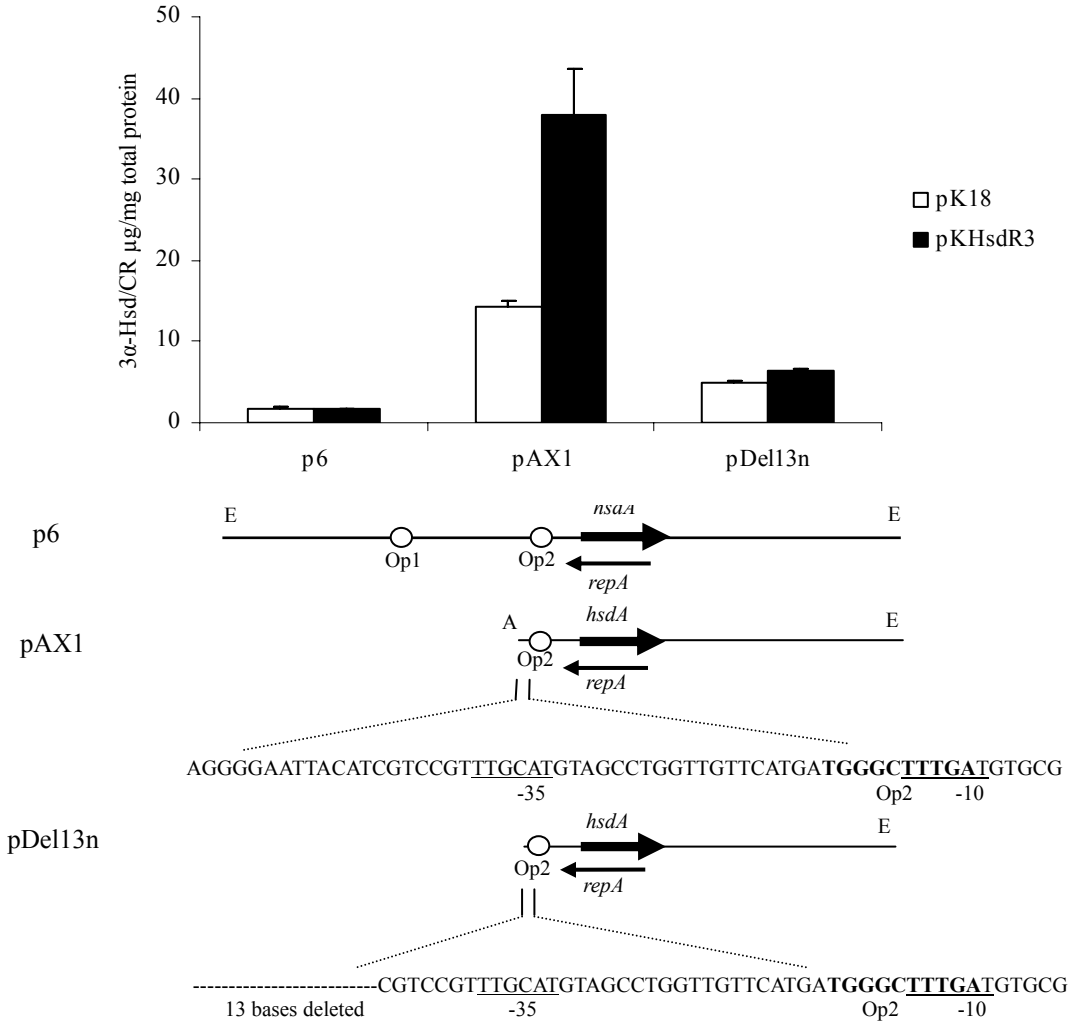

Fig. 3-5. HsdR activates expression of 3α-HSD/CR. 3α-HSD/CR (µg/mg protein) was assayed by ELISA after co-transformation of *E. coli* with pKHsdR3 and plasmids containing the *hsdA* gene. Induced expression of 3α-HSD/CR is observed with plasmid pAX1, but not with p6 (control) nor with pDel13n. E: *Eco*RI; A: *Avr*II. Bars represent the average and standard deviation of at leat three independent measurements.

Co-transformation of pDel13n, in which 13 bases were deleted upstream of the *Avr*II-*Eco*RI fragment, with pK18 also leads to a slight increase in 3α-HSD/CR expression compared to p6. Also here, the DNA-loop structure could not be formed due to the lack of bases important for RepA binding (Xiong and Maser, 2001). Interestingly, co-transformation of the *hsdR* gene

(pKHsdR3) did not significantly enhance 3α-HSD/CR expression with pDel13n, a fact which lead us conclude that the deleted nucleotides may be necessary for HsdR action (Fig. 3-5).

In order to prove that the ability of HsdR to activate *hsdA* expression is affected by RepA binding, a series of plasmids p67, p67-3, p67-5 and p67-7, in which a various number of bases were present between the two operators Op1 and Op2, were employed. With these plasmids, our group has previously shown that a critical distance between Op1 and Op2 together with additional -3, -5 and -7 nucleotides deletions result in DNA rotations that lead to altered orientations of both operators to each other (Xiong *et al*., 2003b). As a consequence, RepA binding and subsequent *hsdA* repression was influenced (Xiong *et al*., 2003b).

Here, these plasmids were transformed into *E. coli* strain HB101 with plasmid pKtacHsdR1 (Fig. 3-6). 3α-HSD/CR expression was the lowest with plasmid p67-3, probably because the 64 bp distance and orientation between Op1 and Op2 is suitable for a strong RepA binding and *hsdA* repression (Xiong and Maser, 2001; Xiong *et al*., 2003b). In this conformation, RepA is able to prevent HsdR from activating the *hsdA* promoter. With plasmid p67-7, which habours a 60 bp spacing between Op1 and Op2, co-transformation of HsdR lead to a significant increase in 3α-HSD/CR expression when compared to the empty control vector pK18. Obviously, the altered DNA conformation, in which repression by RepA is not as strong as that in p67-3, allows HsdR to perform its action on *hsdA* expression. This effect becomes most clear with plasmids p67 and p67-5, in which the positioning between Op1 and Op2 was turned by at least 72º along the DNA axis, such that RepA-Op1 and RepA-Op2 binding became sterically unlikely (Xiong *et al*., 2003b). In the absence of the Op1-RepA-Op2, HsdR could bind to the *hsdA* promoter domain and activate 3α-HSD/CR expression (Fig. 3-6). This result shows that the activity of the transcriptional regulator HsdR is dependent on the decreased repression by RepA.

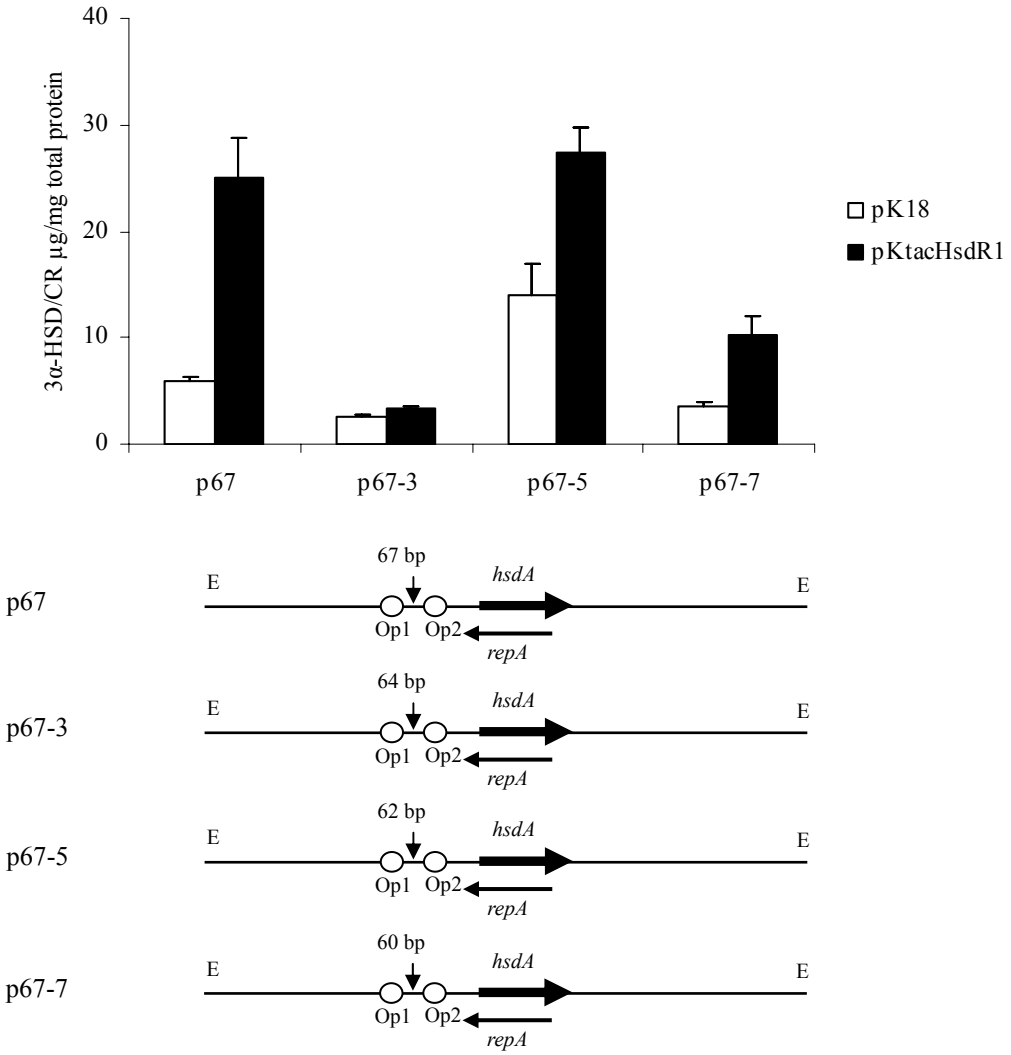

Fig. 3-6. HsdR activity is associated with *hsdA* repression by RepA. Plasmids p67, p67-3, p67-5 and p67-7 with varying distances between Op1 and Op2 (67, 64, 62 and 60 bp, respectively) upstream of the *hsdA* gene, were co-transformed into *E. coli* HB101 with plasmids pK18 (control) or pKtacHsdR1 (containing *hsdR*). 3α-HSD/CR expression in *E. coli* was determined by ELISA. Bars represent the average and standard deviation of at leat three independent measurements.

3.1.4 Binding of HsdR to the Promoter Region of the *hsdA* Gene

The specific interaction between HsdR and the promoter of the *hsdA* gene was demonstrated by gel mobility shift assays. A DNA fragment from -65 to +137 bp relative to the *hsdA* transcriptional start site (Fig. 3-7A) was labeled with digoxigenin and incubated with purified HsdR protein. After electrophoresis, formation of the HsdR-DNA complex was seen as shifted bands in Fig. 3-7B (lanes 2 and 3). Two shifted bands were observed when 100 pmole of HsdR protein was present. It seems that there are several binding sites at the *hsdA* promoter, including high affinity binding sites and low affinity binding sites, the former being occupied after addition of small amounts of HsdR protein which resulted in the formation of the fast-migrating band. When large amounts of HsdR protein are present, both high affinity and low affinity binding sites are bound and the slower migrating band is formed. The extent of the shifted bands became weaker upon reducing the amount of HsdR protein as shown in Fig. 3-7B (lane 3). This result indicates that HsdR can bind to the *hsdA* promoter.

To figure out if RepA competes with HsdR to bind to the *hsdA* promoter, the same DNA fragment used above was also used for competition binding of RepA with HsdR. This fragment contained one high affinity binding site (Op2) of RepA (Xiong and Maser, 2001). The shifted bands formed by RepA (Fig. 3-7C, lane 1) and HsdR (Fig. 3-7C, lane 4), respectively, indicated that HsdR and RepA can independently bind to the same DNA probe. It was proposed that if they compete for the same binding site, formation of the HsdR-DNA complex will be inhibited by RepA. However, it turned out that two shifted bands occurred after addition of 6 pmole of RepA to the HsdR reaction mixtures (Fig. 3-7C, lane 3): one shifted band compares to that formed by HsdR, and the other one, with slower electrophoretic mobility, obviously represents an HsdR-DNA-RepA complex. Furthermore, the shifted band of the HsdR-DNA-RepA complex became very strong after addition of more RepA protein (12 pmole) to the HsdR reaction mixtures (Fig. 3-7C, lane 2). Taken together, HsdR and RepA can simultaneously bind to different sites of the *hsdA* promoter.

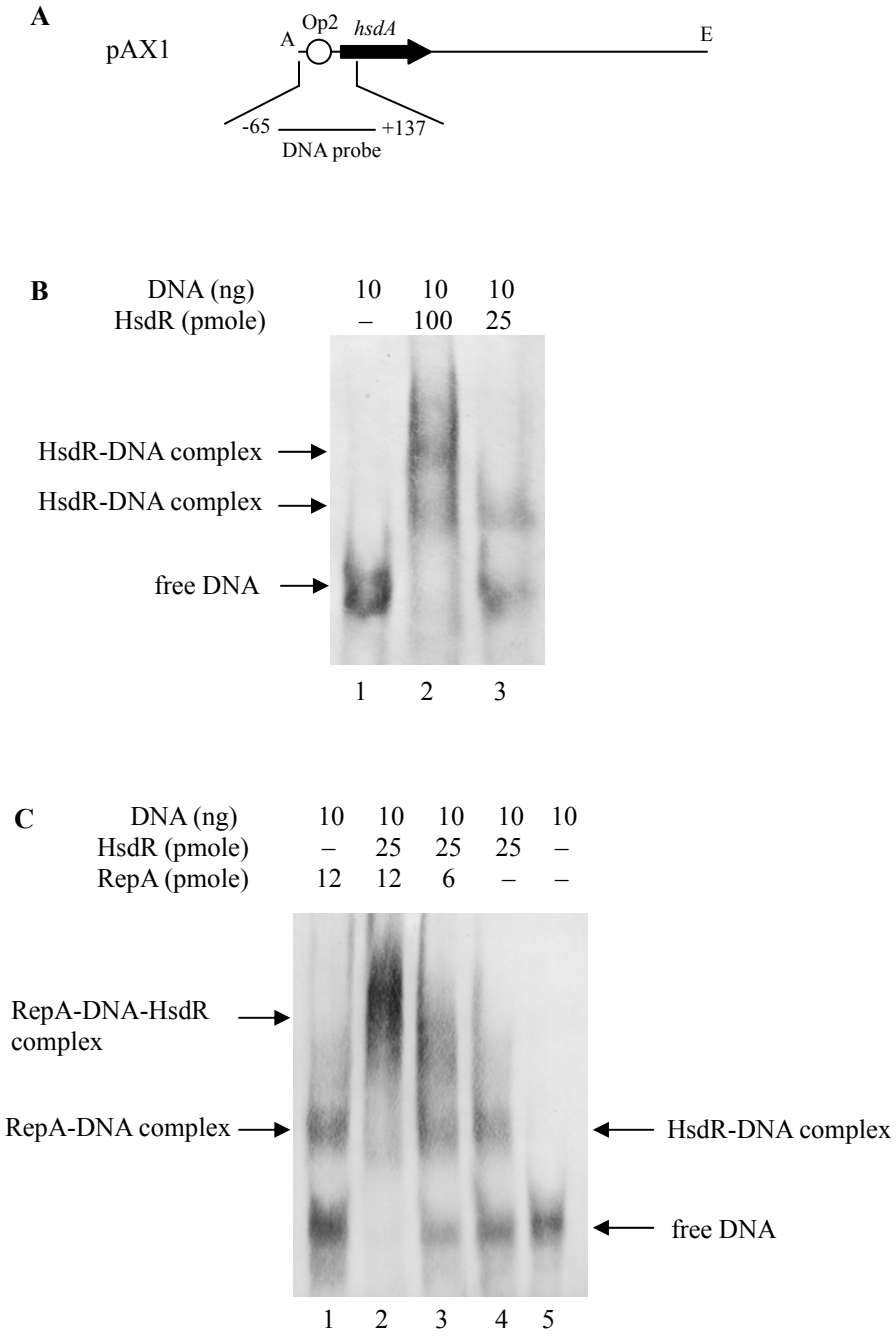

Fig. 3-7. HsdR binds to the *hsdA* promoter region. A, a 203-bp DNA fragment from -65 to +137 relative to the transcriptional start site of the *hsdA* promoter was used as DNA probe for HsdR-DNA binding. B, 10 ng of DNA probe containing the *hsdA* promoter was incubated with different amounts of HsdR protein. Compared to free DNA (lane 1), HsdR-DNA binding leads to a shift of the corresponding bands (lanes 2 and 3). C, different concentrations of purified RepA were added to the HsdR-DNA reaction mixtures. Compared to the control (lane 5), RepA and HsdR were shown to bind to different sites of the *hsdA* promoter (lanes 1 to 4) (for details see text).

3.1.5 Interaction between HsdR and RNA polymerase

To determine HsdR as an activator at the transcription level for the target gene, binding activity of HsdR and RNA polymerase was measured (Fig. 3-8). In this ELISA experiment, two distinct negative controls were set up, one with no RNA polymerase coated to the wells and no HsdR protein added, and the other with only HsdR protein (20 ng) added. As shown in Fig. 3-8, the optical density value with 20 ng HsdR and 300 ng RNA polymerase was approximately 3-fold of that with 0.625 ng HsdR. At the same time the value gradually decreased with decreasing amounts of HsdR protein as shown in Fig. 3-8. This indicates that HsdR binds to RNA polymerase, thereby potentially increasing the concentration of RNA polymerase in the promoter domain of the target gene and enhancing its expression.

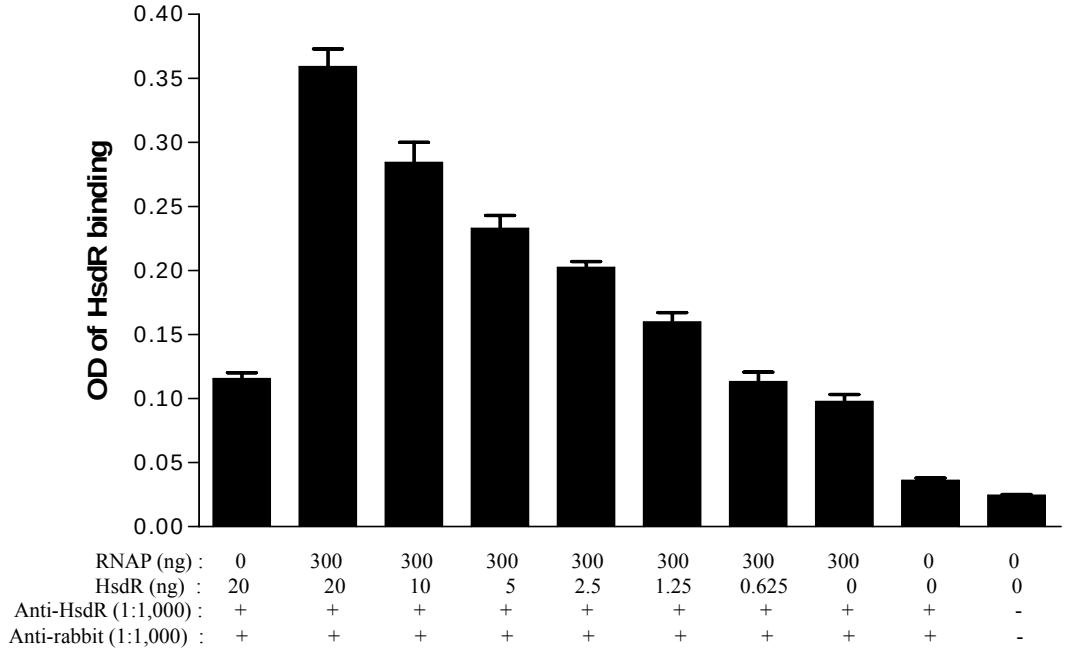

Fig. 3-8. HsdR interacts with RNA polymerase. RNA polymerase (RNAP) was first coated onto the ELISA plates followed by addition of various concentrations of HsdR protein. After incubation with primary antibodies against HsdR, peroxidase-conjugated swine anti-rabbit immunoglobulin (anti-rabbit) was added as secondary antibodies. Finally, the samples were assayed in an ELISA reader (BIO-RAD). A clear and concentration dependent binding of RNAP to HsdR is seen. Bars represent the average and standard deviation of at leat three independent measurements.

3.1.6 HsdR is Essential for the Induced Expression of the *hsdA* Gene

To elucidate if HsdR is involved in the induction of *hsdA* expression, an *hsdR* gene knock-out mutant of *C. testosteroni* (CT-HsdR-Ko) was prepared by homologous integration. Wild type *C. testosteroni* and the *hsdR* knock-out mutant strain CT-HsdR-Ko were induced overnight with 0.5 mM testosterone, and ELISA was used to measure *hsdA* expression. As shown in Fig. 3-9, the expression levels of 3α-HSD/CR with testosterone induction in wild type *C. testosteroni* was 30-fold higher that that in the absence of testosterone, which was not the case in the *hsdR* knock-out mutant (about 4-fold higher than that without testosterone induction). Furthermore, in the absence of the inducer testosterone, 3α-HSD/CR expression in both the wild type strain and the *hsdR* knock-out mutant was at the same basal level. Obviously, testosterone binding to RepA decreases its affinity to the operators Op1 and Op2 such that the loop unfolds. As a consequence, the *hsdA* promoter becomes accessible for the transcription factor HsdR which can perform its function to enhance 3α-HSD/CR expression. According to this result, HsdR is a critical factor for *hsdA* gene regulation.

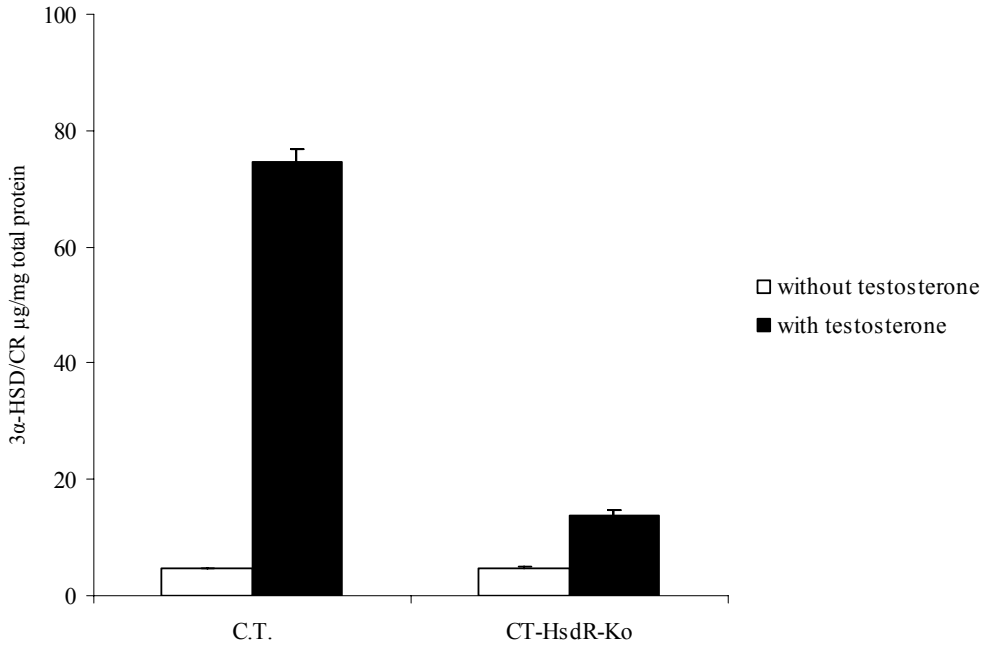

Fig. 3-9. HsdR is necessary for the induced expression of 3α-HSD/CR. ELISA revealed that after testosterone induction 3α-HSD/CR expression increased considerably in wild type *C. testosteroni,* compared to that observed in *hsdR* knock-out mutants. In the absence of the steroidal inducer testosterone, 3α-HSD/CR expression in *hsdR* knock-out mutants and in wild type cells occurred at the same basal level. Bars represent the average and standard deviation of at leat three independent measurements.

3.1.7 HsdR Expression is not Induced by Testosterone

To determine whether the expression of HsdR itself is sensitive to testosterone induction, the amount of HsdR in *C. testosteroni* was measured by ELISA with respective primary antibodies. After addition of testosterone, 3α-HSD/CR expression increased, whereas HsdR expression did not change (Fig. 3-10). This reveals that HsdR expression is not induced by testosterone in *C. testosteroni*.

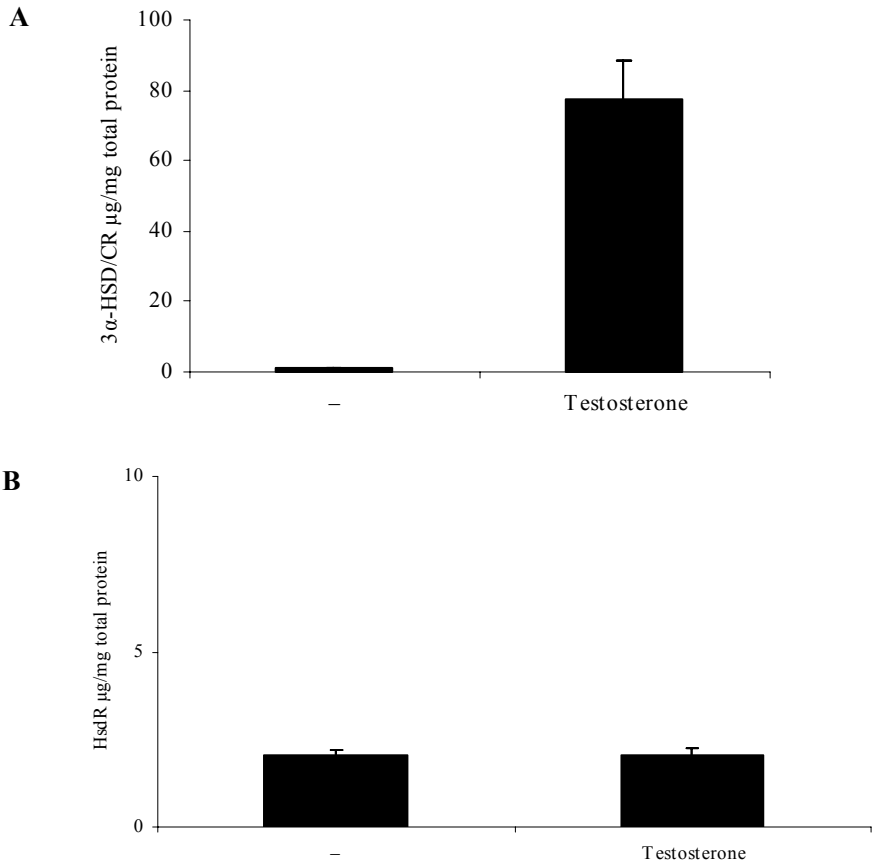

Fig. 3-10. 3α-HSD/CR but not HsdR expression is induced by testosterone. 3α-HSD/CR and HsdR expression in *C. testosteroni* was determined by ELISA. Whereas 3α-HSD/CR expression was induced by testosterone (A), HsdR expression did not change upon testosterone induction (B). Bars represent the average and standard deviation of at leat three independent measurements.

3.2 HsdR Negatively Regulates its Own Expression

3.2.1 Binding of HsdR to the *hsdR-SDRx* Intergenic Region

The specific interaction between HsdR and the *hsdR-SDRx* intergenic region was demonstrated by electrophoretic mobility shift assays. A 200-bp DNA fragment containing 107-bp *hsdR-SDRx* intergenic region was labeled with digoxigenin and incubated with purified HsdR protein. After electrophoresis, formation of the HsdR-DNA complex was seen as shifted bands in Fig. 3-11. The extent of the shifted bands became weaker upon reducing the amount of HsdR protein. To prove the specificity of HsdR-DNA binding, 100-fold unlabeled DNA probe was added to the mixtures (Fig. 3-11). In such case, the shifted band disappeared. This result shows that HsdR binds to its own promoter region.

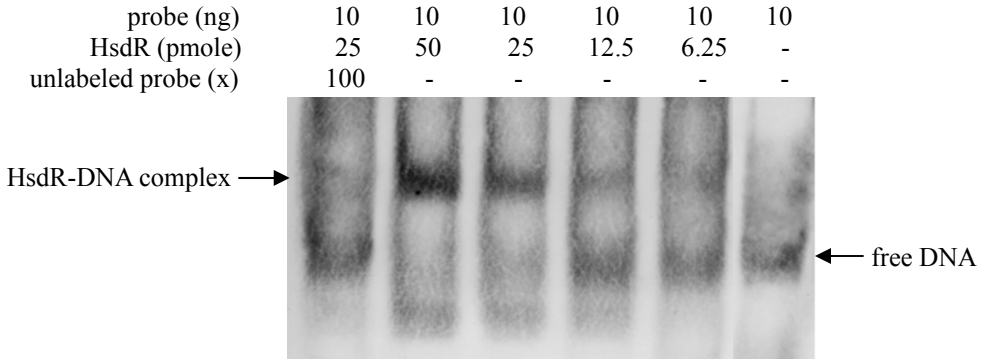

Fig. 3-11. HsdR binds to the *hsdR-SDRx* intergenic region. After incubation of 200-bp DNA probe with HsdR protein, the reaction mixtures were subjected to native PAGE. The DNA bands transferred onto nitrocellulose membrane were analyzed by chemiluminescence.

3.2.2 Construction of an *hsdR-gfp* Fusion Mutant of *C. testosteroni*

As a positive transcriptional regulator for 3α-HSD/CR expression, HsdR may exist as a multimer to perform its function. To test if HsdR negatively regulates its own expression, an *hsdR-gfp* fusion mutant of *C. testosteroni* was constructed. Plasmid pTOPOHsdRGFP containing the combined HsdR-GFP fragment was transformed into *C. testosteroni* by electroporation. Because this plasmid cannot replicate in *C. testosteroni* but contains the homologous fragment of this strain, it can therefore be integrated into the chromosomal DNA of *C. testosteroni* via homologous recombination. PCR was used to check the integration of plasmid pTOPOHsdRGFP

into the chromosomal DNA of *C. testosteroni.* An *hsdR-gfp* fusion mutant C.T. HsdRGFP2 was obtained.

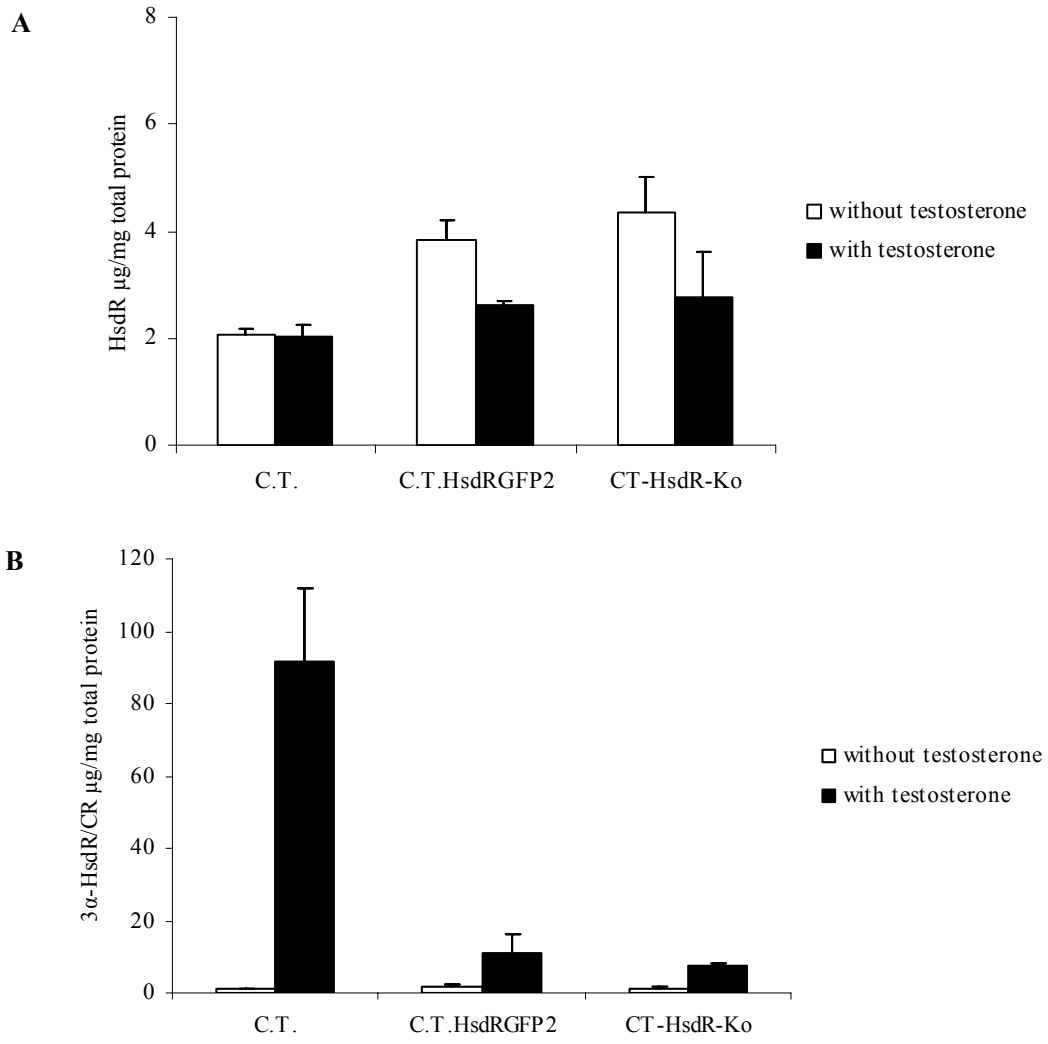

Fig. 3-12. Expression of HsdR and 3α-HSD/CR in the *hsdR* mutant strains of *C. testosteroni*. ELISA was used to measure the expression levels of HsdR (A) and 3α-HSD/CR (B) in wild type and *hsdR* mutant strains of *C. testosteroni*. Bars represent the average and standard deviation of at leat three independent measurements.

3.2.3 Autorepression of HsdR is Prevented in the *hsdR* Gene Mutant Strains of *C. testosteroni*

Since LTTRs often positively regulate their target genes and negatively control their own expression, HsdR may also repress its own expression. To test for HsdR expression in the *hsdR*

knock-out mutant and the *hsdR-gfp* fusion mutant strain, the amount of HsdR expression was detected by ELISA after the mutant strain and the wild type *C. testosteroni* were induced with testosterone. As indicated in Fig. 3-12A, the amount of HsdR in the wild type strain did not change with or without induction by testosterone, while expression of mutated HsdR in the *hsdR* mutant strains was higher than that in the wild type strain without induction by testosterone. This is probably because the HsdR-GFP fusion protein or the disrupted HsdR protein cannot form the correct oligomeric structure as the original HsdR, then the autorepression of HsdR is prevented.

3.2.4 Induction of 3α-HSD/CR Expression Decreased in the *hsdR* Gene Mutant Strains of *C. testosteroni*

The conformation of the mutated HsdR proteins expressed in the *hsdR* mutant strains might be different from that of the original HsdR protein, therefore, it may affect the activity of HsdR. After incubation with 0.5 mM testosterone, 3α-HSD/CR expression in the mutant strains and wild type *C. testosteroni* was measured. ELISA results showed that 3α-HSD/CR expression significantly decreased after testosterone induction, compared to that in the wild type strain as shown in Fig. 3-12B. This probably results from the changed conformation of mutated HsdR proteins, which cannot fold like HsdR to form the correct oligomer and to activate the expression of its target genes.

3.3 Oligomeric State of the HsdR Protein

3.3.1 Construction of *in frame hsdR* Deletion Mutants and Purification of Truncated HsdR Proteins

As described above, HsdR was shown to be a DNA-binding protein. This feature results from its N-terminal winged Helix-Turn-Helix DNA-binding domain, while the C-terminal end was predicted by BLAST to be the substrate binding domain. To test if these two regions are involved in the multimerization of HsdR, we constructed several in frame *hsdR* deletion mutants, HsdRΔN, HsdRΔC and HsdRΔNC, which were deleted for codons 1-86, 221-303, and 1-86 and 221-303, respectively (Fig. 3-13). These truncated alleles were cloned into the pET15b vector and then transformed into *E. coli* BL21(DE3)pLysS. Truncated proteins were overexpressed after induction by 1 mM IPTG, and the corresponding proteins were dissolved with lysis buffer

containing 0.6% SLS and purified through a Ni-NTA His-tag column (Qiagen). The purified proteins were analyzed by 15% SDS-PAGE as indicated below.

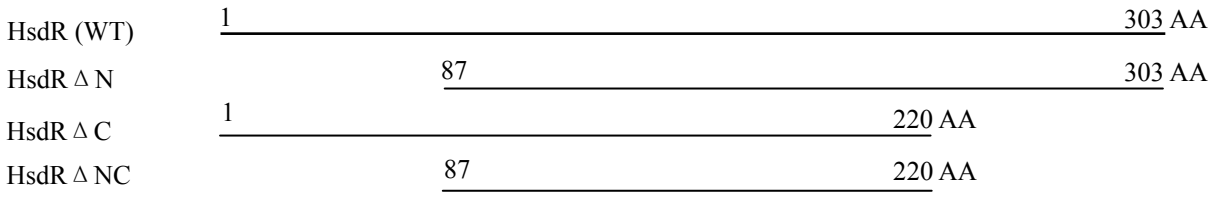

Fig. 3-13. Schematic representation of HsdR and three *in frame hsdR* deletions. WT, wild type; AA, amino acid.

3.3.2 Effect of HsdR Domain Deletions on the Expression of 3α-HSD/CR

To test the effect of different HsdR domain deletions on the transcriptional regulation of 3α-HSD/CR expression, the pK18 descendents pKHsdRΔN, pKHsdRΔC, and pKHsdRΔNC were co-transformed into *E. coli* HB101 with plasmid pAX1, the latter containing the *hsdA* gene together with its regulatory elements. Plasmids pK18 and pKtacHsdR1 were used as the negative and positive control, respectively. ELISA result shows that 3α-HSD/CR expression in *E. coli* HB101 containing pKHsdRΔN, pKHsdRΔC, and pKHsdRΔNC decreased compared to pKtacHsdR1, even lower than that with pK18 (Fig. 3-14). This indicates that all the deleted regions are important for the positive regulation of HsdR on 3α-HSD/CR expression.

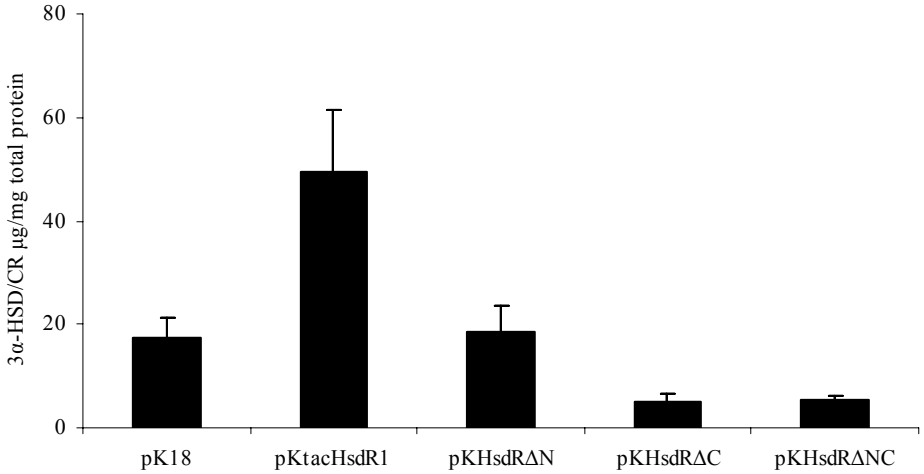

Fig. 3-14. Effect of *in frame hsdR* deletions on 3α-HSD/CR expression. Plasmid pAX1 containing the *hsdA* gene was co-transformed into *E. coli* HB101 with pKtacHsdR1, pKHsdRΔN, pKHsdRΔC, and pKHsdRΔNC, respectively. ELISA was used to quantify 3α-HSD/CR expression. Bars represent the average and standard deviation of at leat three independent measurements.

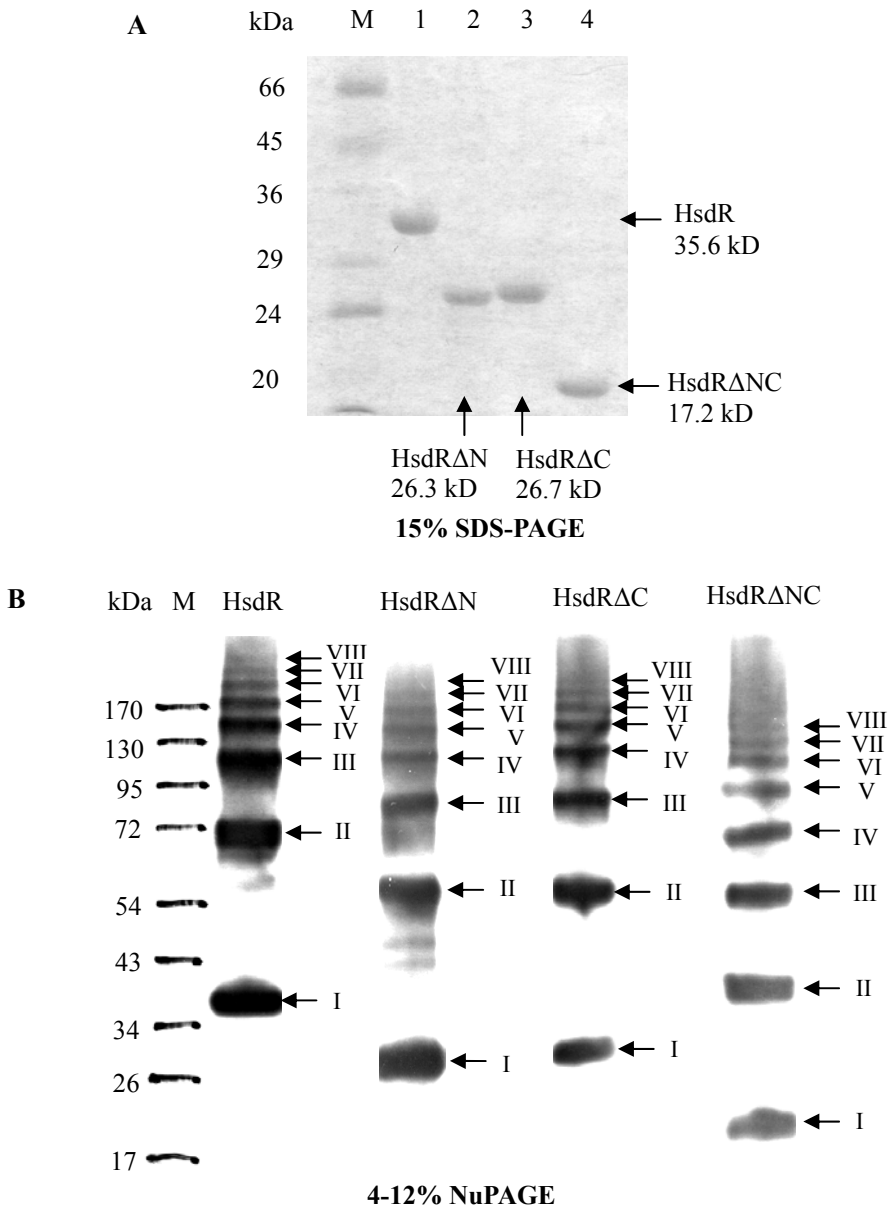

Fig. 3-15. HsdR may exist as an octamer. A, 2 μg of HsdR and its truncated forms were subjected to 15% SDS-PAGE. For each protein, there is only one band (monomer) observed. B, 1 μg of HsdR and its truncated forms were subjected to 4-12% NuPAGE. Interestingly, there are 8 bands observed for each sample.

3.3.3 Oligomerization of the HsdR Protein and Importance of the Central Part of HsdR for its Multimerization

To analyze the multimerization of HsdR and its truncated proteins, all of them were

subjected to polyacrylamide gel electrophoresis. At first 2 μg of HsdR and its truncated forms were analyzed by 15% SDS-PAGE. After gel staining there was only one clear band (monomer) observed for each protein (Fig. 3-15 A). Surprisingly, when the same samples were subjected to 4-12% Nu-PAGE and analyzed by Western blotting using an anti-HsdR polyclonal antibody, there appeared eight bands for each sample (the molecular mass of each band being identical to that of the respective oligomer of HsdR or its truncated forms), even for HsdRΔNC which contains only the central part of HsdR (Fig. 3-15 B). These results reveal that HsdR may exist as an octamer and that the central part of HsdR may be essential for the multimerization of HsdR.

To further determine the oligomerization state of HsdR, the cross-linking reagent DMP was used to identify the multimerization of the purified HsdR protein. After incubation, the reaction mixtures were subjected to SDS-PAGE. As shown in Fig. 3-16, there is one clear band without DMP, representing the HsdR monomer (lane 1). As for HsdR protein treated with DMP, there are three clear bands (corresponding to a dimer, hexamer, and octamer, the latter is the slowest one) in addition to the band of the HsdR monomer. This result also shows that HsdR may exist as an octamer.

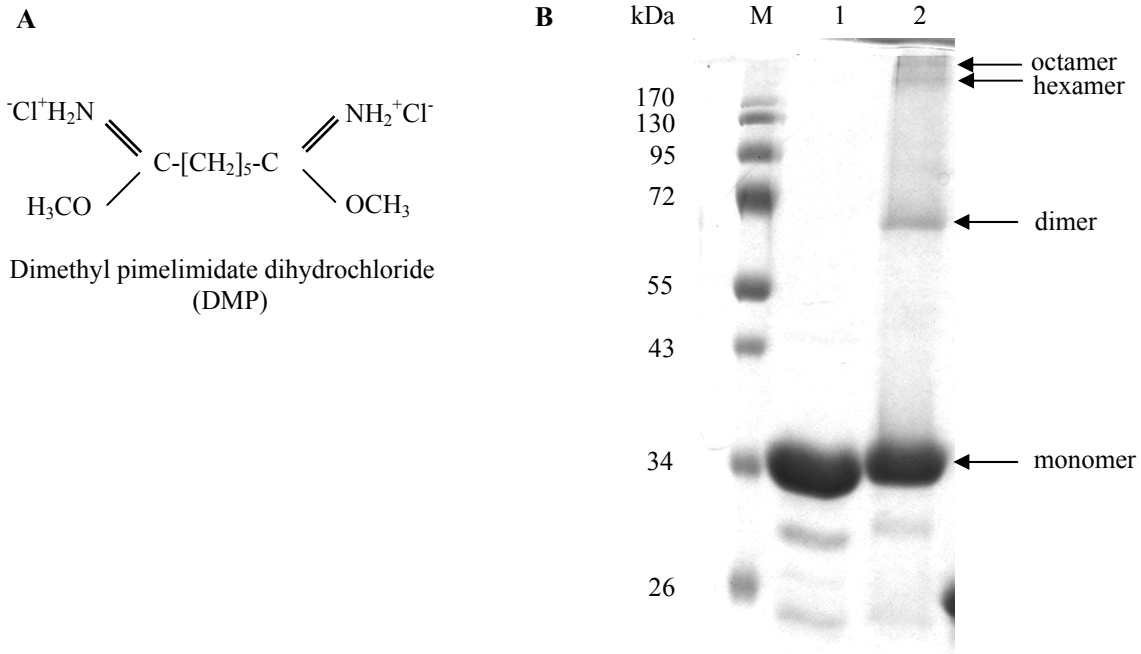

Fig. 3-16. Cross-linking of HsdR with DMP. A, structural formula of dimethyl pimelimidate dihydrochloride (DMP). B. cross-linking of HsdR with DMP. 5 μg purified HsdR protein was mixed with 10 mM cross-linking reagent DMP (lane 2). Lane 1 was without DMP. After incubation at RT for 30 min, the reaction mixtures were subjected to 15% SDS-PAGE.

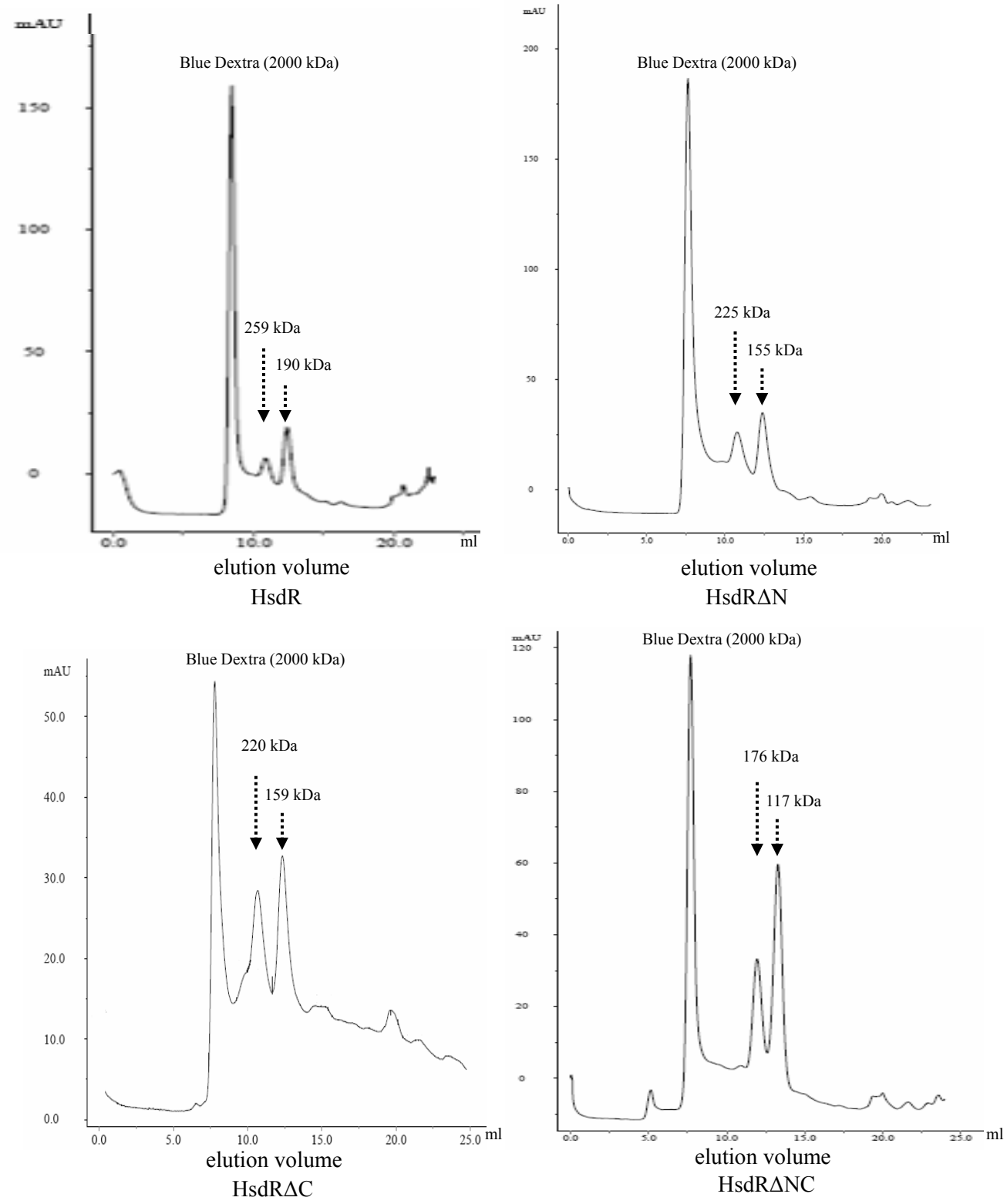

Fig. 3-17. Gel filtration chromatography of HsdR and its truncated forms. Purified proteins were applied to a Superdex 200 column, whereby Dextra served as the control.

SDS-PAGE showed that the molecular mass of one component of HsdR and its truncated forms HsdRΔN, HsdRΔC, and HsdRΔNC is 35.6, 26.3, 26.7 and 17.2 kDa, respectively, which are identical to the molecular weight of these proteins deduced from the amino acid sequence of the respective proteins. Unexpectedly, results based on gel filtration chromatography showed that two peaks are present for each HsdR form. The corresponding molecular masses of these two peaks were: for HsdR 259 kDa and 190 kDa, for HsdRΔN 225 kDa and 155 kDa, for HsdRΔC 220 kDa and 159 kDa, and for HsdRΔNC 176 kDa and 117 kDa (Fig. 3-17), which may represent the octamers and hexamers of the respective forms. Thus, to further understand the active form of HsdR, the purified HsdR protein should be crystalized and/or analyzed by mass spectrometry.

3.4 SDRx is Involved in Steroid Degradation in *C. testosteroni*

3.4.1 Cloning and Sequencing of the *SDRx* Gene

In this study, a novel SDR gene from *C. testosteroni*, *SDRx,* was found to be divergently transcribed from the *hsdR* gene and to locate 3.6 kb downstream of the *hsdA* gene, the latter being extensively characterized in previous work of our group (Fig. 3-1) (Möbus and Maser, 1998; Xiong and Maser, 2001; Xiong *et al*., 2003a, b). The SDRx gene contains 768 base pairs coding for a novel protein of 255 amino acids with a predicted molecular mass of 27 kDa. The GenBank accession number of the nucleotide sequence of *SDRx* is HQ637462.

3.4.2 Sequence Alignments and Phylogenetic Analyses

The deduced amino acid sequence of SDRx reveals that it belongs to the short-chain dehydrogenase/reductase (SDR) superfamily. Some consensus sequences of the SDR superfamily are indicated in the SDRx primary structure in Fig. 3-18. The N-terminal Gly-*X*-*X*-*X*-Gly-*X*-Gly sequence (Gly-13, Gly-17 and Gly-19; numbering according to the SDRx amino acid sequence) is one of the amino acid "fingerprints" of the SDR superfamily that characterizes the cofactor-binding motif. In addition, the conserved Tyr-*X*-*X*-*X*-Lys catalytic motif (Jörnvall *et al*., 1995; Oppermann *et al*., 1997) comprises the catalytically active site in SDRx from *C. testosteroni* (at amino acid positions 160-164). Further SDR sequence motifs found in SDRx are N-N-A-G (around position 96-99) for stabilization of the central β-sheet (Filling *et al*., 2002) and an I-A-V-N sequence preceding the P-G motif for reaction direction (Filling *et al*., 2001) around

position 190, followed by a conserved Thr at amino acid position 195.

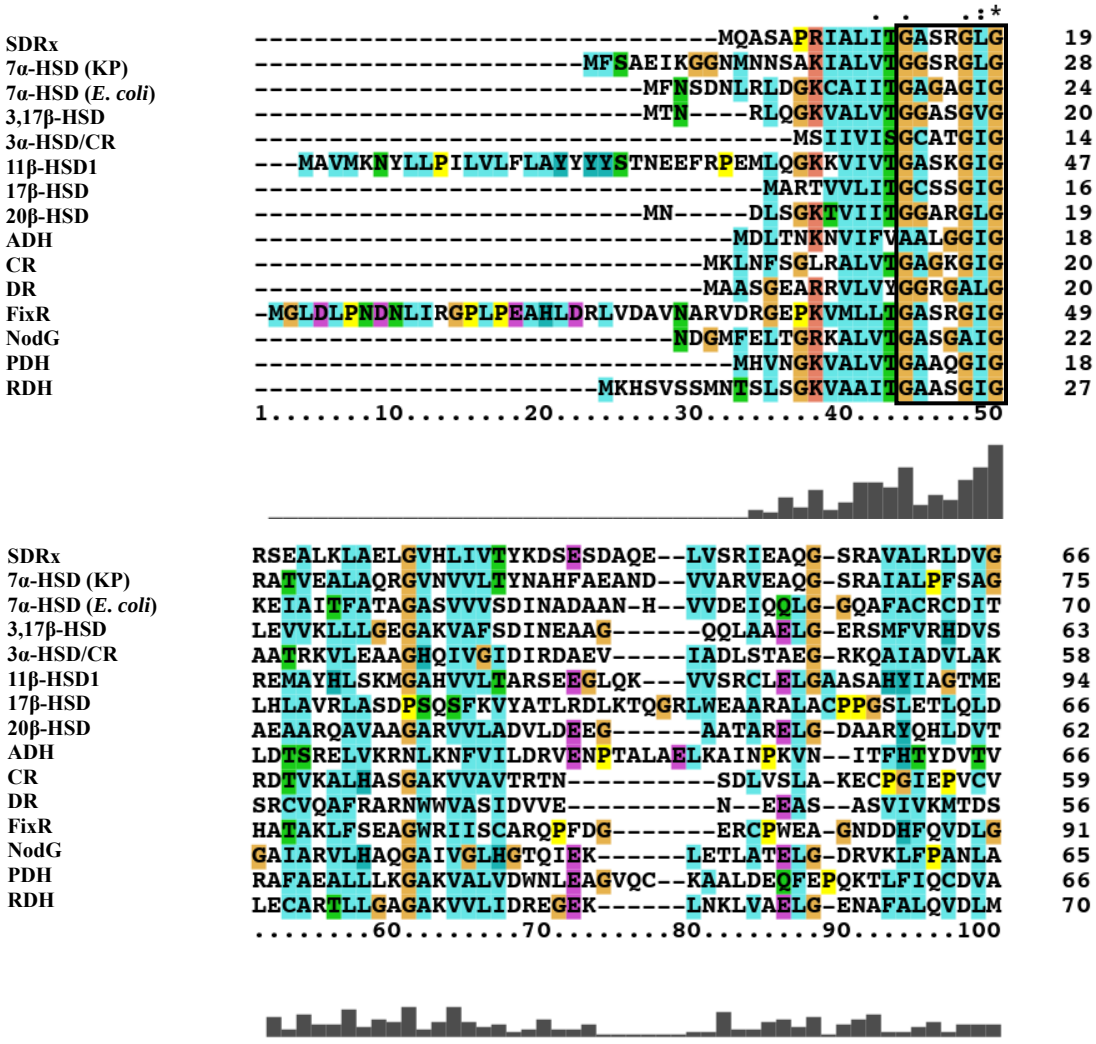

Fig. 3-18. Multiple alignment of amino acid sequences of SDRx and other SDRs. The N-terminal cofactor binding site and the catalytically active site were highlighted by boxes. "*" indicates amino acids identical among all the proteins; ":" and "." indicate amino acids of high and low similarity, respectively. 7*α*-HSD (KP) =7alpha-hydroxysteroid dehydrogenase from *Klebsiella pneumoniae* NTUH-K2044 (GenBank BAH63072.1); 7*α*-HSD (*E. coli*) =7alpha-hydroxysteroid dehydrogenase from *E. coli* (Swiss-Prot P25529); *3,17*β*-HSD* =3β,17β-hydroxysteroid dehydrogenase from *C. testosteroni* (Swiss-Prot P19871.5); *20*β*-HSD* =3*α*,20β-hydroxysteroid dehydrogenase from *S. hydrogenans* (Swiss-Prot P19992); *CR* =carbonyl reductase from mouse lung (PDB 1CYD_A); *NodG* =NodG protein from *Rhizobium meliloti* (Swiss-Prot P06234); *FixR* =FixR protein from *B. japonicum* (Swiss-Prot P05406); *3α-HSD/CR* =3*α*-hydroxysteroid dehydrogenase/carbonyl reductase from *C. testosteroni* ATCC11996 (GenBank AF092031); *PDH* =15-hydroxyprostaglandin dehydrogenase from human placenta (Swiss-Prot P15428); *RDH* =ribitol dehydrogenase from *K. aerogenes* (Swiss-Prot P00335); *17β-HSD* =17β-hydroxysteroid dehydrogenase from human placenta (PDB 1BHS); *11β-HSD1* =11β-hydroxysteroid dehydrogenase from mouse liver (Swiss-Prot P50172); *ADH* =alcohol dehydrogenase from *Drosophila lebanonensis* (Swiss-Prot P10807); *DR* =dihydropteridine reductase from rat liver (Swiss-Prot P11348).

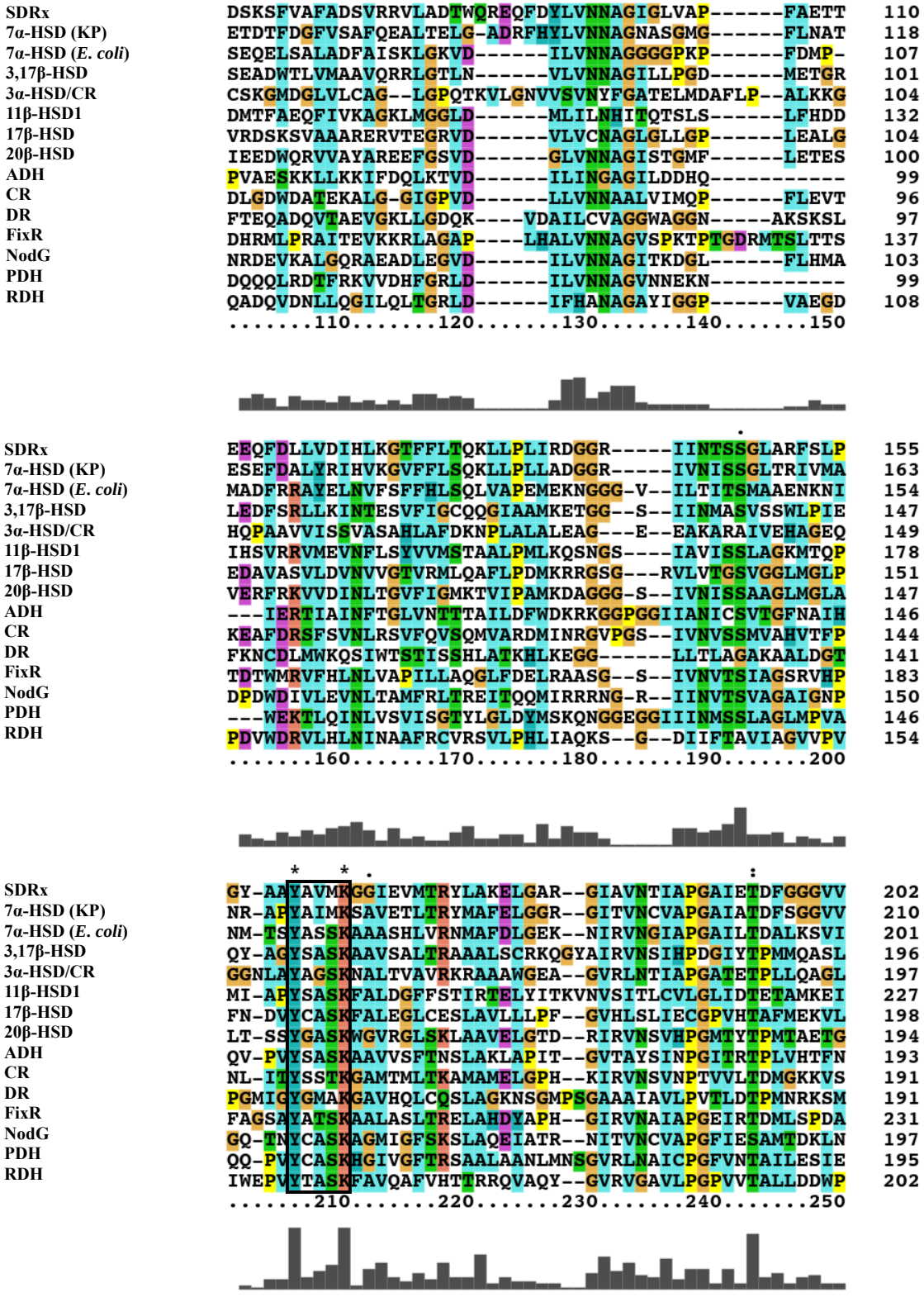

Fig. 3-18. (Continued)

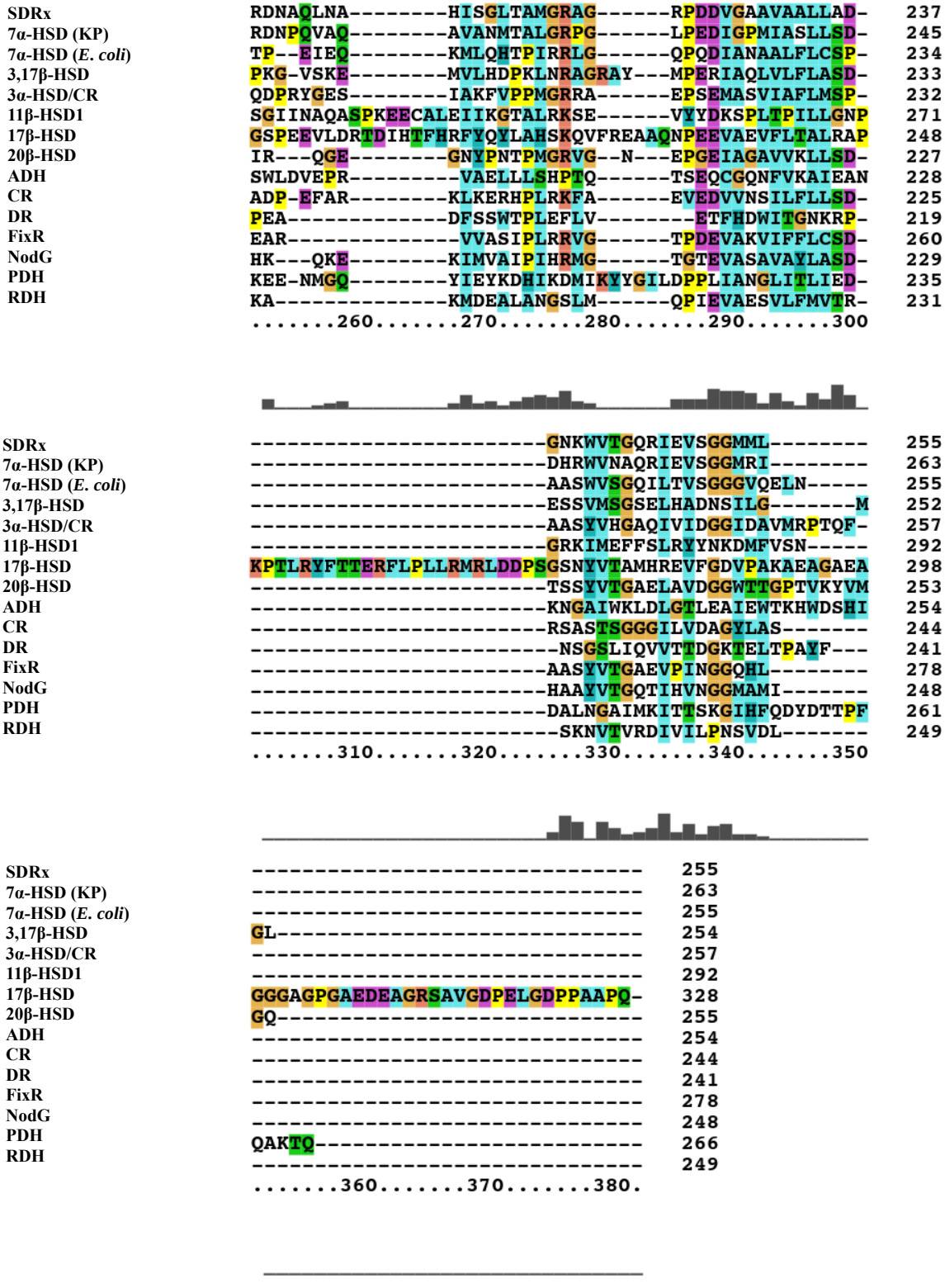

Fig. 3-18. (Continued)

Based on the sequence alignment, a phylogenetic tree was constructed and depicted in Fig. 3-19. According to the bootstrap analyses, SDRx from *C. testosteroni* is seemingly related to 7α-hydroxysteroid dehydrogenase (7α-HSD). The amino acid identity between SDRx and 7α-HSD from *Klebsiella pneumoniae* NTUH-K2044 and between SDRx and 7α-HSD from *E. coli* are 50% and 31%, respectively.

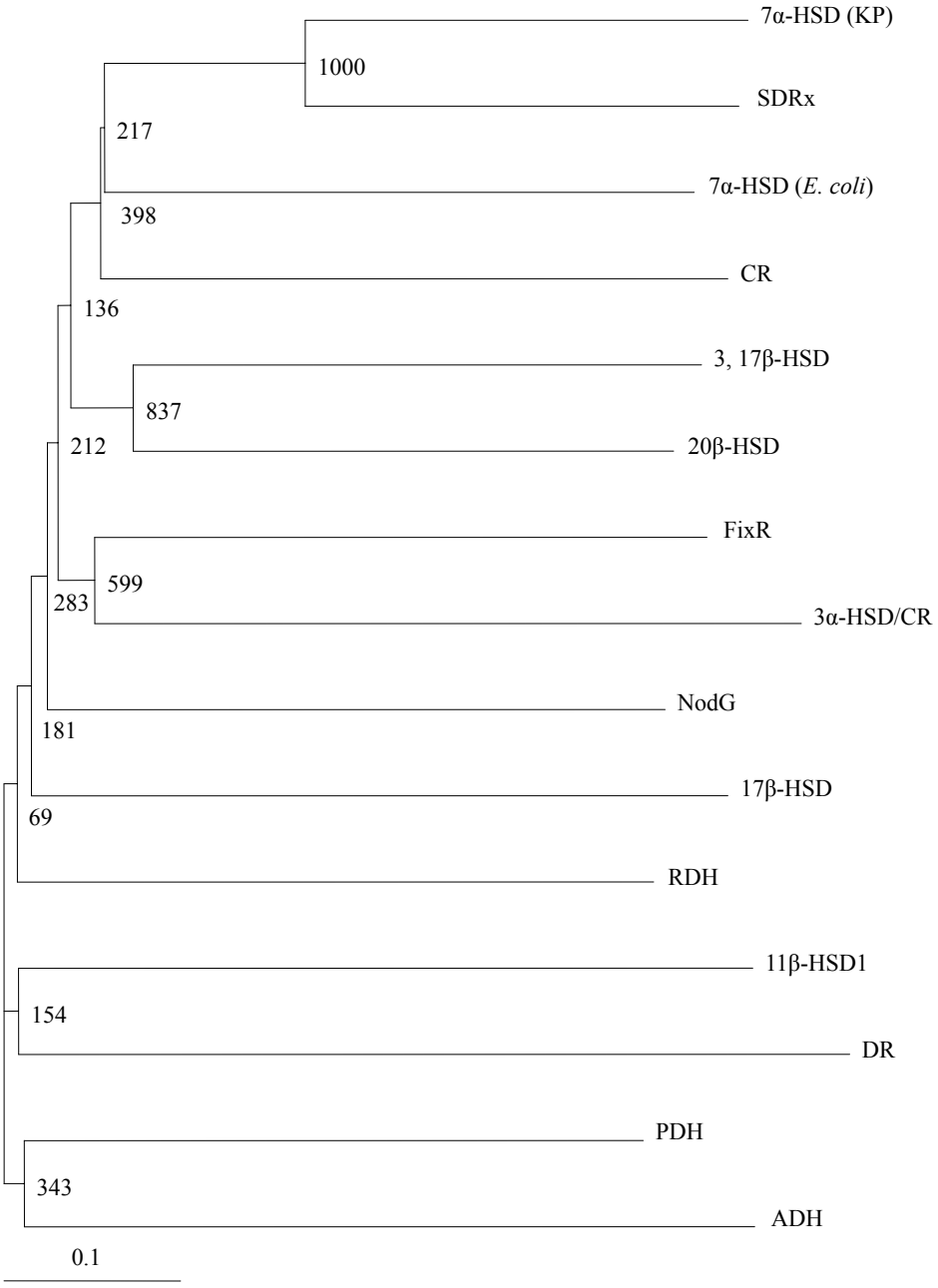

Fig. 3-19. Phylogenetic tree of selected SDR proteins. The tree was constructed by the neighbour-joining method using the CLUSTAL W program. Bootstrap analyses was performed by generating 1000 reiterations. Branch lengths are arbitrary, and bootstrap values are indicated for each node. KP: *Klebsiella pneumoniae* NTUH-K2044.

3.4.3 Preparation of an *SDRx* Disrupted Mutant Strain of *C. testosteroni*

To elucidate the biological function of SDRx, an *SDRx* gene knock-out mutant of *C. testosteroni*, C.T.SDR-6, was prepared by homologous integration. Knock-out plasmid insertion was ensured due to the sensitivity of *C. testosteroni* to kanamycin and due to the kanamycin resistance gene of plasmid pCR2.1-TOPO, which was inserted into the chromosomal DNA during growth of *C. testosteroni* in kanamycin-containing medium. In addition, plasmid integration into the chromosomal DNA was proven by PCR and sequencing. The knock-out strain of *C. testosteroni* was used in subsequent studies for steroid degradation.

3.4.4 Steroid Degradation in the *SDRx* Disrupted Mutant Strain

To test if SDRx is involved in the degradation of steroid compounds such as testosterone or estradiol, HPLC analyses was performed regarding the ability of the *SDRx* knock-out mutant to degrade the steroids. After extraction with ethyl acetate, culture medium samples collected at different time points were subjected to HPLC. The results of steroid degradation are shown in Fig. 3-20 (A and B). After incubation for 12 h, testosterone was completely degraded in wild-type *C. testosteroni*, which was not the case with medium samples from the *SDRx* knock-out mutant strain. Even after 24 h, there is still a small part of testosterone left in the mutant strain medium. With estradiol, the rate of degradation in the *SDRx* mutant strain is also slower compared to that of the wild-type *C. testosteroni*. These results indicate that SDRx is somehow involved in steroid degradation but obviously not absolutely necessary for this pathway.

3.4.5 Growth Impairment of *C. testosteroni* on Steroids after Disruption of the *SDRx* Gene

To further confirm if disruption of the *SDRx* gene affects the utilization of steroids, wild type *C. testosteroni* and the *SDRx* knock-out mutant strain were incubated with 0.5 mM of different steroids overnight. Whereas growth of wild type *C. testosteroni* improved in the presence of the steroids estradiol, testosterone and cholic acid, growth of the mutant strain C.T.SDR-6 with a disrupted *SDRx* gene was impaired with all steroids (Fig. 3-21). This result indicates that the capacity to use steroids in *C. testosteroni* was greatly affected after disruption of the *SDRx* gene.

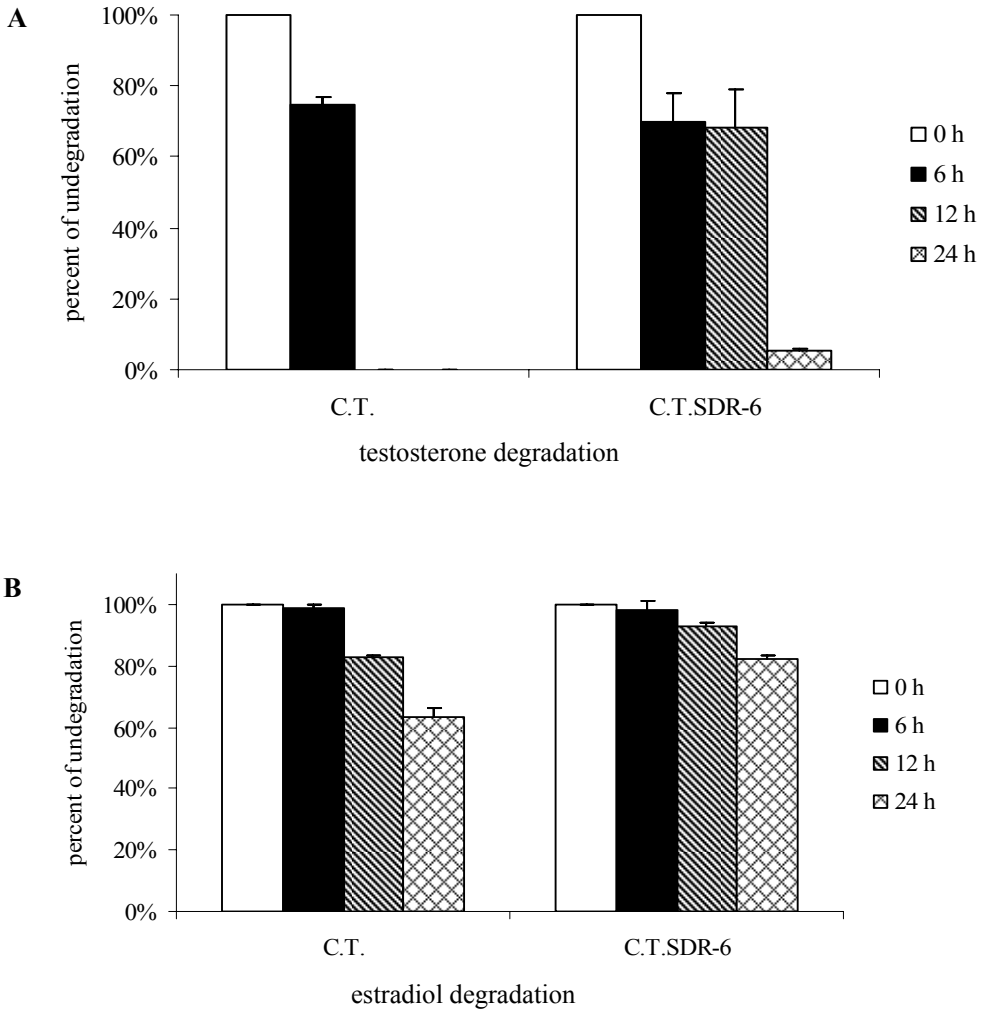

Fig. 3-20. Degradation of testosterone and estradiol in *SDRx* knock-out mutant strain. 0.5 mM testosterone or estradiol was incubated with *C. testosteroni* wild type (C.T.) or the knock-out mutant (C.T.SDR-6), respectively. Degradation of testosterone (A) or estradiol (B) occurred in the mutant strain, however, at lower rates as compared to the wild-type strain. Bars represent the average and standard deviation of at leat three independent measurements.

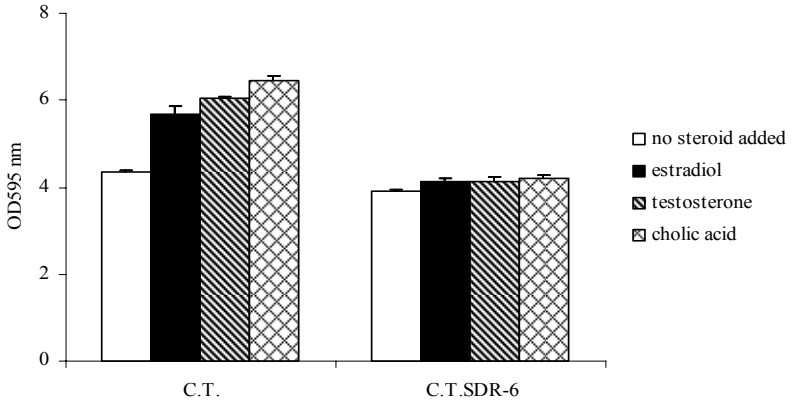

Fig. 3-21. Growth of wild type *C. testosteroni* and the *SDRx* knock-out mutant strain in the presence of various steroids. After incubation with 0.5 mM of steroids, the OD_{595} of cell culture was measured. Bars represent the average and standard deviation of at leat three independent measurements.

3.4.6 Overexpression and Purification of SDRx

The *SDRx* gene from *C. testosteroni* ATCC11996 was subcloned into the vector pET15b and subsequently overexpressed in *E. coli* BL21(DE3)pLysS cells. After incubation with IPTG, recombinant SDRx could be purified in one step by nickel-chelate chromatography. The predicted molecular mass of the SDRx protein (27 kDa) plus its His-tag sequence (2.2 kDa) was calculated to be 29.2 kDa, which corresponds to the protein bands seen on the SDS-polyacrylamide gel (Fig. 3-22).

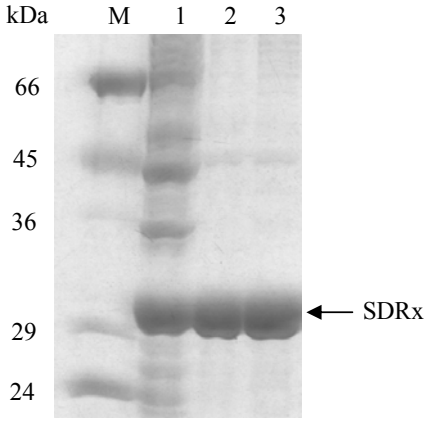

Fig. 3-22. Purification of the SDRx protein under denaturing conditions. The recombinant SDRx protein was purified on a Ni-NTA His tag column. M: molecular mass marker; lane 1, cellular lysate; lane 2, first eluate; lane 3, second eluate.

4. Discussion

The elimination of a wide range of pollutants and wastes from the environment is an absolute requirement to promote a sustainable development of our society with low environmental impact. Biological processes play a major role in the removal of environmental contaminants (Díaz, 2008). Microorganisms capable of utilizing various naturally occurring steroids as carbon and energy sources are relatively widespread in nature (Mahato and Majumdar, 1993; Mahoto and Garai, 1997; Zhang *et al*., 2011). New technological breakthroughs in sequencing, genomics, proteomics, bioinformatics are producing large amounts of information. Genome-based global studies showed that complete assimilation of these substrates is achieved through an adaptive complex metabolic pathway involving many enzymatic steps of oxidation responsible for the breakdown of the steroid nucleus (Leppik and Sinden, 1987; Harder and Probian, 1997; van der Geize *et al*., 2007). The two elements needed for an efficient utilization of steroid compounds by bacteria are the enzymes responsible for their degradation and the regulatory elements that control the expression of the catabolic operons. Until now, catabolic enzymes involved in steroid degradation were extensively studied, but little is known about the regulation mechanism of these enzymes in the degradation pathways. 3α-HSD/CR from *C. testosteroni* involved in the initial step of steroid degradation can be induced by steroids testosterone, progesterone, and cholic acid, and the induction of its expression was controlled by several regulators (Marcus and Talalay, 1956; Oppermann and Maser, 1996; Möbus *et al*., 1997; Xiong and Maser, 2001; Xiong *et al*., 2003a; Göhler *et al*., 2008). In the present study, we focus on characterization of a novel transcriptional regulator HsdR for 3α-HSD/CR expression. In addition, the initial characterization of a short-chain dehydrogenase/reductase gene, *SDRx,* which is divergently transcribed from the *hsdR* gene, was also performed.

4.1 HsdR, a LysR-type Regulator for 3α-HSD/CR Expression

To search for further *cis*- or *trans*-acting elements for 3α-HSD/CR expression which might locate upstream or downstream from the *hsdA* gene, a 5.257-kb *Eco*RI genomic fragment containing *hsdA* was extended leftward or rightward. Sequence analyses revealed that a

LysR-type transcriptional regulator gene (which we later named "*hsdR*") is located 2.58 kb downstream of the *hsdA* gene. The common features of the LTTRs comprise sequence lengths of around 300 residues, conserved N-terminal winged helix-turn-helix (wHTH) motif for DNA binding, an inducer binding C-terminal domain and, with few known exceptions (Sainsbury *et al*., 2009), a homotetrameric quaternary structure of the active species. The HELIXTURNHELIX program (http://www.pasteur.fr) predicted that HsdR contains a winged helix-turn-helix DNA-binding motif in the N-terminal region. Moreover, at the C-terminus a LysR-type substrate binding domain was identified, as revealed by BLAST search. In the course of our further investigation, HsdR was shown to bind to the promoter region of the *hsdA* gene and the binding determinant is distinct from that of RepA at the *hsdA* promoter. Although HsdR is a critical factor for the induction of 3α-HSD/CR expression by testosterone (Fig. 3-9) and HsdR activates 3α-HSD/CR expression in the absence of coinducer (Fig. 3-5 and Fig. 3-6), until now, the appropriate coinducer of HsdR was not found. In general, LysR-type regulators act as tetramers or dimers to perform their function and to recruit RNA polymerase for subsequent gene transcription. Recruitment of RNA polymerase was also shown in this study for HsdR induced *hsdA* expression.

4.2 Production and Purification of Recombinant HsdR Protein

Structural characterization of LysR-type regulators is affected by the fact that many of the family members are insoluble when overexpressed and difficult to obtain in highly purified form. In this study, we also encounter the same problem. Recombinant HsdR protein was present in form of inclusion bodies when induced by IPTG at 37 °C, even after attempting to dissolve it with different detergents such as sodium lauroyl sarcosinate (SLS). To solve this problem, the induction conditions were optimized: HsdR protein was induced at RT overnight and dissolved with SLS. Surprisingly, the solubility of HsdR induced at RT highly increased compared to that induced at 37 °C, especially in the presence of SLS (data not shown). Probably, the low temperature slowed down the speed of protein production and gave the protein enough time to fold properly (Vera *et al*., 2007). As a result, the solubility of the recombinant HsdR protein increased. In addition, we noticed an interesting phenomenon that,

after addition of SLS, the solubility of HsdRΔN and HsdRΔNC induced at RT was almost equal to that induced at 37 °C. In contrast, the solubility of HsdR and HsdRΔC, which harbor the N-terminal DNA binding region compared to HsdRΔN and HsdRΔNC, only increased when they are induced at RT. Thus, the insolubility of LysR-type regulators might be related to their HTH DNA binding motifs.

4.3 Catabolic Operons Controlled by LTTRs

LTTRs constitute the largest family of prokaryotic regulatory proteins identified so far (Pareja *et al*., 2006). The genes regulated by LTTRs have diverse functions including the degradation of organic compounds. In this study, HsdR was identified to regulate the expression of 3α-HSD/CR, which is one of the first enzymes in the steroid-catabolic pathway and also catalyzes the carbonyl reduction of nonsteroidal aldehydes and ketones (Maser *et al*., 2000). In addition, many LTTRs are associated with degradation pathways of aromatic compounds. A large group of LTTRs regulates a single target operon only, such as CatR controlling *catBCA* expression for catechol metabolism in *Pseudomonas putida* (Rothmel *et al*., 1990). Operons such as the *clcABDE* operon of plasmid pAC27 (Coco *et al*., 1993), the *tcbCDEF* operon in plasmid pP51 (van der Meer *et al*., 1991) and the *cbnABDE* operon from *Ralstonia eutropha* (Ogawa *et al*., 1999) involved in chlorocatechol metabolism were controlled by ClcR, TcbR and CbnR (van der Meer *et al*., 1991; Coco *et al*., 1993; Ogawa *et al*., 1999). Two paralogous LTTRs, BenM and CatM from *Acinetobacter* sp. strain ADP1 controlling the expression of several operons involved in benzoate degradation, were extensively studied (Roméro-Arroyo *et al*., 1995; Collier *et al*., 1998). AtzR controlling the *atzDEF* operon is required for cyanuric acid mineralization to carbon dioxide and ammonium in *Pseudomonas* sp. ADP (Wackett *et al*., 2002). TsaR controlling *tsaMBCD* is involved in the degradation of *p*-toluenesulfonate (TSA) in *C. testosteroni* T-2 (Cook *et al*., 1999; Tralau *et al*., 2003a, b). NahR controlled the expression of two plasmid-borne operons, *nah* and *sal*. 14 enzymes encoded by these two operons are required for metabolism of naphthalene or salicylate (Yen and Gunsalus, 1982; Yen and Gunsalus, 1985; Schell, 1990).

In general, LTTRs were described as transcriptional activators of a single divergently transcribed gene, which exhibited negative autoregulation (Lindquist *et al*., 1989; Schell, 1993; Parsek *et al*., 1994). Extensive research has now led to them being regarded as global transcriptional regulators, acting as either activators or repressors of single or operonic genes; they are often divergently transcribed but can be located elsewhere on the bacterial chromosome (Heroven *et al*., 2006; Hernández-Lucas *et al*., 2008). In this study, the target gene *hsdA* was located 2.58 kb upstream of the *hsdR* gene on the *C. testosteroni* chromosome. In addition, a further short-chain dehydrogenase/reductase gene, *SDRx*, was found to be divergently transcribed from the *hsdR* gene. SDRx is seemingly related to 7α-HSDs as revealed by phylogenetic analyses. 7α-HSD is an NADP(H)-dependent oxidoreductase belonging also to the short-chain dehydrogenase/reductase (SDR) superfamily (Tanaka *et al*., 1996). Interestingly, degradation velocities of the steroids cholic acid, testosterone and estradiol decreased in *SDRx* knock-out mutant of *C. testosteroni* (Gong *et al*., 2010). Gel mobility shift assays showed that HsdR also binds to the *hsdR-SDRx* intergenic region (Fig. 3-11). In addition, a putative HsdR binding motif was found to be present in both the *hsdA* promoter (TAC-N_7-GTTT, from position -56 to -43) and the *hsdR-SDRx* intergenic region (TAC-N_7-GTGA, from -72 to -59). Combined, the expression of the *SDRx* gene seems also to be regulated by HsdR. Thus, studies should be further performed to determine the relationship between HsdR and SDRx.

4.4 Autorepression of LTTRs

In general, LTTRs negatively regulate their own expression upon binding to their own promoters (Lindquist *et al*., 1989; Schell, 1993; Parsek *et al*., 1994). It has been demonstrated that there are two conserved binding sites repressor binding site (RBS, -80 to -50) and activation binding site (ABS, -50 to -20) in the target promoters controlled by LTTRs (Schell, 1993; Parsek *et al*., 1994). RBS was characterized by the presence of T-N_{11}-A binding motif (LTTR box). In this study, HsdR binding to the *hsdR-SDRx* intergenic region was demonstrated by EMSA. Sequence analyses indicated that there are ten T-N_{11}-A putative binding sites (PS) in the 107-bp *hsdR-SDRx* intergenic region (Fig. 4-1). In addition, the

putative -10 and -35 elements of *hsdR* and *SDRx* promoters were also predicted, which are overlapping with several putative binding sites (Fig. 4-1). Thus, the expression of the *hsdR* and *SDRx* genes can be affected upon HsdR binding to the *hsdR-SDRx* intergenic region. In the present study, mutated HsdR expression increased in the *hsdR* mutant strains when compared to that in the wild type strain. This is probably because the structure of the mutated HsdR proteins cannot correctly fold like the original HsdR, and then its binding ability and activity are altered. Thus, it provided a possibility for the inhibition of HsdR autorepression in the *hsdR* mutant strains of *C. testosteroni*. Until now, it remains unclear which putative site is corresponding to RBS or ABS of LTTRs. The exact binding pattern of HsdR at this specific region should be elucidated by DNase I footprinting and point mutations.

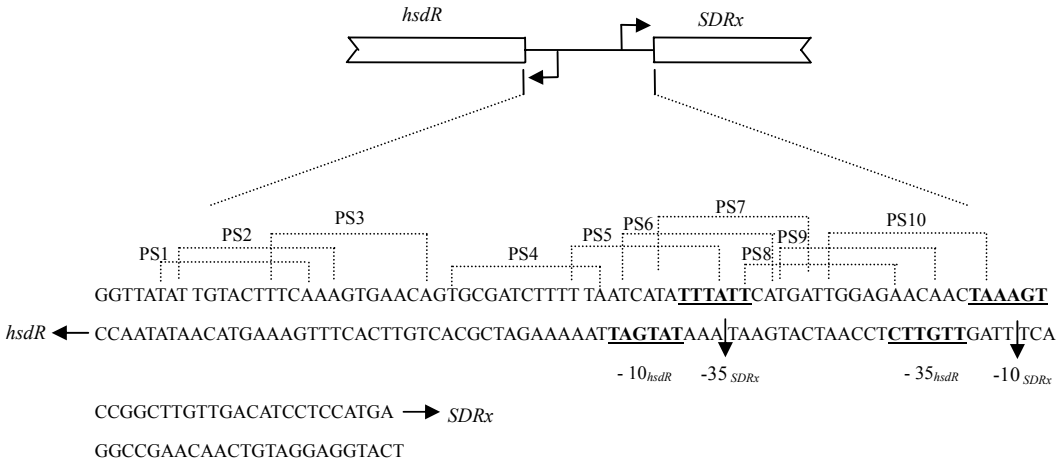

Fig. 4-1. Ten putative LTTR binding motifs (T-N_{11}-A) exist in the *hsdR-SDRx* intergenic region. The putative -10 and -35 elements of the *hsdR* and *SDRx* promoters are underlined in bold. PS: putative binding site.

4.5 Multimerization of LTTRs

In the present investigation, HsdR, an LTTR from *C. testosteroni*, was identified as a positive transcriptional regulator for *hsdA* expression, while it is important to understand the exact regulatory mechanism of HsdR including the active form of HsdR. Phylogenetic analyses revealed that HsdR is related to CrgA, which exists as a homooctamer. Western blotting analyses of HsdR and its truncated proteins revealed that HsdR may form a homooctamer and become a new member of the subclass of LTTRs that form octamers. Unexpectedly, HsdRΔN, which is the N-terminal DNA-binding domain deletion allele of HsdR, and HsdRΔC, in

which part of the C-terminal regulatory domain is deleted, have been shown to still exist as an octamer. This is even the case with HsdRΔNC containing the central part of HsdR. These results revealed that the central part of HsdR plays a pivotal role in the multimerization of HsdR. Gel filtration chromatography results indicated that there are two predominant oligomers present for each protein in solution, which are corresponding to octamers and hexamers of the respective proteins, respectively. Until now, little is known about whether the hexamer is the active form of HsdR or not, and why the oligomeric state of HsdR and its truncated proteins is similar to each other. These questions should be elucidated by the crystal structure of HsdR protein.

As an LTTR, HsdR positively regulates *hsdA* expression and may also perform negative autoregulation. As shown in the present study, HsdR may exist as a multimer to activate *hsdA* expression, and to repress its own expression. The conformation of the HsdR-GFP fusion protein might be changed compared to the original HsdR protein, which then may affect the oligomeric state of HsdR protein, such that it cannot bind to the target promoters with the correct form. Finally its activity is inhibited. This was confirmed in both the *hsdR-gfp* fusion mutant and the *hsdR* gene knock-out mutant strain of *C. testosteroni*. After testosterone induction, 3α-HSD/CR expression significantly decreased compared to the wild type *C. testosteroni*. Whereas, HsdR expression increased in the *hsdR-gfp* fusion mutant and the *hsdR* gene knock-out mutant strain of *C. testosteroni*, because autorepression of HsdR was impaired.

4.6 Electrophoresis of HsdR with NuPAGE

Interestingly, the results of HsdR and its truncated proteins analyzed by SDS-PAGE are dramatically different from that obtained by NuPAGE. With SDS-PAGE, all proteins were denatured and finally only monomer bands were observed. In contrast, there are eight bands for each protein after analyses by NuPAGE and Western blotting. NuPAGE® Bis-Tris Gels (Invitrogen) used in the present study are discontinuous SDS-PAGE systems that operate in the same way as the traditional Tris-Glycine system, but are cast at a lower pH (pH 6.4, and

the gel of the traditional Tris-Glycine system is cast at pH 8.8), which allows for better protein stability during the run. Furthermore, the sampling buffer of NuPAGE gels does contain lithium dodecyl sulphate, but not SDS. After mixing with the sampling buffer, HsdR or its truncated forms were incubated at 72 °C for 10 min, but not heat at 95 °C for 3 min. Thus, during electrophoresis with the NuPAGE gels, the octamer of HsdR may gradually dissociate, which is the reason why the octamer band of each protein is not as clearly visible as the other bands.

4.7 SDRx and the Catabolism of the Steroid Cholic Acid

Despite a residue identity level of only 20-30% between different SDR members, the N-terminal cofactor-binding motif Gly-*X*-*X*-*X*-Gly-*X*-Gly and the catalytic Tyr-*X*-*X*-*X*-Lys motif in all members of the SDR superfamily are well conserved, and the primary structure of SDRx revealed that it belongs to this superfamily. According to phylogenetic analyses, SDRx is seemingly a microbial 7α-hydroxysteroid dehydrogenase (7α-HSD). 7α-HSDs are NADP(H)-dependent oxidoreductases belonging to the SDR superfamily (Tanaka *et al*., 1996). They are widespread among bacterial species such as bacteroides and clostridia and do also occur in *E. coli* and *Ruminococcus* (Akao *et al*., 1987; Coleman *et al*., 1988; Bennett *et al*., 2003). 7α-HSDs catalyze the dehydrogenation of the hydroxyl group at position 7 of the steroid skeleton of bile acids (Tanaka *et al*., 1996). Bile acids are saturated, hydroxylated C-24 cyclopentano-phenanthrene sterols synthesized from cholesterol in hepatocytes. The two primary bile acids synthesized in the human liver are cholic acid (3α, 7α, 12α-trihydroxy-5β-cholan-24-oic acid) and chenodeoxycholic acid (3α, 7α-dihydroxy-5β-cholan-24-oic acid). In humans, bile acids are further metabolized by the liver via conjugation to glycine or taurine. Ridlon *et al*. reported that, in the human intestinum, oxidation of the hydroxyl groups at C-3, C-7 and C-12 of bile acids are carried out by microbial 3α-HSD, 7α-HSD and 12α-HSD, which indicates that the metabolism of bile acids in microorganisms occurs via several pathways (Ridlon *et al*., 2006). Therefore, microbial catabolism of bile acids may still occur, even if one of the above dehydrogenase genes is disrupted.

Accordingly, in our study, growth of an *SDRx* knock-out mutant on cholic acid and other steroids was impaired, because the 7α-HSD reaction could not be performed. However, although being affected, the mutants could grow on steroids, possibly because the steroids could be degraded via alternative pathways. In addition, the rate of metabolism of testosterone or estradiol in the *SDRx* knock-out mutant strain of *C. testosteroni* was slower than that in the wild type strain. Also here, both steroids were finally completely degraded upon longer incubation times. This also indicates that SDRx may be involved in the degradation of steroids in *C. testosteroni,* but testosterone or estradiol might also be catabolized by other pathways.

4.8 Global Regulation of 3α-HSD/CR Expression

With two-dimensional electrophoresis our group previously found that the expression of several steroid catabolizing enzymes in *C. testosteroni* ATCC 11996 was induced by testosterone (Marcus *et al*., 1956; Oppermann *et al*., 1996; Möbus *et al*., 1997). Our group then focused on the regulation of the gene (*hsdA*) encoding 3α-HSD/CR, one of the enzymes being considered at the top of the steroid degradation pathway. Previous investigations lead to the identification of two genes coding for negative regulators of *hsdA* expression, *repA* and *repB*, and two operator sequences, Op1 and Op2, upstream from *hsdA*. With these players, a "two repressor model" of *hsdA* regulation was proposed (Xiong and Maser, 2001; Xiong *et al*., 2003a; Xiong *et al*., 2003b). Two palindromic 10-bp motifs Op1 (TCAAAGCCCA) and Op2 (TGGGCTTTGA), working as *cis*-acting operator elements for *hsdA* regulation, were localized at 0.935 kb and 2.568 kb upstream of *hsdA*, respectively. While Op2 overlaps the -10 binding site (TTTGAT) of the σ70 RNA polymerase by 5 bp, RepA was identified to specifically bind to both operators and to force the DNA between Op1 and Op2 to form a loop structure. The resulting DNA-loop-RepA complex strongly blocks transcription of the *hsdA* gene. In the presence of appropriate steroids, however, they bind to RepA, thereby reducing its ability to bind to the operator region (Xiong and Maser, 2001). Upon dissociation of the repressor from the operators, RNA polymerase may bind to the promoter and transcription of 3α-HSD/CR mRNA is initiated. RepB was demonstrated to bind to the

mRNA of 3α-HSD/CR and to interfere with 3α-HSD/CR translation (Xiong *et al*., 2003a). Later, the *teiR* gene encoding a positive regulator of steroid-degrading enzymes, including 3α-HSD/CR, was identified to mediate steroid sensing and signaling in *C. testosteroni* ATCC 11996 via a kinase mechanism (Göhler *et al*., 2008).

A：in the absence of inducing steroids

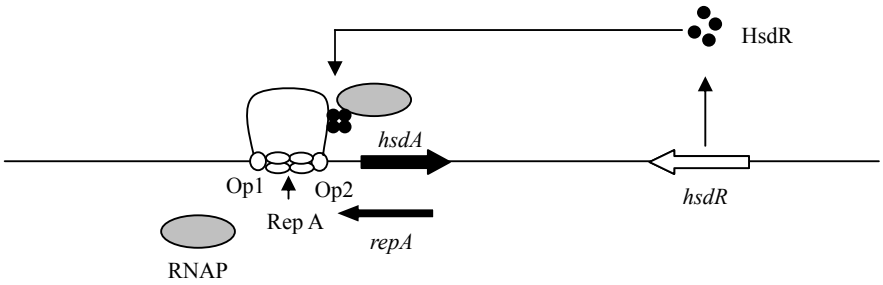

B: in the presence of appropriate steroids

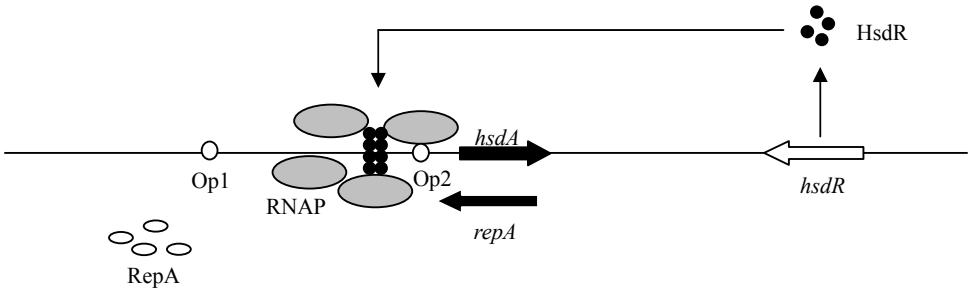

Fig. 4-2. Model for the regulation of *hsdA* expression by HsdR in *C. testosteroni*. A, in the absence of the inducing steroid testosterone, the RepA protein binds to operators Op1 and Op2 and blocks *hsdA* transcription. The loop structure formed by RepA binding does also affect other transcription regulators such as HsdR to activate the *hsdA* promoter. B, in the presence of testosterone, RepA is released from the operators and the loop structure is disrupted. Thus, HsdR can now activate the *hsdA* promoter and recruit RNA polymerase (RNAP) to promote *hsdA* transcription.

Here, the novel transcription factor HsdR was found to serve as an activator of *hsdA* expression and the regulation of *hsdA* expression by HsdR is summarized in Fig. 4-2. In the absence of "inducing" steroids, the transcriptional repressor RepA binds to Op1 and Op2 to form a loop structure which contains the *hsdA* promoter domain. Due to the resulting DNA

configuration, other transcriptional regulators such as HsdR cannot perform their function at the *hsdA* promoter even if already bound to the target promoter. Therefore, 3α-HSD/CR expression is only at basal levels in both wild type *C. testosteroni* and the *hsdR* knock-out mutant strain (cf. Fig. 3-9). In the presence of an inducer such as testosterone, RepA is released from the operators and the loop structure is disrupted, such that HsdR can bind to the *hsdA* promoter and increase the concentration of RNA polymerase at the promoter domain. Finally, *hsdA* expression increases. In conclusion, HsdR is a positive transcription factor for the *hsdA* gene and promotes induction of 3α-HSD/CR expression in *C. testosteroni*.

4.9 LysR-type Transcriptional Regulators in *C. testosteroni* ATCC 11996

It has demonstrated that LTTRs comprise the largest family of prokaryotic regulatory proteins and othologues of these regulators are also found in eukaryote and fungi. In general, LTTRs are present in numerous species of bacteria, such as α-Proteobacteria, β-Proteobacteria and γ-Proteobacteria, and so on (Schell, 1993; Maddocks and Oystom, 2008). Sequence analysis showed that LTTRs have retained a conserved structure and function. Interestingly, multiple paralogues of LTTRs can be present within a given genome, which may result from gene duplication. Subsequent evolutionary pressures and genetic divergence have led to the emergence of groups of orthologous paralogues of LTTRs (Maddocks and Oystom, 2008). Here, 95 LysR-type transcriptional regulator genes were found by analyzing the whole shotgun genome sequence of *C. testosteroni* ATCC 11996, the names of these regulators are arbitrarily designated. The relative information is listed in Table 4-1. Because LTTRs typically regulate the expression of their divergently transcribed genes, so the corresponding divergently transcribed genes of these LysR-type regulators in *C. testosteroni* are included in the table. The length of their amino acid sequences is about 300 AA, and with few exceptions (LysR03 contained 421 AA and LysR95 contained 237 AA). Phylogenetic analyses based on the nucleotide sequence revealed that 95 LysR-type regulators can be divided into three groups, 46 of them form Group I, 26 of them form Group II and 23 of them form Group III (Fig. 4-3). In group I, the divergently transcribed genes of this group of LTTRs are involved in metabolism (catabolic enzymes and substrate transporters), cell division (ATP-dependent

DNA helicase RecG, which is the adjacent gene of LysR55), and cellular mobility. The divergently transcribed genes of Group II regulators are involved in metabolism (catabolic enzymes and substrate transporters), and antibiotic resistance (the divergently transcribed gene of LysR82, beta-lactamase, the presence of which may explain why *C. testosteroni* ATCC 11996 is resistant against antibiotic ampicillin). The functions of genes divergently transcribed from Group III LTTRs include the catabolism and transportation of metabolites. In addition, the functions of some of the LTTR divergently transcribed genes are still unknown.

In general, LTTRs are divergently transcribed from their target genes or operons, but it is not the same case for some LTTRs in *C. testosteroni* ATCC 11996. Here, 15 LysR-type regulators are not divergently transcribed from their adjacent genes: 12 of them marked with * are located at the same strand with their adjacent genes (they have the same transcriptional direction with their upstream and downstream genes). For LysR6 and LysR90, which are marked with #, the transcriptional direction of the upstream genes is opposite to that of both the LysR gene and its downstream gene, while the transcriptional direction of the downstream gene is opposite to that of both the LysR47 gene (marked with §) and its upstream gene. If these LTTRs control the expression of their adjacent genes, the mechanism of regulation may be distinct from the classical regulation mechanism of LTTRs, in which the transcriptional regulation of LTTRs are based on the intergenic region between LTTRs and their divergently transcribed genes. Therefore, these LTTRs may have evolved to use another transcription regulatory way, it should be elucidated by further experiments.

Most LTTRs in *C. testosteroni* have a characteristically high G+C content (above 61%), possibly as a result of low Lys/Arg ratio (Table 4-1): Lys codons contain only A+T, whereas Arg codons contain only G+C. This possibly leads to the selection of Arg over Lys in proteins encoded by high G+C DNA (Maddocks and Oyston, 2008; Viale *et al*., 1991). In addition, the G+C content of some LTTRs is lower than that of the whole genome (61.48%), such as LysR60 (54.74%, and the Lys content is nearly the same as the Arg content (18/19). Interestingly, BLAST analyses revealed that LysR60 is not present in other strains of *C.*

testosteroni, such as *C. testosteroni* KF-1, *C. testosteroni* S44, and *C. testosteroni* CNB-2, thus the LysR60 gene is probably acquired by horizontal gene transfer. Phylogenetic analyses showed that HsdR is closely related to LysR81, which shows 50% nucleotide sequence identity to HsdR, and the G+C content of them is nearly the same (Table 4-1). BLAST results showed that Orthologs of HsdR are present in α-Proteobacteria, β-Proteobacteria and γ-Proteobacteria, which is the same case for LysR81. These results suggest that LysR81 may be the orthologous paralog of HsdR.

The higher Arg content in LysR family members might be related to the specific function of these proteins as transcriptional regulators. Arg residues have been proposed to have at least three specific roles: recognition sites for cell proteases involved in protein turnover, modulating triplets in the control of translation, and positively charged binding sites for proteins that interact with anions (Riordan, 1979). Pherhaps the latter role contributes to the excess of arginines in these DNA-binding proteins, since the guanidinium of Arg, which has the ability to form multiple hydrogen bonds with a phosphate moiety, is better suited than the ε–amino of Lys for interaction with DNA phosphate-containing molecules (Riordan, 1979).

Table 4-1 LTTRs in *C. testosteroni* ATCC 11996

LTTR	G+C content (%)	length (AA)	Lys/Arg (%)	group	divergently transcribed gene
LysR01	61.96	359	11/30 (36.7)	I	formyl-CoA transferase
LysR06#	69.09	302	4/27 (14.8)	I	D-amino-acid dehydrogenase (upstream); ATP-cobalamin adenosyltransferase (downstream)
LysR22	68.19	327	6/29 (20.7)	I	CoA-transferase
LysR41*	65.55	297	5/28 (17.9)	I	phospholipid/glycerol acyltransferase (upstream); hydroxydechloroatrazine ethylaminohydrolase (downstream)
LysR65	60.39	307	14/17 (82.4)	I	5-methyltetrahydropteroyltriglutamate-homocysteine S-methyltransferase
LysR84	62.54	306	4/31 (12.9)	I	orotate phosphoribosyltransferase
LysR09	65.39	312	1/27 (3.7)	I	tRNA-specific 2-thiouridylase MnmA
LysR42	58.13	280	3/13 (23.1)	I	TctC
LysR70	69.76	311	6/27 (22.2)	I	TctC
LysR73	65.19	314	7/33 (21.2)	I	TctC
LysR79	64.69	302	8/20 (40.0)	I	TctC
LysR80	65.57	303	9/24 (37.5)	I	TctC
LysR43*	58.76	315	8/21 (38.1)	I	RNA polymerase, sigma 32 subunit, RpoH (upstream); TctC (downstream)
LysR02	64.52	308	5/19 (26.3)	I	major facilitator superfamily MFS_1
LysR11	67.57	294	3/25 (12.0)	I	extracellular solute-binding protein, family 1
LysR17	63.45	310	7/23 (30.4)	I	sodium symporter
LysR51	62.26	294	8/22 (36.4)	I	amino acid metabolite efflux pump
LysR04	68.09	303	3/25 (12.0)	I	transmembrane pair
LysR38	58.36	296	9/20 (45.0)	I	LivK (leucine ABC transporter)
LysR92*	64.20	310	3/28 (10.7)	I	Molybdenum-pterin binding protein (upstream); ABC transporter ATP-binding subunit (downstream)
LysR20	67.45	298	6/26 (23.1)	I	carbon starvation induced protein
LysR45	58.70	296	8/24 (33.3)	I	fis family transcriptional regulator
LysR48*	64.78	300	6/32 (18.8)	I	MarR family transcriptional regulator (upstream); hypothetical protein (downstream)
LysR55*	63.05	322	13/24 (54.2)	I	ATP-dependent DNA helicase RecG (upstream); Ferritin and Dps (downstream)
LysR13*	64.44	313	5/22 (22.7)	I	ATPase, Mrp (upstream); Respiratory-chain NADH dehydrogenase domain, 51 (downstream)
LysR47§	66.21	293	4/21 (19.0)	I	acyl-CoA dehydrogenase (upstream); aldehyde dehydrogenase (downstream)
LysR60*	54.74	326	18/19 (94.7)	I	short-chain dehydrogenase/reductase SDR (upstream); hypothetical protein (downstream)
LysR61	70.20	301	3/20 (15.0)	I	Permease
LysR62	63.51	295	5/24 (20.8)	I	acyl-CoA dehydrogenase-like protein
LysR72	66.77	315	3/29 (10.3)	I	alcohol dehydrogenase GroES-like protein
LysR54	63.42	297	5/27 (18.5)	I	allantoate amidohydrolase
LysR56	68.04	314	1/27 (3.7)	I	FAD linked oxidase-like protein
LysR66*	64.31	325	4/34 (11.8)	I	Ferrochelatase (upstream); 2OG-Fe(II) oxygenase (downstream)
LysR89	66.24	313	5/26 (19.2)	I	cysteine synthase A
LysR12	70.23	308	1/27 (3.7)	I	diaminopimelate decarboxylase
LysR08	70.47	306	3/27 (11.1)	I	twin-arginine translocation pathway signal
LysR31	66.23	304	5/24 (20.8)	I	LrgA
LysR58	65.84	323	4/27 (14.8)	I	sodium-type flagellar motor component

LysR26	68.78	314	5/24 (20.8)	I	hypothetical protein
LysR37	64.73	326	4/27 (14.8)	I	hypothetical protein
LysR74	64.00	312	4/24 (16.7)	I	hypothetical protein
LysR76	65.58	305	7/18 (38.9)	I	hypothetical protein
LysR77	62.36	316	2/29 (6.9)	I	hypothetical protein
LysR87	66.01	304	4/27 (14.8)	I	hypothetical protein
LysR95	59.94	237	1/19 (5.3)	I	hypothetical protein
LysR03	66.19	421	7/29 (24.1)	II	L-carnitine dehydratase/bile acid-inducible
LysR07*	65.46	302	5/29 (17.2)	II	orotidine 5'-phosphate decarboxylase (upstream); TctC (downstream)
LysR16	67.15	346	3/28 (10.7)	II	UDP-N-acetylglucosamine pyrophosphorylase
LysR19*	63.24	310	4/28 (14.3)	II	diguanylate cyclase with PAS/PAC sensor (upstream); sugar ABC transporterATP-binding protein (downstream)
LysR24*	65.78	300	5/26 (19.2)	II	formyltetrahydrofolate deformylase (upstream); UvrD/REP helicase (downstream)
LysR39	62.58	301	4/28 (14.3)	II	benzoylformate decarboxylase
LysR53	61.24	301	9/21 (42.9)	II	NAD-dependent epimerase/dehydratase
LysR78	56.08	298	5/24 (20.8)	II	peptidyl-arginine deiminase
LysR82	63.89	287	2/26 (7.7)	II	beta-lactamase
LysR34	62.16	302	3/25 (12.0)	II	aldo/keto reductase
LysR68	67.08	318	4/25 (16.0)	II	acyl-CoA dehydrogenase domain-containing protein
LysR21	61.58	307	9/27 (33.3)	II	periplasmic iron binding protein
LysR25	67.44	301	1/29 (3.4)	II	TctC
LysR27	68.47	295	2/21 (9.5)	II	amino-acid ABC transporter binding protein ybeJ precursor
LysR33	64.74	311	11/27 (40.7)	II	phosphonate ABC transporter periplasmic
LysR36	64.78	299	4/25 (16.0)	II	lysine exporter (LYSE/YGGA)
LysR59	65.70	310	4/28 (14.3)	II	major facilitator superfamily MFS_1
LysR91	62.25	316	10/21 (47.6)	II	tripartite ATP-independent periplasmic
LysR23	68.99	300	6/29 (20.7)	II	Pirin-like protein
LysR35	66.77	312	4/27 (14.8)	II	Pirin-like protein
LysR40	56.84	294	9/21 (42.9)	II	UspA
LysR05	65.56	330	3/29 (10.3)	II	hypothetical protein
LysR28	62.04	287	4/9 (44.4)	II	hypothetical protein
LysR29*	64.42	296	8/25 (32.0)	II	hypothetical protein (upstream);
LysR50	57.79	307	13/26 (50.0)	II	hypothetical protein
LysR94	58.01	307	5/25 (20.0)	II	hypothetical protein
LysR14	67.24	291	4/29 (13.8)	III	major facilitator superfamily MFS_1
LysR32	67.40	318	4/27 (14.8)	III	major facilitator superfamily MFS_1
LysR44	61.51	322	7/28 (25.0)	III	major facilitator superfamily MFS_1
LysR75	62.83	303	8/20 (40.0)	III	major facilitator transporter
LysR88	66.88	311	9/27 (33.3)	III	Proline sensor PrlS
LysR15	62.25	305	8/26 (30.8)	III	3-hydroxyacyl-CoA dehydrogenase NAD-binding
LysR30	65.62	288	2/27 (3.4)	III	DSBA oxidoreductase (downstream)
LysR52	63.62	294	7/29 (24.1)	III	GSH-dependent dehydroascorbate reductase
LysR63 (HsdR)	63.71	303	4/27 (14.8)	III	short-chain dehydrogenase/reductase SDRx
LysR64	61.43	311	9/24 (37.5)	III	DSBA oxidoreductase
LysR83	64.44	313	7/28 (25.0)	III	NAD(P)H dehydrogenase (quinone)

LysR86	63.27	313	6/32 (18.8)	III	monooxygenase, FAD-binding protein
LysR90#	62.65	314	7/31 (22.6)	III	LuxR family transcriptional regulator (upstream); alcohol dehydrogenase, zinc-binding protein (downstream)
LysR18	65.47	305	14/26 (53.8)	III	glyoxylate carboligase
LysR67	68.68	297	2/27 (7.4)	III	NAD-dependent epimerase/dehydratase
LysR71	65.17	311	10/31 (32.3)	III	tartrate dehydrogenase
LysR81	63.75	308	10/31 (32.3)	III	alpha/beta hydrolase fold-3 protein
LysR93	61.46	313	6/26 (23.1)	III	alpha/beta superfamily hydrolase
LysR85	57.72	313	7/19 (36.8)	III	(2Fe-2S)-binding protein
LysR10	69.96	303	5/33 (15.2)	III	Pirin-like protein
LysR49	59.85	302	8/28 (28.6)	III	hypothetical protein
LysR57	65.71	314	8/32 (25.0)	III	hypothetical protein
LysR49	59.85	302	8/28 (28.6)	III	hypothetical protein

* indicates LysR genes are located at the same DNA strand with both the upstream gene and the downstream gene;

# indicates the transcriptional direction of the upstream gene is opposite to that of both the LysR gene and its downstream gene;

§ indicates the transcriptional direction of the downstream gene is opposite to that of both the LysR gene and its upstream gene.

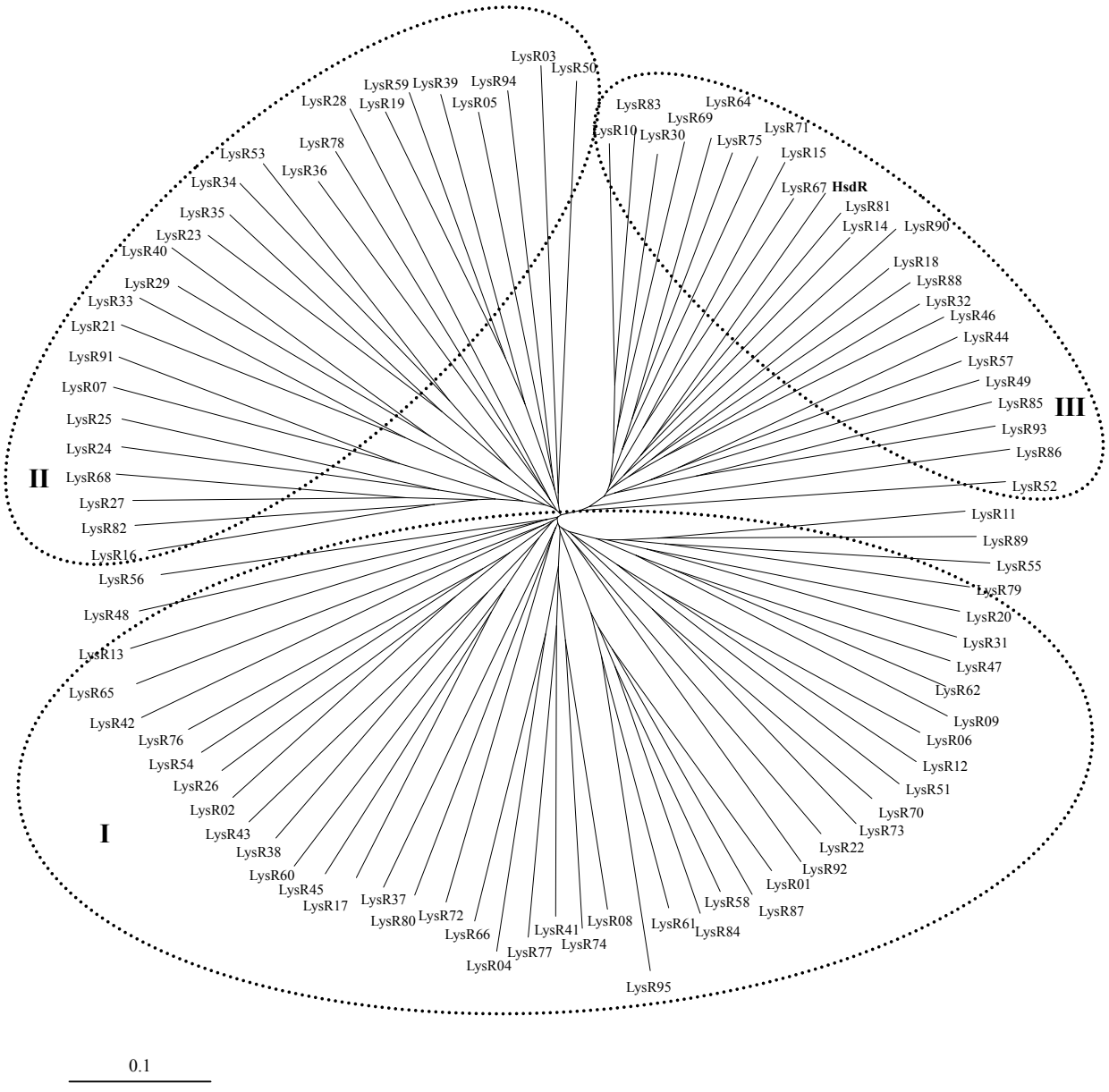

Fig. 4-3. Phylogenetic tree of LTTRs based on the nucleotide sequence. CLUSTAL W was used to construct the phylogenetic tree, which is visualized with Treeview (Page, 1996).

References

Altschul, S. F., Gish, W., Miller, W., Myers, E. W., and Lipman, D. J. (1990) Basic local alignment search tool. *J. Mol. Biol.* 215, 403-410.

Akao, T., Hattori, M., Namba, T., and Kobashi, K. (1987) Enzymes involved in the formation of 3β, 7β-dihydroxy-12-oxo-5β-cholanic acid from dehydrocholic acid by *Ruminococcus sp*. obtained from human intestine. *Biochim. Biophys. Acta.* 921, 275-280.

Aravind, L., Anantharaman, V., Balaji, S., Babu, M. M., and lyer, L. M. (2005) The many faces of the helix-turn-helix domain: transcription regulation and beyond. *FEMS Microbiol. Rev.* 29, 231-262.

Barbaro, D. J., Mackowiak, P. A., Barth, S. S., and Southern, P. M., Jr. (1987) *Pseudomonas testosteroni* infections: Eighteen recent cases and a review of the literature. *Rev. Infect. Dis.* 9, 124-129.

Bartowsky, E., and Normark, S. (1991) Purification and mutant analyses of *Citrobacter freundii* AmpR, the regulator of chromosomal AmpC β-lactamase. *Mol. Microbiol*. 5, 1715-1725.

Balows, A., Trueper, H. G., and Dworkin, M. (1992) A Handbook on the Biology of Bacteria, Ecophysiology, Isolation, Identification and Applications, Springer Verlag, Berlin.

Bell, K. S., Philp, J. C., Aw, D. W. J., and Christofi, N. (1998) The genus *Rhodococcus*. *J. Appl. Microbiol.* 85, 195-210.

Bennett, M. J., McKnight, S. L., and Coleman, J. P. (2003) Cloning and characterization of the NAD-dependent 7α-hydroxysteroid dehydrogenase from *Bacteroides fragilis*. *Curr. Microbiol.* 47, 475-484.

Bradford, M. M. (1976) A rapid and sensitive method for the quantitation of microgram quantities of protein utilizing the principle of protein-dye binding. *Anal. Biochem.* 72, 248-254.

Brennan, R. G., and Matthews, B. W. (1989) The helix-turn-helix DNA binding motif. *J. Biol. Chem.* 264, 1903-1906.

Bundy, B. M., Collier, L. S., Hoover, T. R., and Neidle, E. L. (2002) Synergistic transcriptional activation by one regulatory protein in response to two metabolites. *Proc. Natl. Acad. Sci. U. S. A.* 99, 7693-7698.

Burn, J. E., Hamilton, W. D., Wooton, J. C., and Johnston, A. W. (1989) Single and multiple mutations affecting properties of the regulatory gene *nodD* of *Rhizobium*. *Mol. Microbiol.* 3, 1567-1577.

Byrne, G. A., Russell, D. A., Chen, X., and Meijer, W. G. (2007) Transcriptional regulation of

the *virR* operon of the intracellular pathogen *Rhodococcus equi*. *J. Bacteriol.* 189, 5082-5089.

Cao, H., Krishnan, G., Goumnerov, B., Tsongalis, J., Tompkins, R., and Rahme, L. G. (2001) A quorum sensing-associated virulence gene of *Pseudomonas aeruginosa* encodes a LysR-like transcription regulator with a unique self-regulatory mechanism. *Proc. Natl. Acad. Sci. U. S. A*. 98, 14613-14618.

Choi, H., Kim, S., Mukhopadhyay, P., Cho, S., Woo, J., Storz, G., and Ryu, S. (2001) Structural basis of the redox switch in the OxyR transcription factor. *Cell* 105, 103-113.

Clark, T. J., Momany, C., and Neidle, E. L. (2002) The *benPK* operon, proposed to play a role in transport, is part of a regulon for benzoate catabolism in *Acinetobacter* sp. Strain ADP1. *Microbiology* 148, 1213-1223.

Coco, W. M., Rothmel, R. K., Henikoff, S., and Chakrabarty, A. M. (1993) Nucleotide sequence and initial functional characterization of the *clcR* gene encoding a LysR family activator of the *clcABD* chlorocatechol operon in *Pseudomonas putida*. *J. Bacteriol.* 175, 417-427.

Coco, W. M., Parsek, M. R., and Chakrabarty, A. M. (1994) Purification of the LysR family regulator, ClcR, and its interaction with the *Pseudomonas putida clcABD* chloroactechol operon promoter. *J. Bacteriol.* 176, 5530-5533.

Coleman, J. P., White, W. B., Lijewski, M., and Hylemon, P. B. (1988) Nucleotide sequence and regulation of a gene involved in bile acid 7-dehydroxylation by *Eubacterium* sp. strain VPI 12708. *J. Bacteriol.* 170 2070-2077.

Collier, L. S., Gaines, G. L., and Neidle, E. L. (1998) Regulation of benzoate degradation in *Acinetobacter* sp. strain ADP1 by BenM, a LysR-type transcriptional activator. *J. Bacteriol.* 189, 2493-2501.

Colyer, T. E., and Kredich, N. M. (1994) Residue threonine-149 of the *Salmonella typhimurium* CysB transcription activator: mutations causing constitutive expression of positively regulated genes of the cysteine regulon. *Mol. Microbiol.* 13, 797-805.

Colyer, T. E., and Kredich, N. M. (1994) In vitro characterization of constitutive CysB proteins from *Salmonella typhimurium*. *Mol. Microbiol.* 21, 247-256.

Cook, A. M., Laue, H., and Junker, F. (1999) Microbial desulfonation. *FEMS Microbiol. Rev.* 22, 399-419.

Deghmane, A. E., Petit, S., Topilko, A., Pereira, Y., Giorgini, D., Larribe, M., and Taha, M. K. (2000) Intimate adhesion of *Neisseria meningitidis* to human epithelial cells is under the control of the *crgA* gene, a novel LysR-type transcriptional regulator. *EMBO J.* 19, 1068-1078.

Deghmane, A. E., Giorgini, D., Larribe, M., Alonso, J. M., and Taha, M. K. (2002) Down-regulation of pili and capsule of *Neisseria meningitidis* upon contact with epithelial cells is mediatd by CrgA regulotary protein. *Mol. Microbiol.* 43, 1555-1564.

Deghmane, A. E., and Taha, M. K. (2003) The *Neisseria meningitidis* adhesion regulatory protein CrgA acts through oligomerization and interaction with RNA polymerase. *Mol. Microbiol.* 47, 135-143.

DiBella, L. M., Benashshi, S. E., Tedford, H. W., Harrison, A., Patel-King, R. S., and King, S. M. (2001) The Tctex1/Tctex2 Class of Dynein Light Chains. *J. Biol. Chem.* 276, 14366-14373.

Díaz, E. (2008) Microbial Biodegradation: Genomics and Molecular Biology. Caister Academic Press.

Duax, W.L., Ghosh, D., and Pletnev, V. (2000) Steroid dehydrogenase structures, mechanism of action, and disease. *Vitam. Horm.* 58, 121-148.

Efron, B., Hallorant, E., and Holmes, S. (1996) Bootstrap confidence levels for phylogenetic trees, *Proc. Natl. Acad. Sci. U. S. A.* 93, 7085-7090.

Ezezika, O. C., Sollier-Hyams, L. S., Dale, H. A., Burk, A. C., and Neidle, E. L. (2006) CatM regulation of the *benABCDE* operon: functional divergence of two LysR-Type paralogs in *Acinetobacter baylyi* ADP1. *Appl. Environ. Microbiol.* 72, 1749-1758.

Ezezika, O. C., Haddad, S., Clark, T. J., Neidle, E. L., and Momany, C. (2007) Distinct effector-binding sites enable synergistic transcriptional activation by BenM, a LysR-type regulator. *J. Mol. Biol.* 367, 616-629.

Filling, C., Berndt, K. D., Benach, J., Knapp, S., Prozorovski, T., Nordling, E., Ladenstein, R., Jörnvall, H., and Oppermann, U. C. T. (2002) Critical residues for structure and catalysis in short-chain dehydrogenase/reductases. *J. Biol. Chem.* 277, 25677-25684.

Filling, C., Nordling, E., Benach, J., Berndt, K. D., Ladenstein, R., Jörnvall, H., Oppermann, U. C. T. (2001) Structural role of conserved Asn 179 in the short-chain dehydrogenase/reductase scaffold. *Biochem. Biophys. Res. Commun.* 289 (2001) 712-717.

Garcia Valdes, E., Cozar, E., Rotger, R., Lalucat, J., and Ursing, J. (1988) New naphthalene-degrading marine *Pseudomonas* strains. *Appl. Environ. Microbiol.* 54, 2478-2485.

Gerischer, U. (2002) Specific and global regulation of genes associated with the degradation of aromatic compounds in bacteria. *J. Mol. Microbiol. Biotechnol.* 4, 111-121.

Grimm, C., Maser, E., Möbus, E., Klebe, G., and Reuter, K. (2000) The crystal structure of 3α-Hydroxysteroid Dehydrogenase/Carbonyl Reductase from *Comamonas testosteroni* show a novel oligomerization pattern within the short chain dehydrogenase/reductase family. *J. Biol. Chem.* 275, 41333-41339.

Gong, W., Xiong, G., and Maser, E. (Nov 24, 2010) Cloning, expression and characterization of a novel short-chain dehydrogenase/reductase (SDRx) in *Comamonas testosteroni*. *J. Steroid Biochem. Mol. Biol.* 10.1016/j.jsbmb.2010.11.008

Göhler A., Xiong, G. M., Paulsen, S., Trentmann, G., and Maser, E. (2008) Testosterone-inducible Regulator is a kinase that drives steroid sensing and metabolism in *Comamonas testosteoni*. *J. Biol. Chem.* 283, 17380-17390.

Harder, J., and Probian, C. (1997) Anaerobic mineralization of cholesterol by a novel type of denitrifying bacterium. *Arch. Microbiol.* 167, 269-274.

Henikoff, S., Haughn, G. W., Calvo, J. M., and Wallace, J. C. (1998) A large family of bacterial activator proteins. *Proc. Natl. Acad. Sci. U. S. A.* 85, 6602-6606.

Hernández-Lucas, I., Gallego-Hernández, A. L., Encarnación, S., Fernández-Mora, M., Martínez-Batallar, A. G., Salgado, H., Oropeza, R., and Calva, E. (2008) The LysR-type transcriptional regulator LeuO controls expression of several genes in *Salmonella enterica* serovar Typhi. *J. Bacteriol.* 190, 1658-1670.

Heroven, A. K., and Dersch, P. (2006). RovM, a novel LysR-type regulator of the virulence activator gene *rovA*, controls cell invasion, virulence and motility of *Yersinia pseudotuberculosis*. *Mol. Microbiol.* 62, 1469-1483.

Higgins, D., Thompson, J., Gibson, T., Thompson, J. D., and Gibson, J. (1994) CLUSTAL W: improving the sensitivity of progressive multiple sequence alignment through sequence weighting, position-specific gap penalties and weight matrix choice, *Nucleic Acids Res.* 22, 4673-4680.

Hoffmann, F., Sotriffer, C., Evers, A., Xiong, G. M., and Maser, E. (2007) Understanding oligomerization in 3α-hydroxysteroid dehydrogenase/carbonyl reductase from Comamonas testosteroni: An in silico approach and evidence for an active protein. *J. Biotechnol.* 129, 131-139.

Hong, Y., Wang, G., and Maier, R. J. (2008) The NADPH quinine reductase MdaB confers oxidative stress resistance to *Helicobacter hepaticus*. *Microb. Pathog.* 44, 169-174.

Horiguchi, T., Miwa, Y., and Shigesada, K. (1997) The quaternary geometry of transcription termination factor rho: assignment by chemical cross-linking, *J. Mol. Biol.* 269, 514-528.

Horinouchi, M., Yamamoto, T., Taguchi, K., Arai, H., and Kudo, T. (2001) Meta-cleavage enzyme gene tesB is necessary for testosterone degradation in *Comamonas testosteroni* TA441. *Microbiology* 147, 3367-3375.

Horinouchi, M., Hayashi, T., Yamamoto, T., and Kudo, T. (2003a) A new bacterial steroid

degradation gene cluster which consists of aromatic compound degradation genes for seco-steroids and 3-ketosteroid dehydrogenase genes in *Comamonas testosteroni* TA441. *Appl. Environ. Microbiol.* 69, 4421-4430.

Horinouchi, M. Hayashi, T., Koshino, H., Yamamoto, T., and Kudo, T. (2003b) Gene encoding the hydrolase for the product of the meta-cleavage reaction in testosterone degradation by *Comamonas testosteroni*. *Appl. Environ. Microbiol.* 69, 2139-2152.

Horinouchi, M., Hayashi, T., and Kudo, T. (2004a) The genes encoding the hydroxylase of 3-hydroxy-9,10-secoandrosta-1,3,5(10)-triene-9,17-dione in steroid degradation in *Comamonas testosteroni* TA441. *J. Steroid Biochem. Mol. Biol.* 92,143-154.

Horinouchi, M., Kurita, T., Yamamoto, T., Hatori, E., T., and Kudo, T. (2004b) Steroid degradation gene cluster of *Comamonas testosteroni* consisting of 18 putative genes from meta-cleavage enzyme gene *tesB* to regulator gene *tesR*. *Biochem. Biophys. Res. Commun.* 324, 597-604.

Horinouchi, M., Hayashi, T., Kurita, T., and Kudo, T. (2005) Identification of 9,17-dioxo-1,2,3,4,10,19-hexanorandrostan-5-oic acid, 4-hydroxy-2-oxohexanoic acid, and 2-hydroxyhexa-2,4-dienoic acid and related enzymes involved in testosterone degradation in *Comamonas testosteroni* TA441, *Appl. Environ. Microbiol.* 71, 5275-5281.

Horinouchi, M., Hayashi, T., and Kudo T. (2010) Steroid degradation in *Comamonas testosteroni*. *J. Steroid Biochem. Mol. Biol.* doi:10.1016/j.jsbmb.2010.10.008

Huffman, J. L., and Brennan, R. G. (2002) Prokaryotic transcription regulators: more than just the helix-turn-helix motif. *Curr. Opin. Struct. Biol.* 12, 98-106.

Ieva, R., Alaimo, C., Delany, I., Spohn, G., Rappuoli, R., and Scarlato, V. (2005) CrgA is an inducible LysR-type regulator of *Neisseria meningitidis*, acting both as a repressor and as an activator of gene transcription. *J. Bacteriol.* 187, 3421-3430.

Jornvall, H., Persson, B., Krook, M., Atrian, S., Gonzalez-Duarte, R., Jeffery, J., and Ghosh, D. (1995) Short-chain dehydrogenases/reductases (SDR). *Biochemistry* 34, 6003-6013.

Jourdan, A. D., and Stauffer, G. V. (1998) Mutational analyses of the transcriptional regulator GcvA: amino acids important for activation, repression, and DNA binding. *J. Bacteriol.* 180, 4865-4871.

Kallberg, Y., Oppermann, U., Jornvall, H., and Persson, B. (2002) Short-chain dehydrogenase/reductase (SDR) relationships: a large family with eight cluster common to human, animal, and plant genomes. *Protein Sci.* 11, 636-641.

Kieslich, K. (1985) Microbial side-chain degradation of sterols. *J. Basic. Microbiol.* 25, 461-474.

Kim, J., Kim, J. G., Kang, Y., Jang, J. Y., Jog, G. J., Lim, J. Y., Kim, S., Suga, H., Nagamatsu, T., and Hwang, I. (2004) Quorum sensing and the LysR-type transcriptional activator ToxR regulate toxoflavin biosynthesis and transport in *Burkholderia glumae*. *Mol. Microbiol.* 54, 921-934.

Kullik, I., Stevens, J., Toledano, M. B., and Storz, G. (1995) Mutational analyses of the redox-sensitive transcriptional regulator OxyR: regions important for DNA binding and multimerization. *J. Bacteriol.* 177, 1285-1291.

Laemmli, U. K. Cleavage of structural proteins during the assembly of the head of (1970) bacteriophage T4. *Nature* 227, 680-685.

Leppik, R. A., and Sinden, D. J. (1987) *Pseudomonas* mutant strains that accumulate androstane and seco-androstane intermediates from bile acids. *Biochem. J.* 243, 15-21.

Lindquist, S., Lindberg, F., and Normark, S. (1989) Binding of the *Citrobacter freundii* AmpR regulator to a single DNA site provides both autoregulation and activation of the inducible *ampC* beta-lactamase gene. *J. Bacteriol.* 171, 3746-3753.

Lochowska, A., Iwanicka-Nowick, R., Plochocka, D., and Hryniewicz, M. M. (2001) Functional dissection of the LysR-type CysB transcriptional regulator. Regions important for DNA binding, inducer response, oligomerization, and positive control. *J. Biol. Chem.* 276, 2098-2107.

Lochowska, A., Iwanicka-Nowick, R., Zaim, J., Witkowska-Zimny, M., Bolewska, K., and Hryniewicz, M. M. (2004) Identification of activating region (AR) of *Escherichia coli* LysR-type transcription factor CysB and CysB contact site on RNA polymerase alpha subunit at the *cysP* promoter. *Mol. Microbiol.* 53, 791-806.

Lu, Z., Takeuchi, M., and Sato, T. (2007) The LysR-type transcriptional regulator YofA controls cell division through the regulation of expression of *ftsW* in *Bacillus subtilis*. *J. Bacteriol.* 189, 5642-5651.

Maddocks, S. E., and Oyston, P. C. F. (2008) Structure and function of the LysR-type transcriptional regulator (LTTR) family proteins. *Microbiology* 154, 3609-3623.

Mahato, S. B., and Majumdar, I. (1993) Current trends in microbial steroid biotransformation. *Phytochemistry* 34, 883-898.

Mahoto, S. B., and Garai, S. (1997) Advances in microbial steroid biotransformation. *Steroids* 62, 332-345.

Marcus, P. I., and Talalay, P. (1956) Induction and purification of α- and β-hydroxysteroid dehydrogenases. *J. Biol. Chem.* 218, 661-674.

Maser, E., Möbus, E., and Xiong, G. M. (2000) Functional expression, purification, and

characterization of 3α-Hydroxysteroid Dehydrogenase/Carbonyl Reductase from *Comamonas testosteroni*. *Biochem. Biophys. Res. Commun.* 272, 622-628.

McFall, S. M., Parsek, M. R., and Chakrabarty, A. M. (1997a) 2-Chloromuconate and ClcR-mediated activation of the *clcABD* operon: in vitro transcriptional and DNase I footprint analyses. *J. Bacteriol.* 179, 3655-3663.

McFall, S. M., Klem, T. J., Fujita, N., Ishihama, A., and Chakrabarty, A. M. (1997b) DNase I footprinting, DNA bending and in vitro transcription analyses of ClcR and CatR interactions with the *clcABD* promoter: evidence of a conserved transcriptional activation mechanism. *Mol. Microbiol.* 24, 965-976.

Mclver, J., Djordjevic, M. A., Weinman, J. J., Bender, G. L., and Rolfe, B. G. (1989) Extension of host range of *Rhizobium leguminosarum* bv. *Trifolii* caused by point mutations in *nodD* that result in alterations in regulatory function and recognition of inducer molecules. *Mol. Plant Microbe Interact.* 2, 97-106.

Miclo, A., and Germain, P. (1992) Hexahydroindanone derivatives of steroids formed by *Rhodococcus equi*. *Appl. Microbiol. Biotechnol.* 36, 456-460.

Möbus, E., Jahn, M., Schmid, R., Jahn, D., and Maser, E. (1997) Testosterone-regulated expression of enzymes involved in steroid and aromatic hydrocarbon catabolism in *Comamonas testosteroni*. *J. Bacteriol.* 179, 5951-5955.

Möbus, E., and Maser, E. (1999) Cloning and sequencing of a new *Comamonas testosteroni* gene encoding 3 alpha-hydroxysteroid dehydrogenase/carbonyl reductase. *Adv. Exp. Med. Biol.* 463, 395-402.

Möbus, E., and Maser, E. (1998) Molecular cloning, overexpression, and characterization of steroid-inducible 3α-Hydroxysteroid Dehydrogenase/Carbonyl Reductase from *Comamonas testosteoni*. *J. Biol. Chem.* 273, 30888-30896.

Monferrer, D., Tralau, T., Kertesz, M., Dix, I., Solà, M., and Usón, I. (2010) Structural studies on the full-length LysR-type regulator TsaR from *Comamonas testosteroni* T-2 reveal a novel open conformation of the tetrameric LTTR fold. *Mol. Microbiol.* 75, 1199-1214.

Morelle, S., Carbonnelle, E., and Nassif, X. (2003) The REP2 repeats of the genome of *Neisseria meningitides* are associated with genes coordinately regulated during bacterial cell interaction. *J. Bacteriol.* 185, 2618-2627.

Muraoka, S., Okumura, R., Ogawa, N., Nonaka, T., Miyashita, K., and Senda, T. (2003) Crystal structure of a full-length LysR-type transcriptional regulator, CbnR: unusual combination of two subunit forms and molecular bases for causing and changing DNA bend. *J. Mol. Biol.* 328, 555-566.

Ogawa, N., McFall, S. M., Klem, T. J., Miyashita, K., and Chakrabarty, A. M. (1999)

Transcriptional activation of the chlorocatechol degradative genes of *Ralstonia eutropha* NH9. *J. Bacteriol.* 181, 6697-6705.

Oppermann, U. C. T., Netter, K. J., and Maser, E. (1993) Carbonyl reduction by 3 alpha-HSD from *Comamonas testosteroni*--new properties and its relationship to the SCAD family. *Adv. Exp. Med. Biol.* 328, 379-390.

Oppermann, U. C. T., Belai, I., and Maser, E. (1996) Antibiotic resistance and enhanced insecticide catabolism as consequences of steroid induction in the Gram-negative bacterium *Comamonas testosteroni*. *J. Steroid Biochem. Mol. Biol.* 58, 217-223.

Oppermann, U. C. T., and Maser, E. (1996) Characterization of a 3α-αhydroxysteroid dehydrogenase/carbonyl reductase from the Gram-negative bacterium *Comamonas testosteroni*. *Eur. J. Biochem.* 241, 744-749.

Oppermann, U. C. T., Filling, C., Berndt, K. D., Persson, B., Benach, J., Ladenstein, R., and Jörnvall, H. (1997) Active site directed mutagenesis of 3 beta/17 beta-hydroxysteroid dehydrogenase establishes differential effects on short-chain dehydrogenase/reductase reactions. *Biochemistry* 36, 34-40.

Page, R. (1996) Treeview: an application to display phylogenetic trees on personal computers. *Comput. Appl. Biosci.* 12, 357-358.

Pareja, E., Pareja-Tobes, P., Manrique, M., Pareja-Tobes, E., Bonal, J., and Tobes, R. (2006) ExtraTrain: a database of Extragenic regions and Transcriptional information in prokaryotic organisms. *BMC Microbiol.* 6, 29.

Parsek, M. R., Shinabarger, D. L., Rothmel, R. K., and Chakrabarty, A. M. (1992) Roles of CatR and *cis,cis*-muconate in activation of the *catBC* operon, which is involved in benzoate degradation in *Pseudomonas putida*. *J. Bacteriol.* 174, 7798-7806.

Parsek, M. R., McFall, S. M., Shinabarger, D. L., and Chakrabarty, A. M. (1994) Interaction of two LysR-type regulatory proteins CatR and ClcR with heterologous promoters: functional and evolutionary implications. *Proc. Natl. Acad. Sci. U. S. A.* 91, 12393-12397.

Renna, M. C., Najimudin, N., Winik, L. R., and Zahler, S. A. (1993) Regulation of the *Bacillus subtilis alsS*, *alsD*, and *alsR* genes involved in post-exponential-phase production of acetoin. *J. Bacteriol.* 175, 3863-3875.

Persson, B., Krook, M., and Jornvall, H. (1991) Characteristics of short-chain alcohol dehydrogenases and related enzymes. *Eur. J. Biochem.* 200, 537-543.

Pérez-Rueda, E., and Collado-Vides, J. (2001) Common history at the origin of the position-function correlation in transcriptional regulators in archaea and bacteria. *J. Mol. Evol.* 53, 172-179.

Ridlon, J. M., Kang, D. J., and Hylemon, P. B. (2006) Bile salt biotransformations by human intestinal bacteria. *J. Lipid. Res.* 47, 241-259.

Riordan, J. F. (1979) Arginyl residues and anion binding sites in proteins. *Mol. Cell. Biochem.* 26, 71-92.

Porrúa, O., García-Jaramillo, M., Santero, E., and Govantes, F. (2007) The LysR-type regulator AtzR binding site: DNA sequence involved in activation, repression and cyanuric acid-dependent repositioning. *Mol. Microbiol.* 66, 410-427.

Roméro-Arroyo, C. E., Schell, M. A., Gaines, G. L., and Neidle, E. L. (1995) *catM* encodes a LysR-type transcriptional activator regulating catechol degradation in Acinetobacter calcoaceticus. *J. Bacteriol.* 177, 5891-5898.

Rothmel, R. K., Aldrich, T. L., Houghton, J. E., Coco, W. M., Ornston, L. N., and Chakrabarty, A. M. (1990) Nucleotide sequencing and characterization of *Pseudomonas putida catR*: a positive regulator of the *catBC* operon is a member of the LysR family. *J. Bacteriol.* 172, 922-931.

Russell, D. A., Byrne, G. A., O'Connell, E. P., Boland, C. A., and Meijer, W. G. (2004) The LysR-type transcriptional regulator VirR is required for expression of the virulence gene *vapA* of *Rhodococcus equi* ATCC 33701. *J. Bacteriol.* 186, 5576-5584.

Sainsbury, S., Lane, L. A., Ren, J., Gilbert, R. J., Saunders, N. J., Robinson, C. V., Stuart, D. I., and Owens, R. J. (2009) The structure of CrgA from *Neisseria meningitides* reveals a new octameric assembly state for LysR transcriptional regulators. *Nucleic Acids Res.* 37, 4545-4558.

Sambrook, J., and Russel, D. W. (2001) Molecular cloning: A Laboratory Manual, 2nd ed. Cold Spring Harbor Laboratory Press, Cold Spring Harbor, NY.

Schell, M. A., Brown, P. H., and Raju, S. (1990) Use of saturation mutagenesis to localize probable functional domains in the NahR protein, a LysR-type transcription activator. *J. Biol. Chem.* 265, 3844-3850.

Schell, M. A. (1990) Regulation of naphthalene degradation genes of plasmid NAH7: example of a generalized positive control system in *Pseudomonas* and related bacteria. In: *Pseudomonas*: Biotransformations, Pathogenesis, and Evolving Biotechnology. Chakrabarty, A. M., Kaplan, S., Iglewski, B., Silver, S., eds. (1990) Washington, DC: Am. Soc. Microbiol. 165-177.

Schell, M. A. (1993) Molecular biology of the LysR family of transcriptional regulators. *Annu. Rev. Microbial.* 47, 597-626.

Sperandio, V., Li, C. C., and Kaper, J. B. (2002) Quorum-sensing *Escherichia coli* regulator A: a regulator of the LysR family involved in the regulation of the locus of enterocyte effacement pathogenicity island in enterohemorrhagic *E. coli*. *Infect. Immum.* 70, 3085-3093.

Stec, E., Witkowska-Zimny, M., Hryniewicz, M. M., Neumann, P., Wilkinson, A. J., Brzozowski, A. M., Verma, C. S., Zaim, J., Wysocki, S., and Bujacz, G. D. (2006) Structural basis of the sulphate starvation response in *E. coli*: crystal structure and mutational analyses of the cofactor-binding domain of the Cbl transcriptional regulator. *J. Mol. Biol.* 364, 309-322.

Storz, G., Tartaglia, L. A., and Ames, B. N. (1990) The OxyR regulon. *Antonie Van Leeuwenhoek* 58, 157-161.

Sumpter, J. B., and Johnson, A. C. (2005) Lessons from endocrine disruption and their application to other issues concerning trace organics in the aquatic environment. *Environ. Sci. Technol.* 39, 4321-4332.

Sun, J., and Klein, A. (2004) A LysR-type regulator is involved in the negative regulation of genes encoding selenium-free hydrogenases in the archaeon *Methanococcus voltae*. *Mol. Microbiol.* 52, 563-571.

Suzuki, M., and Brenner, S. E. (1995) Classification of multi-helical DNA-binding domains and application to predict the DBD structures of sigma factor, LysR, OmpR/PhoB, CENP-B, Rapl, and Xy1S/Ada/AraC. *FEBS Lett.* 372(2-3), 215-221.

Talalay, P., Dobson, M. M., and Tapley, D. F. (1952) Oxidative degradation of testosterone by adaptive enzymes. *Nature* 170, 620-621.

Tanaka, N., Nonaka, T., Tanabe, T., Yoshimoto, T., Tsuru, D., and Mitsui, Y. (1996) Crystal structures of the binary and ternary complexes of 7 alpha-hydroxysteroid dehydrogenase from *Escherichia coli*. *Biochemistry* 35, 7715-7730.

Tamaoka, J., Ha, D. M., and Komagata, K. (1987) Reclassification of *Pseudomonas acidovorans* den Dooren de Jong 1926 and *Pseudomonas testosteroni* Marcus and Talahay 1956 as *Comamonas acidovorans* comb. nov. and *Comamonas testosteroni* comb. nov. with an emended description of the genus Comamonas. *Int. J. Syst. Bacteriol.* 37, 52-59.

Tellinghuisen, T. L., and Kuhn, R. J. (2000) Nucleic acid-dependent cross-Linking of the nucleocapsid protein of Sindbis Virus, *J. Virol.* 74 4302-4309.

Tralau, T., Mampel, J., Cook, M. A., and Ruff, J. (2003a) Charaterization of TsaR, an Oxygen-Sensitive LysR-type Regulator for the degradation of *p*-Toluenesulfonate in *Comamonas testosteroni* T-2. *Appl. Environ. Microbiol.* 69, 2298-2305.

Tralau, T., Cook, M. A., and Ruff, J. (2003b) An additional regulator, TsaQ, is involved with TsaR in regulation of transport during the degradation of *p*-toluenesulfonate in *Comamonas testosteroni* T-2. *Arch. Microbiol.* 180, 319-326.

Tropel, D., and van der Meer, J. R. (2004) Bacterial transcriptional regulators for degradative pathways of aromatic compounds. *Microbiol. Mol. Biol. Rev.* 68, 474-500.

Tyrrell, R., Verschueren, K. H., Dodson, E. J., Murshudov, G. N., Addy, C., and Wilkinson, A. J. (1997) The structure of the cofactor-binding fragment of the LysR family member, CysB: a familiar fold with a surprising subunit arrangement. *Structure* 5, 1017-1032.

Vera, A., Gonzalez-Montalban, N., Aris, A., and Villaverde, A. (2007) The conformational quality of insoluble recombinant proteins is enhanced at low growth temperatures. *Biotechnol. Bioeng.* 96, 1101-1106.

van der Geize, R., Hessels, G. I., van Gerwen, R., Vrijbloed, J. W., van der Meijden, P., and Dijkhuizen, L. (2000a) Targeted disruption of the *kstD* gene encoding a 3-ketosteroid delta (1) -dehydrogenase isoenzyme of *Rhodococcus erythropolis* strain SQ1. *Appl. Environ. Microbiol.* 66, 2029-2036.

van der Geize, R., Hessels, G. I., van Gerwen, R., van der Meijden, P., and Dijkhuizen, L. (2000b) Unmarked gene deletion mutagenesis of *kstD*, encoding 3-ketosteroid Delta (1) –dehydrogenase, in *Rhodococcus erythropolis* SQ1 using *sacB* as counter-selectable marker. *FEMS Microbiol. Lett.* 205, 197-202.

van der Geize, R., Hessels, G. I., and Dijkhuizen, L. (2002a) Molecular and functional characterization of the *kstD2* gene of *Rhodococcus erythropolis* SQ1 encoding a second 3-ketosteroid Delta (1) –dehydrogenase isoenzyme. *Microbiology* 148, 3285-3292.

van der Geize, R., Hessels, G. I., van Gerwen, R., van der Meijden, P., and Dijkhuizen, L. (2002b) Molecular and functional characterization of *kshA* and *kshB*, encoding two components of 3-keto-steroid 9 alpha-hydroxylase, a class IA monooxygenase, in *Rhodococcus erythropolis* strain SQ1. *Mol. Microbiol.* 45, 1007-1018.

van der Geize, R., and Dijkhuizen, L. (2004) Harnessing the catabolic diversity of *rhodococci* for environmental and biotechnological applications. *Curr. Opin. Microbiol.* 7, 255-261.

van der Geize, R., Yam, K., Heuser, T., Wilbrink, M. H., Hara, H., Anderton, M. C., Sim, E., Dijkhuizen, L., Davies, J. E., Mohn, W. W., and Eltis, L, D. (2007) A gene cluster encoding cholesterol catabolism in a soil actinomycete provides insight into *Mycobacterium tuberculosis* survival in macrophages. *Proc. Natl. Acad. Sci. U. S. A.* 104, 1947-1952.

van der Geize, R., Hessels, R. G., Nienhuis-Kuiper, I. M., and Dijkhuizen, L. (2008) Characterization of a second *Rhodococcus erythropolis* SQ1 3-ketosteroid 9α-Hydroxylase activity comprising a terminal oxygenase homologue, KshA2, active with oxygenase-reductase component KshB. *Appl. Environ. Microbiol.* 74, 7197-7203.

van der Meer, J. R., Frijters, A. C., Leveau, J. H. J., Eggen, R. I. L., Zehnder, A. J. B., and de Vos, W.M. (1991) Characterization of the *Pseudomonas* sp. strain P51 gene tcbR, a LysR-type transcriptional activator of the *tcbCDEF* chlorocatechol oxidative operon, and analyses of the regulatory region. *J. Bacteriol.* 173, 3700-3708.

Viale, A. M., Kobayashi, H., Akazawa, T., and Henikoff, S. (1991) *rbcR*, a gene coding for a member of the LysR family of transcriptional regulators, is located upstream of the expressed set of ribulose 1,5-bisphosphate carboxylase/oxygenase genes in the photosynthetic bacterium *Chromatium vinosum*. *J. Bacterol.* 173, 5224-5229.

Wang, L., Helmann, J. D., and Winans, S. C. (1992) The *A. tumefaciens* transcriptional activator OccR causes a bend at a target promoter, which is partially relaxed by a plant tumor metabolite. *Cell* 69, 659-667.

Wackett, L. P., Sadowsky, M. J., Martinez, B., and Shapir, N. (2002) Biodegradation of atrazine and related s-triazine compounds: from enzymes to field studies. *Appl. Microbiol. Biotechnol.* 58, 39-45.

Warhurst, A. M., and Fewson, C. A. (1994) Biotransformations catalyzed by the genus Rhodococcus. *Crit. Rev. Biotechnol.* 14, 29-73.

Xiong, G. M., and Maser, E. (2001) Regulation of the steroid-inducible 3α-Hydroxysteroid Dehydrogenase/Carbonyl Reductase gene in *Comamonas testosteroni*. *J. Biol. Chem.* 276, 9961-9970.

Xiong, G. M., Martin, H., and Maser, E. (2003a) Identification and characterization of a novel translational repressor of the steroid-inducible 3α-Hydroxysteroid Dehydrogenase/Carbonyl Reductase gene in *Comamonas testosteroni*. *J. Biol. Chem.* 278, 47400-47407.

Xiong, G. M., Markowetz, S., and Maser, E. (2003b) Regulation of 3α-Hydroxysteroid Dehydrogenase/Carbonyl Reductase in *Comamonas testoteroni*: function and relationship of two operators. *Chem. Biol. Interact.* 143-144, 411-423.

Yen, K.-M., Gunsalus, I. C. (1982) Plasmid gene organization: naphthalene/salicylate oxidation. *Proc. Natl. Acad. Sci. U. S. A.* 79, 874-878.

Yen, K.-M., Gunsalus, I. C. (1985) Regulation of naphthalene catabolic plasmid NAH7. *J. Bacteriol.* 162, 1008-1013.

Zhang, T. D., Xiong, G. M., and Maser, E. (2011) Characterization of the steroid degrading bacterium S19-1 from the Baltic Sea at Kiel, Germany. *Chem. Biol. Interact.* 191, 83-88.

Acknowledgements

The present study was carried out in Institute of Toxicology and Pharmacology for Natural Scientists, University Medical School, Schleswig-Holstein, Campus Kiel. First, I would like to express my most sincere acknowledgement to my supervisor Prof. Dr. Edmund Maser. Thank Prof. Maser for providing me an opportunity to study in our institute. In particular, I'm totally inspired by his tireless working enthusiasms, and his encouragement always motivates me to make progress.

I would like to thank my co-supervisor Dr. Guangming Xiong. Thank Dr. Xiong for bringing me to the institute. With the patient guidance from Dr. Xiong, I've made great progress in the field of molecular biology. To say the least, my Ph.D thesis wouldn't be possible without the help from Prof. Maser and Dr. Xiong.

Warm thank to our institute secretary Frau Kubach for her very kindly help in study and lives, especially for helping us rent a wonderful apartment. Thank Dr. Martin for providing technical support whenever we need. I'd also like to thank Michael Kisiela's help in computer and Bioinformatics. Thanks to all colleagues in our institute for their friendly help and smiles, I'm very happy to study years in such a nice environment.

I would like to devote this thesis to my parents and my girlfriend Tingdi for their love and support. Last but not least, I would like to thank China Scholarship Council for the financial support of Ph.D study.

Curriculum vitae

Name: Wenjie Gong

Gender: Male

Date of birth: 20. 10. 1983

Birth place: Wugang city, Hunan province, P. R. China

Nationality: Chinese

Education

01/2009-	Institute of Toxicology and Pharmacology for Natural Scientists, University Medical School, Schleswig-Holstein, Campus Kiel, Germany (PhD candidate)
09/2006-12/2008	College of Animal Science and Veterinary Medicine, Jilin University (Master Degree)
09/2002-08/2006	College of Scientific Technology and Normal, Hunan Agriculture University (Bachelor Degree)
09/1999-08/2002	Wugang Vocational Technical School, Hunan province (high school)

Publication

Gong, W., Jiang, Y., and Za, Y. F., *et al*. (2010) Temporal and spatial dynamics of rabies viruses in China and Southeast Asia. *Virus Res.* 150 (1-2), 111-118.

Gong, W., Xiong, G., and Maser, E. (Nov 24, 2010) Cloning, expression and characterization of a novel short-chain dehydrogenase/reductase (SDRx) in *Comamonas testosteroni*. *J. Steroid Biochem. Mol. Biol.*, in press.

Gong, W., Xiong, G., and Maser, E. Identification and characterization of the LysR-type transcriptional regulator HsdR for steroid-inducible expression of the 3α-hydroxysteroid dehydrogenase/carbonyl reductase gene in *Comamonas testosteroni*. *Appl. Environ. Microbiol.*, accepted.

Gong, W., Xiong, G., and Maser, E. Characterization of oligomeric state and negative autorepression of LysR-type transcriptional regulator HsdR in *Comamonas testosteroni* (to be submitted).

Erklärung

Eidesstattliche Erklärung:

Hiermit erkläre ich an Eides statt, dass ich die vorgelegte Dissertation mit dem Titel "Characterization of the LysR-type Transcriptional Regulator HsdR Gene and Its Adjacent Short-chain Dehydrogenase/Reductase SDRx Gene in *Comamonas testosteroni* ATCC 11996" selbständig und ohne unerlaubte Hilfe angefertigt habe und dass ich die Arbeit noch keinem anderen Fachbereich bzw. noch keiner anderen Fakultät vorgelegt habe.

Kiel, 2011

_____

(Wenjie Gong)